Hydrogen and strontium isoscapes for the African Palearctic range to reconstruct insect migration and connectivity

Sana Ghouri

Thesis submitted to the University of Ottawa
in partial Fulfillment of the requirements for the M. Sc. Degree in the Ottawa Carleton Institute of Biology.

Department of Biology
Faculty of Science
University of Ottawa

Acknowledgements

First, I wanted to thank the funders for supporting this research. This study received funding from the New Frontiers in Research Fund 2018 (Dr. Clément Bataille and Dr. Gerard Talavera). Dr. Gerard Talavera's contributions were further supported by the grant PID2020-117739GA-I00 from MCIN/AEI/10.13039/501100011033 and the grant LINKA20399 from the CSIC iLink program. I would also like to acknowledge the University of Ottawa for awarding a start-up account to Dr. Bataille. Additionally, I am grateful to the University of Ottawa for funding my Master's degree through scholarships and teaching assistant positions.

To my thesis advisor, Dr. Clément Bataille for the valuable insight and guidance throughout these projects. His attention to detail and profound knowledge have not only been a constant source of inspiration but also a guiding light throughout these projects. His mentorship has set a stellar example for my future work. I'm also deeply grateful for the numerous opportunities he provided to showcase my research at conferences.

My heartfelt thanks extend to my thesis advisory committee, Dr. Frances Pick and Dr. Jayne Yack, for their invaluable guidance in my research project.

To the SAiVE labmates, both past and present. Thank you for a friendly and helpful atmosphere. Special thanks to my SAiVE bestie and office neighbor Zoe Landry, you made my master’s experience better by adding fun and laughter.

Aside from my lab members, I would like to thank all our collaborators who made this research possible with their expertise. I extend my gratitude to the members of the PhyloMigration Lab and to Dr. Gerard Talavera, who not only was an amazing co-supervisor during my honours and my Master’s project but also played a crucial role in this research.

I thank Gerard Talavera, Ivy Ng’iru, Anna Orteu and Elena Plana for their instrumental role in collecting samples.

I wish to show a heartfelt appreciation to the team at the Ján Veizer Stable Isotope Laboratory, where I spent countless hours microweighing my samples. A special thank you note to Kerry,

whose guidance was indispensable in understanding the intricacies of exchangeable hydrogen and for being a great microweighing buddy. Thank you to Dr. Nimal De Silva and Ms. Smita Mohanty for helping me with any lab issues in such a cheerful mood that is contagious.

I am deeply thankful for my sister, Heeba Ghouri, and my best friend, Leila Ben-Ohoud. These two amazing strong women were my constant cheerleaders and believed in me from start to end.

Finally to my younger self. You wanted to become a scientist and you did!

Table of Contents

List of Figures

List of Tables

Abstract

Insect migration stands as a phenomenon of paramount ecological importance, influencing ecosystems through a myriad of mechanisms, from facilitating pollination to aiding at disease transmission. Many insect species undertake multi-generational migrations in the Afro-tropical and Palearctic ranges, and increasing evidence highlights a number of migratory circuits across the entire Afro-Palearctic. Yet unravelling the migratory connectivity of the successive generations of these insects remains challenging given the impossibility to apply traditional biologger technology (e.g., radiotelemetry, light loggers), because of the small size, short life span and often large population sizes and ranges of insects. To address this challenge, this research pioneers the application of dual stable isotopic geolocation techniques based on hydrogen (δ^2H) and strontium ($^{87}Sr/^{86}Sr$). Isotope geolocation consists of comparing the isotopic signatures of a mobile individual (e.g., migratory insect) to a map predicting isotope variations on the landscape (i.e., isoscape). Consequently, applying isotope geolocation to reconstruct insect migratory routes and connectivity requires the development of isoscapes across the migratory circuit.

We first developed a novel δ^2H isoscape in insect wing tissues across the Afro-Palearctic range. We analyzed wing tissue from resident butterflies across the Afro-Palearctic. A strong linear relationship between δ^2H in local known-origin butterfly wings and local growing-season precipitation δ^2H values was found across the Afro-Palearctic allowing the development of a robust isoscape. However, the relationship was weaker in the Afrotropics due to the region's unique environmental characteristics, notably highly variable evaporation rates and relative humidity. Achieving increased geolocation precision in this region will necessitate the development of novel modeling approaches, incorporating more time-specific environmental and climate data as well as combining other independent geolocation tools.

To enhance the isotope geolocation potential of migratory butterflies across the Afro-Palearctic range, we developed a bioavailable strontium isoscape. Strontium isotope variations on the landscape are usually independent from those of hydrogen providing a second level of geolocation evidence and enhancing geolocation potential. To build a $^{87}Sr/^{86}Sr$ isoscape, we first

compiled bioavailable $^{87}Sr/^{86}Sr$ data across the range and analyzed a series of plant samples to fill existing spatial gaps. We then applied a novel spatial interpolation ensemble machine learning approach to predict bioavailable $^{87}Sr/^{86}Sr$ ratios across the range. Our analysis emphasizes the influence of factors such as geology, lithology, soil properties but also desert dust and volcanic aerosol deposition on bioavailable $^{87}Sr/^{86}Sr$. The novel ensemble machine learning approach outperforms the traditional random forest regression approach and provides a better assessment of spatial uncertainty to produce the most accurate and unbiased bioavailable $^{87}Sr/^{86}Sr$ isoscape across the Afro-Palearctic range.

As a first test to demonstrate the potential of this dual δ^2H-$^{87}Sr/^{86}Sr$ geolocation approach, we applied it to study the migratory routes and connectivity of *Vanessa cardui* individuals collected from each side of the Sahara Desert. Dual isotope-based metrics elucidated painted lady migration across the Sahara in unprecedented detail, notably moderate population connectivity across the Sahara with dominance of latitudinal migratory trajectories, a leapfrog migration during the southern leg across the Sahara, and incremental shorter distance migration during the northern leg of the migratory cycle. The study also highlighted the important role of the Arabian Peninsula as a significant stepping-stone for individuals traveling between Europe, Africa, and Asia. Such patterns and knowledge of this species' connectivity level will help conservation practitioners better assess risks and improve conservation strategies.

In conclusion, this thesis presents two novel isoscapes, each with a range of applications. The δ^2H isoscape is applicable to trace regional dispersal or migration of insects across the Palearctic, including both bidirectional migration and one-way dispersive behavior. The $^{87}Sr/^{86}Sr$ isoscape provides a basis to study mobility across the African continent and is applicable not only to trace the mobility of terrestrial insects but also the origin of other animals, humans, and manufactured materials across Africa. Together those isoscapes considerably advance the possibility of reconstructing the mobility of migratory insects to solve novel questions as evidenced by our case study on painted ladies.

Résumé

La migration des insectes est un phénomène d'une importance écologique majeure, qui influence les écosystèmes par le biais de divers mécanismes, que ce soit la pollinisation ou la transmission de maladies infectieuses. De nombreuses insectes entreprennent des migrations multigénérationnelles dans les régions afro-tropicales et paléarctiques, et des nombreuses données mettent en évidence un grand nombre de circuits migratoires dans l'ensemble de la région afro-paléarctique. La connectivité migratoire des différentes générations de ces insectes reste difficilement traçable étant donné leur petite taille, leur courte durée de vie et la grande taille et étendue de leurs populations, ce qui les rend difficiles à localiser à l'aide de techniques traditionnelles, telles que la radiotélémétrie ou les enregistreurs de lumière. Cette recherche relève ce défi en utilisant des techniques de géolocalisation isotopique stable basées sur l'hydrogène (δ^2H) et le strontium (^{87}Sr/^{86}Sr). La géolocalisation isotopique consiste à comparer les signatures isotopiques d'un individu en mouvement (par exemple, un insecte en migration) à une carte prédisant les variations isotopiques dans le paysage (c.-à-d. isoscape). Par conséquent, l'application de la géolocalisation isotopique pour reconstruire les trajets migratoires des insectes et leur connectivité nécessite le développement d'isoscapes sur l'ensemble du parcours migratoire.

Nous avons tout d'abord développé un nouvel isoscape δ^2H dans les ailes d'insectes spécifique à l'afro-paléarctique. Nous avons analysé des ailes de papillons locaux dans l'ensemble de l'afro-paléarctique. Une forte relation linéaire entre le δ^2H dans les ailes de papillons d'origine locale connue et le δ^2H des précipitations pendant la saison de croissance a été établie dans l'ensemble de l'Afro-Paléarctique, permettant le développement d'un isoscape. Cependant, la relation était plus faible dans les Afrotropiques en raison des caractéristiques environnementales uniques de la région, notamment des taux d'évaporation et d'humidité très variables. Alors que le nouvel isoscape permet une géolocalisation δ^2H dans l'ensemble de l'Afro-Paléarctique, le pouvoir prédictif plus faible de l'isoscape δ^2H dans l'Afro-tropique limite le potentiel de la géolocalisation par le δ^2H dans cette aire de répartition. Pour améliorer la précision de la géolocalisation dans cette région, il faudra développer de nouvelles approches de modélisation, incorporer des données environnementales et climatiques plus spécifiques et combiner d'autres outils de géolocalisation.

Pour améliorer le potentiel de géolocalisation isotopique des papillons migrateurs dans l'afro-paléarctique, nous avons développé un isoscape du strontium biodisponible. Les variations isotopiques du strontium dans le paysage sont généralement indépendantes par rapport à celles de l'hydrogène. Pour construire un isoscape $^{87}Sr/^{86}Sr$, nous avons d'abord compilé les données $^{87}Sr/^{86}Sr$ biodisponibles dans l'ensemble de l'aire de répartition et analysé une série d'échantillons de plantes afin de combler les déficits de données en Afrique. Nous avons ensuite développé une nouvelle méthode pour prédire les rapports $^{87}Sr/^{86}Sr$ biodisponibles basée sur l'« apprentissage ensembliste » (ou *ensemble machine learning*). Notre analyse souligne l'influence de facteurs tels que la géologie, la lithologie, les propriétés du sol, mais aussi la poussière du désert et les dépôts d'aérosols volcaniques sur le $^{87}Sr/^{86}Sr$ biodisponible. La nouvelle approche par *ensemble machine learning* est plus performante que l'approche traditionnelle de l'algorithme des « forêts aléatoires » (ou *random forest*) et fournit une meilleure évaluation de l'incertitude spatiale pour produire l'isoscape de $^{87}Sr/^{86}Sr$ le plus précis et le moins biaisé pour l'afro-paléarctique.

Notre étude présente deux isoscapes, chacun avec une variété d'applications et d'avantages. Notre analyse du δ^2H dans les ailes de papillons locaux représente la première tentative d'analyse du δ^2H dans les ailes d'insectes pour les climats tropicaux. Cela élargit l'ensemble des données existantes, qui se limitaient jusqu'à présent aux régions boréales et tempérées. Notre isoscape δ^2H est calibré pour la région paléarctique avec une quantification appropriée de l'incertitude et est utile pour retracer la dispersion ou la migration des insectes à travers le paléarctique. L'isoscape de $^{87}Sr/^{86}Sr$ est un outil polyvalent applicable à l'étude des insectes terrestres, des populations humaines, des tissus et des matériaux manufacturés à travers l'Afrique, couvrant des domaines tels que la reconstruction du mouvement des espèces existantes et éteintes, l'identification du trafic illégal de matériaux, la détermination des origines des esclaves et la contribution à la technologie criminalistique.

Comme premier essai pour démontrer le potentiel de cette approche de géolocalisation δ^2H-$^{87}Sr/^{86}Sr$, nous avons étudier la connectivité des papillons *Vanessa cardui* collectés de part et d'autre du Sahara. Cette approche visait à capturer les migrants trans-sahariens, effectuant deux vagues migratoires distinctes, l'une vers le sud en automne et l'autre vers le nord à la fin de l'hiver et au début du printemps, avec des générations qui se croisent, ce qui entraîne des variations dans le temps. Les mesures basées sur les isotopes ont révélé des tendances à grande

échelle dans la migration près du Sahara avec un niveau de détail sans précédent, montrant notamment une connectivité élevée et soulignant le rôle important de la péninsule arabique pour les papillons voyageant entre l'Europe, l'Afrique et l'Asie. Ces tendances et ces données sur le niveau de connectivité peuvent aider les écologistes à améliorer les stratégies de conservation.

Introduction

Migratory insects and their connectivity

Insect migration occurs on an enormous scale around the globe and plays a critical role in influencing terrestrial ecosystems (Satterfield et al., 2020). Their potential ecological impact can be in the form of ecosystem services, such as pollination, biological control of pests, and provision of food to higher trophic levels (Satterfield et al., 2020). Conversely, these migratory insects can also pose risks to ecosystems, food systems, and even human societies when they behave like pests or when they transport harmful pathogens, genes, or viruses (Hu et al., 2016; Satterfield et al., 2020).

During their migration, insect populations display spatial and temporal linkages across their migratory range (i.e., migratory connectivity) that strongly influence spatiotemporal population dynamics between seasons and are thought to have critical implications for ecosystems (Gao et al., 2020; García-Berro et al., 2023). High connectivity is characterized by individuals predominantly moving from one area of their migratory range to another with little or no mixing of individuals from other regions (Gao et al., 2020). In stark contrast to the well-explored migratory connectivity of many bird species in the Palearctic-Afrotropical migration system (Chowdhury et al., 2021; Menz et al., 2019; Wotton et al., 2019), very little is known about the migratory connectivity of insects that cross the Sahara (Talavera et al., 2023; Talavera and Vila, 2017). Among insects, numerous species of dragonflies, locusts, flies, moths and butterflies are known to actively migrate (Satterfield et al., 2020). Unlike birds or mammals, insects breed across multiple generations in various locations and at different times throughout the year, further adding to the complexity of their migratory patterns (García-Berro et al., 2023; Talavera et al., 2023).

When studying insect population connectivity across the Afro-tropical Palearctic range, insect population ecologists face the unique challenge of investigating sequential and reciprocal connectivity between tropical and subtropical, subtropical and temperate, and temperate and boreal regions (Vickery et al., 2023). This approach differs from the typical focus on direct connectivity between tropical and boreal realms as commonly seen in bird studies (Vickery et al., 2023). Understanding the migration routes of specific insect populations is crucial, as it is a

valuable tool for biosecurity, conservation, and management, especially given the sensitivity of migratory species to ongoing climate change (Gao et al., 2020). For example, environmental changes at a specific location along the migratory route could have more profound impacts on species with high connectivity compared to those with lower degrees of connectivity that can compensate population losses from other regions (Gao et al., 2020).

Despite the ecological significance of insect migrations, several significant knowledge gaps persist concerning insect movement. These gaps include (but are not limited to) poor understanding of: specific migration routes, connectivity patterns, population dynamics, and population sizes (Satterfield et al., 2020). The complexities surrounding dispersal patterns and their underlying drivers present challenges in predicting and managing outbreaks, particularly for numerous small pest species (García-Berro et al., 2023; Suchan et al., 2019). These knowledge gaps are largely attributed to the absence of effective tools to track small and short-lived individuals across long distances within these large and complex populations (Chapman et al., 2015). Furthermore, the complexity of multi-generational migration cycles requires separate investigations for each generation of the annual migration cycle.

Isotope geolocation of insects

The analysis of intrinsic biomarkers such as isotopes is one of the most widely adopted methods for tracking and investigating insect migration (Hobson, 2008; Hobson et al., 1999; Wassenaar and Hobson, 1998). This approach is based on the concept that local isotopic signatures assimilated during the larval stage are retained reliably in some animal tissues (e.g., wings), following metamorphosis (Lindroos et al., 2023). The successful application of isotope geolocation to trace migratory insects requires the development of spatial models predicting variations in isotope signatures over the study area (i.e., isoscape) in the tissue of interest, in this case, insect wings (Bowen and West, 2018). Isoscapes can then serve as a baseline against which the isotope signatures of migratory individuals can be compared to estimate their natal origins through isotope-based geographic assignment (i.e. a heat map of probable natal origin) (Wunder et al., 2005).

Isotopes of hydrogen (δ^2H) and strontium (^{87}Sr/^{86}Sr) are intrinsic markers of geographic origin because they reflect the environment in which an organism developed (Hobson et al.,

1999). In stable isotope geolocation, metabolically inert tissues, like wings, preserve the isotopic signature acquired from the local diet and environment. For more than two decades, comparing δ^2H values in inert tissues with continent-wide patterns expected from the δ^2H of amount-weighted mean growing season precipitation has been a primary method for tracing the large-scale movements of insects (Hobson et al., 1999; Wassenaar and Hobson, 1998).These δ^2H values exhibit well-documented variations, across broad latitudinal gradients driven by global hydrological processes, indicating large-scale seasonal and spatial patterns.(Bowen et al., 2005). A strong gradient in precipitation δ^2H exists between western Europe and Scandinavia indicating promising potential for using δ^2H values to pinpoint the origins of insect species from these regions. However, there is less variation in δ^2H values in the Afro-tropics (Bowen et al., 2005).

Multiple δ^2H isoscapes have been developed between the δ^2H in insect wings of known-origin individuals and δ^2H isoscape of precipitation including in United Kingdom and Ireland (Newton, 2021), Europe (Brattström et al., 2010), New Zealand and Australia (Holder et al., 2014), China (Qin and Shi, 2020) and North America (Hobson et al., 2019, 2012a). However, their application for tracking insect origins in the Afro-Palearctic, which features tropical climates with high evapotranspiration rates, can lead to incomplete ecological interpretations due to uncertainties. It is also unclear if a calibration relationship used to link wing and precipitation δ^2H established for North American or European insects can be reliably applied to Africa (Magozzi et al., 2019). An alternate approach is to derive a wing δ^2H directly by collecting butterfly wing samples from known origins across the Afro-Palearctic for a precisely calibrated isoscape.

Some challenges with using δ^2H geolocation are also specific to the Afro-Palearctic. For example, the Afrotropic experiences irregular and intermittent rainfall events with significant variation in timing and intensity, both on an annual and seasonal basis (e.g., drought vs. wet years and wet and dry season). These variations can cause significant deviations in δ^2H values in precipitation from long-term averaged isotopic values in precipitations (Vander Zanden et al., 2014). The primary reason for limited precision in δ^2H -based assignment is the relatively flat gradient of δ^2H in precipitation across sub-Saharan Africa (Reichlin et al., 2013).

Therefore, while hydrogen isotopes have proven invaluable, especially for large-scale geographic assignments (i.e., Borisov et al., 2020; Clem et al., 2022; Flockhart et al., 2013, 2017;

Hobson et al., 2019, 2012, 1999; Holder et al., 2014), their limitations in achieving finer-scale resolution have led to the exploration of complementary isotope system such as $^{87}Sr/^{86}Sr$ ratios. The combination of δ^2H values and $^{87}Sr/^{86}Sr$ ratios can improve the specificity of geographic assignments (Reich et al., 2021). The redundancy decreases substantially when combining these isotope tools because of their independent patterns and scales of variation (Reich et al., 2021). Together, δ^2H values and $^{87}Sr/^{86}Sr$ ratios, have enough discriminatory power to investigate the dispersal of small insect species across both small and large spatial scales within the extensive Afro-Palearctic range (Reich et al., 2021).

Bioavailable $^{87}Sr/^{86}Sr$ ratios in herbivorous insects are valuable for reconstructing geographic origins, mainly because they show patterns of variations driven by fundamentally different processes compared to δ^2H (Bataille et al., 2020). Multiple studies have demonstrated the potential of strontium isotopes in geolocation studies in Africa (e.g., Copeland et al., 2016; Janzen et al., 2020; van der Merwe et al., 1990; Wang et al., 2023), owing to the continent's large geological diversity (Bataille et al., 2020; Janzen et al., 2020). $^{87}Sr/^{86}Sr$ ratios in herbivorous insects directly mirror the $^{87}Sr/^{86}Sr$ ratios of their food, primarily influenced by local geology and, to a lesser extent, by hydrological and atmospheric inputs such as aeolian dust, sea spray and fertilizers (Bataille et al., 2020; Bataille and Bowen, 2012). The incorporation of $^{87}Sr/^{86}Sr$ into soil, plants and herbivores predominantly reflects the large-scale underlying geology (Flockhart et al., 2015). When considering the construction of strontium isoscapes, plants have repeatedly emerged as the most suitable candidates. This choice is attributed to their ease of collection, being demonstrably local and their position at the base of the food chain from which strontium enters the diet of animals (Holt et al., 2021). After analysing the $^{87}Sr/^{86}Sr$ in plant samples and compiling a dataset, we can use random forest regression or ensemble machine learning to create a regional $^{87}Sr/^{86}Sr$ isoscape.

Case study

The Painted Lady butterfly (*Vanessa cardui*) is renowned for its remarkable migratory journey, spanning 8-10 overlapping generations, making it one of the longest multigenerational migrations of any insect species (Talavera and Vila, 2017). These butterflies travel as far north

as Scandinavia during the summer, returning southward for the winter and dispersing across both sides of the Sahara, including the Mediterranean region and sub-Saharan Africa (Suchan et al., 2019; Talavera et al., 2018). This butterfly species has become a model for insect migration studies due to being virtually distributed worldwide and being in continuous movement year-round without entering a diapause phase (Talavera et al., 2023). *V. cardui* in the Palearctic and the Afrotropic are strongly connected by regular trans-Saharan migrations relying on temperate and tropical regions to complete their annual migration (Talavera et al., 2023). This intricate, multi-generational, worldwide migration pattern provides a unique opportunity to investigate insect migratory connectivity within each step of the migratory cycle using dual isotopes of hydrogen and strontium.

Dual δ^2H and ^{87}Sr/^{86}Sr assignments demonstrated higher precision than single-isotope assignment (Reich et al., 2021). Since the patterns of δ^2H and ^{87}Sr/^{86}Sr are independent, the precision improvement in dual-isotope assignments depends on the complementarity of their isotope patterns (Reich et al., 2021). With the development of both δ^2H (Chapter 1) and ^{87}Sr/^{86}Sr isoscapes (Chapter 2) calibrated for butterfly wings for the Afro-Palearctic region, this study has unlocked the potential to use δ^2H and ^{87}Sr/^{86}Sr -based geographic assignments in this region. The dual δ^2H and ^{87}Sr/^{86}Sr framework will be tested on a case study, focusing on unravelling connectivity and migration routes of *V. cardui* across the Sahara. This case study aims to demonstrate the practical application of this approach and assess its effectiveness in enhancing our comprehension of migratory insect dynamics.

Objectives & Significance

In this study, the aim is to provide a framework combining isotopes of strontium and hydrogen in the wing of migratory insects to improve our scientific understanding of insect migration. The application of this framework requires reliable isoscapes of δ^2H and ^{87}Sr/^{86}Sr calibrated for butterfly wings for the Afro-Palearctic region. My first objective is to generate a novel δ^2H wing isoscape broadly applicable to studying the migratory cycle of butterflies, moths, and other terrestrial herbivorous insect species across the Afro-Palearctic (Chapter 1). My second objective is to develop a novel and accurate bioavailable ^{87}Sr/^{86}Sr isoscape across this study region (Chapter 2). My third and last objective is to test this dual δ^2H and ^{87}Sr/^{86}Sr framework for

tracing the migration patterns and connectivity of the painted ladies across the Sahara and Arabian Desert (Chapter 2). I conclude by underlining the applicability of this new dual isotope geolocation tool across the Afro Palearctic range for a range of fields (Conclusion).

Chapter 1: A hydrogen isoscape for tracing the migration of herbivorous lepidopterans across the Afro-Palearctic range

Published in *Rapid Communication in Mass Spectrometry* December 15th, 2023
(https://doi.org/10.1002/rcm.9675)

Authors: Sana Ghouri[1]*, Megan S. Reich[1], Roger Lopez-Mañas[2], Gerard Talavera[2], Gabriel J. Bowen[3], Roger Vila[4], Valery N. K. Talla[5], Steve C. Collins[6], Dino J. Martins[7,8], Clement P. Bataille[9]*

[1]Department of Biology, University of Ottawa, Ontario, Canada

[2]Institut Botànic de Barcelona (IBB), CSIC-Ajuntament de Barcelona, Barcelona, 08038 Catalonia, Spain

[3]Geology and Geophysics, University of Utah, Utah, USA

[4]Institut de Biologia Evolutiva, CSIC-UPF, Barcelona, 08003 Catalonia, Spain

[5]Laboratory of Applied Biology and Ecology, Faculty of Science, University of Dschang, PO Box 67, Dschang, West Region, Cameroon

[6]African Butterfly Research Institute (ABRI), Nairobi, Kenya

[7]Mpala Research Centre, PO Box 555-10400, Nanyuki 10400, Kenya

[8]Turkana Basin Institute, Stony Brook University NY 11794

[9]Department of Earth and Environmental Sciences, University of Ottawa, Ontario, Canada

Author Contributions

Sana Ghouri: Writing - original draft, Methodology, Validation, Visualization, Writing - review & editing, Formal analysis, Data curation

Megan Reich: Validation, Writing - review & editing

Roger Lopez-Mañas: Data curation

Gerard Talavera: Resources, Conceptualization, Funding acquisition, Writing - review & editing

Gabriel J. Bowen: Writing - review & editing

Roger Vila: Resources

Valery N. K. Talla: Resources

Steve C. Collins: Resources

Dino J. Martins: Resources

Clement P. Bataille: Conceptualization, Funding acquisition, Writing - original draft, Writing - review & editing, Supervision, Data curation, Validation

1.1 Introduction

Insect migration occurs on an enormous scale around the globe, with quadrillions of individuals performing bidirectional long-range multigenerational migration cycles which influence terrestrial ecosystems through biomass and energy transfer and the spread of diseases and pests (Hu et al., 2016; Satterfield et al., 2020). During their migration, insect populations display spatial and temporal linkages across their migratory range (i.e., migratory connectivity) that strongly influence spatiotemporal population dynamics and are thought to have critical implications for associated ecosystems (García-Berro et al., 2023). Among insects, many species of dragonflies, locusts, flies, moths and butterflies are known to actively migrate (Satterfield et al., 2020). Unlike bird or mammal species, insect species breed across multiple generations at different places and times throughout the year (García-Berro et al., 2023; Stefanescu et al., 2013; Talavera et al., 2023). When studying insect population connectivity across the Afro-tropical Palearctic range, insect population ecologists need to investigate the sequential and back-and-forth connectivity between tropical and subtropical, subtropical and temperate, and temperate and boreal regions, instead of focusing solely on the direct connectivity between tropical and boreal realms as observed in bird studies (Vickery et al., 2023). Despite insects being the most diverse and abundant group of animals on earth, the spatiotemporal connectivity of most migratory and highly dispersive species is poorly understood. This knowledge gap is concerning given the pressing need to untangle the spatiotemporal connectivity of the vast bioflows of insects in circulation, especially in a context of rapid environmental change. The primary reason for this dearth of knowledge is the challenge of tracking small and short-lived individuals within these large and intricate populations (García-Berro et al., 2023; Suchan et al., 2019). Consequently, investigating multi-generational insect migratory cycles requires tools capable of tracing individuals across multiple generations at different periods and across large spatial scales.

Hydrogen isotope composition (referred to subsequently as δ^2H (Coplen, 2011)) is a promising tool to trace insect mobility and has been applied to a few insect species to study specific dispersal events (e.g., Borisov et al., 2020; Dargent et al., 2023; Hobson et al., 2018; Torniainen and Mikonranta, 2018; Zeng et al., 2020), single generations within the migratory cycle (e.g., Clem et al., 2022; Hobson et al., 2019, 2012b; Talavera et al., 2018; Wassenaar and Hobson, 1998), and more rarely multi-generational migration (e.g., Flockhart et al., 2013, 2017;

Hallworth et al., 2018). The basis behind this approach is that the δ^2H in water varies spatiotemporally and predictably on the landscape with temperature, elevation and continentality (Bowen et al., 2005; Bowen and Revenaugh, 2003). These patterns are transmitted from water to ecosystems, including to animal tissues that are grown at a specific location (Bowen and West, 2008). If carefully sampled by avoiding metabolically active wing veins (Lindroos et al., 2023), the δ^2H in the wings of holometabolic insects should reflect the δ^2H of the larval plant host environment because most of the wing tissue shows little remodeling during subsequent adult life (Lindroos et al., 2023). Interestingly, as hydrogen isotopes are preserved post-mortem in insect wings, individuals collected across a multi-generational migratory cycle can be analyzed a posteriori and provide a complete picture of the migration cycle across space and time.

A pre-requisite to use δ^2H to trace migratory insects is to develop spatial models predicting δ^2H variations over the study area (i.e., isoscape) in the tissue of interest (in this case, insect wings). These models can then act as a baseline against which the δ^2H of migratory individuals can be compared to estimate their natal origins (Wunder et al., 2005). While δ^2H isoscapes of insect wings usually follow the patterns of δ^2H in precipitation, the relationship is not 1:1 for both the plant host and the insect as environmental, metabolic and physiological isotope fractionations occur prior to and during the assimilation of hydrogen isotopes in tissues (Hobson et al., 1999). To assess this relationship, the δ^2H in the wings of a sample set of known-origin individuals is analyzed and compared using a transfer function, which relates the δ^2H values in the wings to the corresponding local predicted δ^2H values in precipitation (Brattström et al., 2010; Hobson et al., 2019, 2012b, 1999; Holder et al., 2014; Ma et al., 2020; Newton, 2021; Qin and Shi, 2020).

Mean annual precipitation isoscapes have been traditionally used when applying hydrogen isotopes in provenance studies. However, in certain situations, time-specific (monthly) precipitation isoscapes can offer advantages over multi-year mean isoscapes. For instance, many insect species have relatively short larval stages lasting weeks to months and therefore assimilate the isotopic composition of local water and food over a short period. Additionally, the length of time for the larval stage often varies with latitude in resident insects, introducing further complexity and variability into the tissue isoscape (Newton, 2021). In these cases, monthly isoscapes could help capture the short-term temporal variation of δ^2H in precipitation occurring during the larval stages (Bowen et al., 2019).

Multiple transfer functions have been developed between the δ^2H in insect wings of known-origin individuals and δ^2H isoscape of precipitation (e.g., Brattström et al., 2010; Hobson et al., 2019, 2012b, 1999; Quinby et al., 2020). These different equations exist because 1) approaches and standards used for δ^2H analysis have not been consistent between studies (Magozzi et al., 2020; Soto et al., 2017), 2) different known-origin individual sample sets have been produced for different regions, time periods, and species (Alquezar et al., 2022; Brattström et al., 2010; Hobson et al., 2018, 2012c; Marx et al., 2022), 3) distinct sampling strategies of known-origin sample sets on a given area can produce different equations (Contina et al., 2022) and 4) distinct global isoscapes of δ^2H in precipitation have been used as base maps to compare to known-origin sample sets (Bowen et al., 2005; Ehleringer et al., 2008; Terzer et al., 2013). Despite these inconsistencies, the existing δ^2H transfer functions, which might be specific to a species, time, location and reference material, are often applied indiscriminately to study insect dispersal and migration, yielding ecological interpretations that might not rigorously incorporate uncertainty. For example, Hobson et al. (2019) report an 8‰ mean uncertainty associated with their transfer function between the δ^2H values of known-origin monarchs reared locally across the eastern USA and the amount-weighted growing season (i.e., those months with a mean daily temperature >0°C) precipitation (GSP) isoscape of Bowen et al. (2005). This constant uncertainty value is often used by other researchers to estimate the uncertainty of their δ^2H isoscape, assuming thereby that this uncertainty is valid for different study areas (e.g., Hobson et al., 2012a; Stefanescu et al., 2016; Talavera et al., 2018), entire migration cycles (e.g., Flockhart et al., 2013) and different insect species (e.g., Hobson et al., 2021; Stefanescu et al., 2016; Talavera et al., 2018).

In practice, the transfer function equation and its uncertainty are dependent on many factors because isotopes might cycle and fractionate differently between precipitation and insects for different locations, climate zones, landcovers, periods or species (Magozzi et al., 2019). A major shortcoming of this calibration approach is that post-precipitation isotope cycling is not taken into account. Precipitation accumulating in soils, ponds or other reservoirs on the landscape can evaporate prior to being uptaken by plants and insects. Evaporation fractionates hydrogen isotopes leading δ^2H values of evaporated surface water to be more enriched in ^{2}H from those of precipitation. Consequently, insect wings developing during the short larval stages may have a high sensitivity to the specific environmental and climatic as well as microclimatic conditions

and water cycling processes occurring on the landscape during this period (Hobson et al., 2010). Additionally, across very large study areas like the Afro-Palearctic, evaporation rates and post-precipitation processes might vary between regions due to different climate seasonality. For example, arid regions exhibit a very different seasonality and evaporation rates than temperate regions complicating the use of standardized time-specific precipitation isoscapes over the large continental scale area used by migratory insects.

In this study, we aim to generate a δ^2H isoscape broadly applicable to understanding the migratory cycle of herbivorous lepidopterans with a focus on butterflies across the Afrotropical and West-Palearctic biogeographic realms (longitudinal range: 36.8° in the east to −16.25° in the west, latitudinal range: 69.94° in the north to −23.87° in the south). The few isotope studies focusing on migratory insects in this region have used the transfer function generated by Brattström et al. (2010) using locally reared red admiral butterflies, *Vanessa atalanta*, at a few sites across Europe (e.g., Stefanescu et al., 2016; Talavera et al., 2018). This transfer function equation and the accompanying uncertainty propagation do not incorporate known-origin data from the Afro-tropics which is essential to obtain a properly calibrated isoscape (Contina et al., 2022). Here, we first analyze δ^2H in wings (δ^2H_{wing}) of known-origin butterfly collected across the Afro-Palearctic range. Butterfly samples from different time periods and climates were used to encompass the entire spatiotemporal range of migratory insects across the Afro-Palearctic. We develop a δ^2H isoscape of butterfly wings using the typical calibration approach by comparing known-origin insect δ^2H to δ^2H_{GSP} values. We then explore the potential climatic and environmental controls of variance of this calibration relationship by using high spatiotemporal-resolution remote sensing products to account for factors such as vegetation and topography. We conclude with recommendations for the development of hydrogen isoscapes for insect provenancing.

1.2 Material and Methods

1.2.1 Known-origin sample set

We gathered a sample set of 142 butterfly individuals using an existing collection of lepidopteran specimens curated at the *Institut Botànic de Barcelona* (IBB, CSIC) and the *Institut de Biologia Evolutiva* (IBE, CSIC-UPF) and collected over the last decades (2007 to 2023).

Upon collection, samples were processed immediately by separating wings from bodies. The bodies were stored in ethanol, and the wings were kept dry in glycine envelopes. This preservation method limits contamination or deterioration of wing tissue that could potentially affect δ^2H values (Bugoni et al., 2008; Fraser et al., 2008). We followed recommendations from Contina et al. (2022) of sampling the isotope extremes of the range by selecting samples from regions with the highest and lowest δ^2H_{GSP} values within the Afro-Palearctic (i.e., Scandinavia (-156.6‰) and tropical regions (-8.0‰). We also included samples from geographic locations spread throughout the range. We screened the collection using a series of criteria to obtain a known-origin sample set and minimize the confounding factors influencing δ^2H_{wing} values. First, we targeted species with sedentary behavior and a low-dispersive rate to ensure we analyzed only resident individuals (i.e., species that do not migrate and likely remain within five kilometres of their location of larval growth during adult life). Second, since we did not have access to an appropriate number of specimens from any single sedentary species that covers the entire study area, we limited the number of sampled species to a minimum of widespread species from three families (i.e., Lycaenidae (n=135), Nymphalidae (n=6), Pieridae (n=1)) which allowed us, within the bounds of practicality, to cover the studied range and minimize inter-specific differences in diet, behavior or metabolism that could influence δ^2H values (Magozzi et al., 2019; Rubenstein and Hobson, 2004). Third, we selected sites where multiple specimens of the same species were available per site (≈3 per site) to ensure the within-species reproducibility of isotope data and investigate intra-site variability. Fourth, we only targeted sites for which precise geographic coordinates were available. Our selected dataset consisted of 142 individuals from 17 butterfly genera from 56 sites in 30 countries (≈ 3 individuals per site) across the study area (Fig. 1.1). Details on the species, locations and associated collecting data are summarized in Table S1.2. While the time of sampling is also an important variable due to the seasonal and inter-annual variations in δ^2H values (Vander Zanden et al., 2014), we could not gather individuals collected synchronically as to build a monthly-resolution known-origin dataset. Hence, specimens in our dataset were collected at different months and years which will add some isotopic variability.

1.2.2 Hydrogen isotope analysis

Butterfly wings were shipped to the Jan Veizer Stable Isotope Laboratory at the University of Ottawa for hydrogen isotope analysis. Before measuring δ^2H_{wing} values, we cleaned the wings with a series of three 2:1 chloroform:methanol baths (1h, 30 min and 5 min, respectively) to remove lipids, dust and contaminants from the wings that could have impacted the δ^2H values. For each individual, small pieces of the cleaned hindwing were cut from the same distal section of the wing to reduce inter-sample variance and avoid large veins (Lindroos et al., 2023). Those samples were then weighed (with weight ranging from 0.076 mg to 0.253 mg) into pressed silver 3.5 × 5 mm capsules. The samples were then put in the oven at 40°C for 1 hour to ensure there was no surface moisture on the capsules. We analyzed the samples using a Costech Zero Blank autosampler attached to a Thermo TCEA, coupled to a Thermo Scientific Delta-V Plus isotope ratio mass spectrometer using a Thermo Conflo IV interface (Thermo Finnigan, Bremen, Germany). The air in the autosampler was purged out and replaced with helium carrier gas. The autosampler was then held under positive helium pressure for the duration of the analytical run. The glassy carbon tube inside of the ceramic tube, normally used for the TC/EA, was removed and instead a ceramic tube was filled from the bottom to the top with 5 cm of silver wool, 10 cm of glassy carbon chips, 0.8 cm of quartz wool, and 1.5 cm of chromium powder (Coplen and Qi, 2016). The δ^2H of the non-exchangeable hydrogen of the butterfly wing was determined using the comparative analysis approach described by Wassenaar and Hobson (2003) based on a calibration line using three USGS calibrated keratin hydrogen-isotope reference materials Caribou Hoof Standard (CBS: −157±0.9‰,), Kudo Horn Standards (KHS: −35.3±1.1‰) and USGS43 hair (δ^2H: −44.4 ± 2.0‰). USGS42 hair (δ^2H: −72.9 ±2.2‰) was used as a quality check. The measured values for USGS42 (−73.2±1.7‰, n =18) were within the reported value and uncertainty, thus verifying this approach. Analytical precision of these measurements is based on the reproducibility of USGS42 and is better than ± 2‰. As butterfly wings are made of chitin, we also used two chitin internal standards in each run as a quality check standards. We ground and homogenized spongy moth wings (*Lymantria dispar*, Linnaeus, 1758) and used a commercial shrimp chitin material (Alfa Aesar). Those quality check standards gave the following δ^2H = −64.0±0.8‰ (n=14) for the spongy moth and δ^2H = −22.7±2.2‰ (n=13) for the commercial chitin, those values support analytical precision of ± 2‰. All δ^2H

values are reported as the δ-notation relative to the international Vienna Standard Mean Ocean Water – Standard Light Antarctic Precipitation scale (VSMOW-SLAP) in per mil (‰).

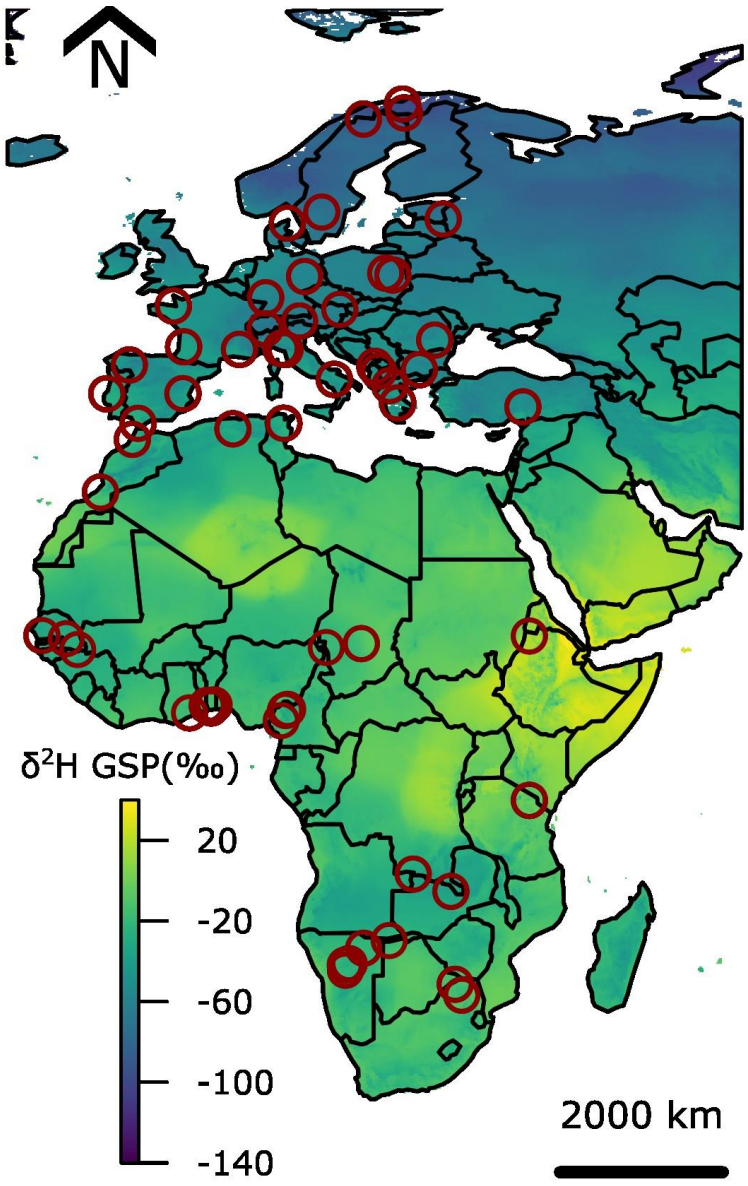

Figure 1.1. Map representing the predicted δ^2H values in growing season precipitation across the Afro-Palearctic range with the location of the known-origin samples. The amount-weighted mean global growing-season precipitation (GSP) map is from waterisotope.org and are made using the OIPC v3.2 database following the approach of Bowen et al. (2005). In that approach, δ^2H of GSP is defined as the average δ^2H in precipitation for all the months with a mean temperature greater than 0°C. The red circles represent the location of 56 sample sites of known-origin butterfly in 30 countries. Sampling data is available in Table 2. The shapefile for country boundaries was obtained from *rnaturalearth package*.

1.2.3 Development of the hydrogen isoscape

All statistical analyses were conducted in the R environment (version 4.2.2). We generated a δ^2H_{wing} isoscape following the procedure described in the *assignR* package. The process requires a tissue-specific isotope dataset of known-origin individuals to develop a transfer function between an isoscape and the tissue of interest. We first carefully screened the known-origin dataset for potential outliers. Outliers δ^2H_{wing} values were defined as per the *outlier()* function from the package *outliers* in R. Based on the *outlier()* function, we identified 2 outliers (Fig. 1.2). The first outlier (ID= 18A228; Table S1.2) is from the genus *Leptotes* and was collected in January 2018 in Cameroon, Africa (δ^2H= −11.2‰). The second outlier (ID= 15D265; Table S1.2) is from the genus *Zizeeria* and was collected in April 2019 in Namibia, Africa (δ^2H= −107.5‰) (Table S1.2). After removing outliers, we calibrated a linear model between δ^2H_{wing} values and δ^2H values of the growing-season precipitation (GSP) isoscape using the *calRaster()* function in the *assignR* package. We also tested a linear model between δ^2H_{wing} values and δ^2H values of monthly precipitation isoscapes using *The Online Isotopes in Precipitation Calculator* (OIPC3.1) by extracting precipitation δ^2H values for the month prior to sampling or the average δ^2H values of the two months prior to sampling (Fig. S1.7).

1.2.4 Statistical analysis of uncertainty

1.2.4.1 Covariates

To explore the controls of uncertainty of the linear model, we investigated potential causes of variance in the relationship between δ^2H_{wing} and δ^2H_{GSP} by calculating intra-site standard deviation at each sampling site and exploring the model residuals (observed δ^2H_{wing} - predicted δ^2H_{wing}). We first tested if some spatial autocorrelation was present in the intra-site standard deviation and model residuals. We then tested whether the intra-site standard deviation and/or the residuals of the linear model was significantly related to different landcover, topographic, geographic or climatic variables. We tested these environmental variables because they are known to strongly influence δ^2H values of local waters (Bowen et al., 2019; Magozzi et al., 2019). The type of landcover, geography, topography and climate can affect the intra-site variance and residuals because 1) different host-plant species might occur in different climate

zones and countries, each with their specific hydrophysiology fractionating hydrogen isotopes differently (Bowen et al., 2019), 2) specific landscapes (e.g., urban, irrigated, mountainous) might have varied water sources or fractionation processes that lead to locally heterogeneous δ^2H values in plants (Yamanaka et al., 2015), 3) differences in environmental conditions (e.g., temperature, relative humidity) of a specific year or month might lead to distinct evaporation regimes and isotopic fractionation between precipitation, surface water, soil water and plants (Magozzi et al., 2019; Vander Zanden et al., 2014) and 4) the δ^2H_{GSP} predictions might be less accurate in certain regions due to the scarcity of precipitation stations (Bowen et al., 2005; West et al., 2014).

Spatial surfaces (i.e., raster and polygon files) of the relevant explanatory variables were obtained from multiple geospatial repositories. All data was accessed and retrieved from its original providers, except topography and landcover, which were retrieved and clipped from the Google Earth Engine data catalogue. We performed the analysis using the *raster* package. For landcover, we used a multi-year averaged landcover classification derived from NASAs remote sensing product MCD12Q1 BGC (Table 1.1). For landcover, the only categorical auxiliary variable, we reported the dominant landcover class within the buffers. For climate we used the multi-year averaged monthly aridity index (AI), year specific monthly vapor pressure (VAP), year-specific monthly rainy days count (precipitation >0.1 mm) (WET), Seasonality Index (SI) and relative humidity index (RH). For vegetation, we used the year-specific monthly Enhanced Vegetation Index (EVI) provided in NASA's MOD13C2 remote sensing product. For topography, we used the Shuttle Radar Topography Mission (SRTM) (Table 1.1). To assess the topographic heterogeneity, we also calculated the difference between minimum and maximum elevation within a 5 km circular buffer of the sampling site. For the relative humidity auxiliary variable, we also reported the relative humidity anomaly of the month which is calculated as the difference between the value of the relative humidity of the month and the average relative humidity of the same month for the period 1991-2020 (Table 1.1). Depending on the temporal resolution of the auxiliary variable, we extracted the annual values and monthly values for the month prior to sampling dates from the specific sampling year or from multi-year averaged data for the covariates described in Table 1.1. Most of the species selected in the known-origin dataset have an expected adult life span of 2-3 weeks and a larval stage of 2-4 weeks (Table S1.2). The values of the month prior to sampling were selected because they represent the best estimate of

environmental conditions during larval development. Most of the resident species used in the known-origin dataset have an expected foraging range of less than 5 km, with the majority having an expected reported foraging range of 1 km (Table S1.2). Assuming a foraging range of <5 km for our resident species, we calculated the statistical distribution of values within a 1 km and 5 km circular radius of the sample site, including minimum, maximum, mean, median and standard deviation values for all continuous auxiliary variables. We buffered the sample's location at 1 and 5 km radius and extracted all cell values falling inside the buffer areas. We then calculated the corresponding statistics at each sampling location (Table S1.2).

Table 1.1. | List and metadata for the geospatial environmental variables used in the regression models. The temporal resolution column reports whether the monthly resolution data are available as a multi-year average ("Month average") or for the specific year of collection ("Month"). The last two columns list the statistics calculated within a 5 km buffer zone and 1 km buffer zone around each sample site.

Variable	Abbreviation	Spatial resolution (m)	Temporal resolution	Source	Statistics 5 km	Statistics 1 km
Land Cover	LC	500	Year	(NASA JPL, 2020)	Mode	Mode
Topography	DEM	30	Static	(NASA JPL, 2020)	Min, Max, Median, Mean, Standard Deviation	Min, Max, Median, Mean, Standard Deviation
Aridity index	AI	873.98	Month average	(Zomer et al., 2022)	Min, Max, Median, Mean, Standard Deviation	Min, Max, Median, Mean, Standard Deviation
Vapor Pressure	VAP	55,569.5	Month	(Harris et al., 2020)	Value	Value
Count of rainy days	WET	55,569.5	Month	(Harris et al., 2020)	Value	Value

Seasonality Index	SI	55,569.5	Static	(Feng et al., 2013)	Value	Value
Relative Humidity	RH	27,784.75	Month	(Hersbach et al., 2020)	Value, Value of Climatic month, Anomaly	Value, Value of Climatic month, Anomaly
Enhanced Vegetation Index	EVI	5,556.95	Month	(Didan, 2015)	Min, Max, Median, Mean, Standard Deviation	Min, Max, Median, Mean, Standard Deviation

1.2.4.2 Multivariate regression model for intra-site variance

We ran a multivariate linear regression model to test the correlation between the intra-site standard deviation and the continuous and categorical potential predictors extracted from each sampling site listed in Table 1.1. Many of the variables in Table 1.1 are collinear, violating assumptions for building a multivariate linear model. We used the variance inflation factor *vif()* function in the *car* package to iteratively remove non-independent variables. A conservative vif threshold of 2 was chosen to ensure no collinearity in the final model. We used the *cooks.distance()* function in the *stats* package to verify that no influential outliers were affecting the model results (RDocumentation, 2009). We assessed the significance of the predictors using the p-values associated with the t-statistics for each covariate and also visualized that the final model met multivariate linear model assumptions using typical diagnostic plots (i.e., residuals and absolute residuals vs predicted values plots, Normal Q-Q plot of residuals, and residuals vs. leverage plots).

1.2.4.3 Mixed effect model for predicting residuals and for predicting hydrogen isotope in wings

For testing the variables correlated with model residuals, we proceeded similarly as for the intra-site standard deviation by building a multivariate linear regression model. However, in this case, all the observations are not independent because multiple individuals were collected per site and have distinct residuals. We accounted for this pseudo-replication by using a mixed effect model with the *lmer()* function in the *lme4* package and allowing within-site correlation

(Bates et al., 2015). The *lmer()* function fit a linear mixed model by Restricted Maximum Likelihood (REML). We used the *vif()* function from the *car* package to iteratively remove non-independent variables (Naimi et al., 2014). A Moran's I test for spatial autocorrelation was also done on residuals. Selection and screening procedures were used as in section 1.2.4.2.
As a second step, we used a similar multivariate linear mixed model approach to improve predictions of δ^2H_{wing} values relative to when a simple linear regression with δ^2H_{GSP} values was used as done in the *assignR* package. We used δ^2H_{GSP} values and the auxiliary variables in Table 1.1 as potential predictors and δ^2H_{wing} values as response variables. To evaluate the performance of the model, we compared the result of this modeling with the univariate linear model using only δ^2H_{GSP} values as predictor.

1.3 Results

1.3.1 Known-origin dataset and isoscape

The δ^2H_{wing} values from the known-origin samples ranged from −119.2 to −12.8‰ (n=142; Fig. 1.2), the lowest value being from Austria (−119.2‰) and the highest from South Africa (−12.8‰). The δ^2H_{wing} values generally followed the expected patterns with higher δ^2H_{wing} values when moving towards the tropics and closer to coastal areas. The range of δ^2H_{wing} values observed in Africa varied from −94.1‰ in Zambia to −12.8‰ in South Africa. However, the majority of values were clustered between −70.0 and −40.0‰. A larger amplitude of δ^2H_{wing} variations and stronger gradients were observed along the temperate and boreal regions with values as low as −119.2‰ in Austria and Scandinavia to −39.3‰ in the circum-Mediterranean regions. A few sites stood out with unexpected δ^2H_{wing} values including very low δ^2H_{wing} values in a low altitude region of Austria and very high δ^2H_{wing} values in South Africa. Italy and Spain had the highest values for Europe with values sometimes overlapping with some regions of Africa.

As most sites had three samples collected, we calculated the standard deviation of δ^2H_{wing} values at each site. The intra-site standard deviation varied greatly spatially with a mean value of 7.1‰ and a range of 0.9‰ to 24.8‰. Intra-site standard deviation was higher in Africa (e.g., Ethiopia, Algeria) and lower in Europe (e.g., Denmark, Sweden).

We found a strong relationship between δ^2H_{wing} and δ^2H_{GSP} (δ^2H_{wing}= –39.80 + 0.80 x δ^2H_{GSP}, r^2=0.53, n=142, Fig. 1.2). We also found a strong relationship between δ^2H_{wing} and δ^2H in precipitation of the month prior to sampling (δ^2H_{wing}= –53.49 + 0.71 x δ^2H_{MP}, r^2=0.45, n=142, Fig. S1.7A) and between δ^2H_{wing} and the average δ^2H in precipitation of the two months prior to sampling (δ^2H_{wing}= –52.47 + 0.66 x δ^2H_{2MP}, r^2=0.46, n=142, Fig. S1.7B). However, those relationships differed substantially from previous equations (Fig. 1.2). The resulting δ^2H_{wing} isoscape (Fig. 1.3) displays a strong spatially coherent pattern, both north-south with increasingly more negative δ^2H values from the tropics towards the poles (Fig. 1.3) and an east-west longitudinal gradient across the African continent with the highest values found in and around the horn of Africa whereas lower values are found further east in Namibia, Angola and Zambia. The spatially explicit uncertainty map of the δ^2H_{wing} isoscape displays values ranging from 16.8‰ to 21.1‰ with a mean uncertainty of 17.3‰. Most of the value's range between 16.8‰ to 17.5‰ (Fig. 1.3).

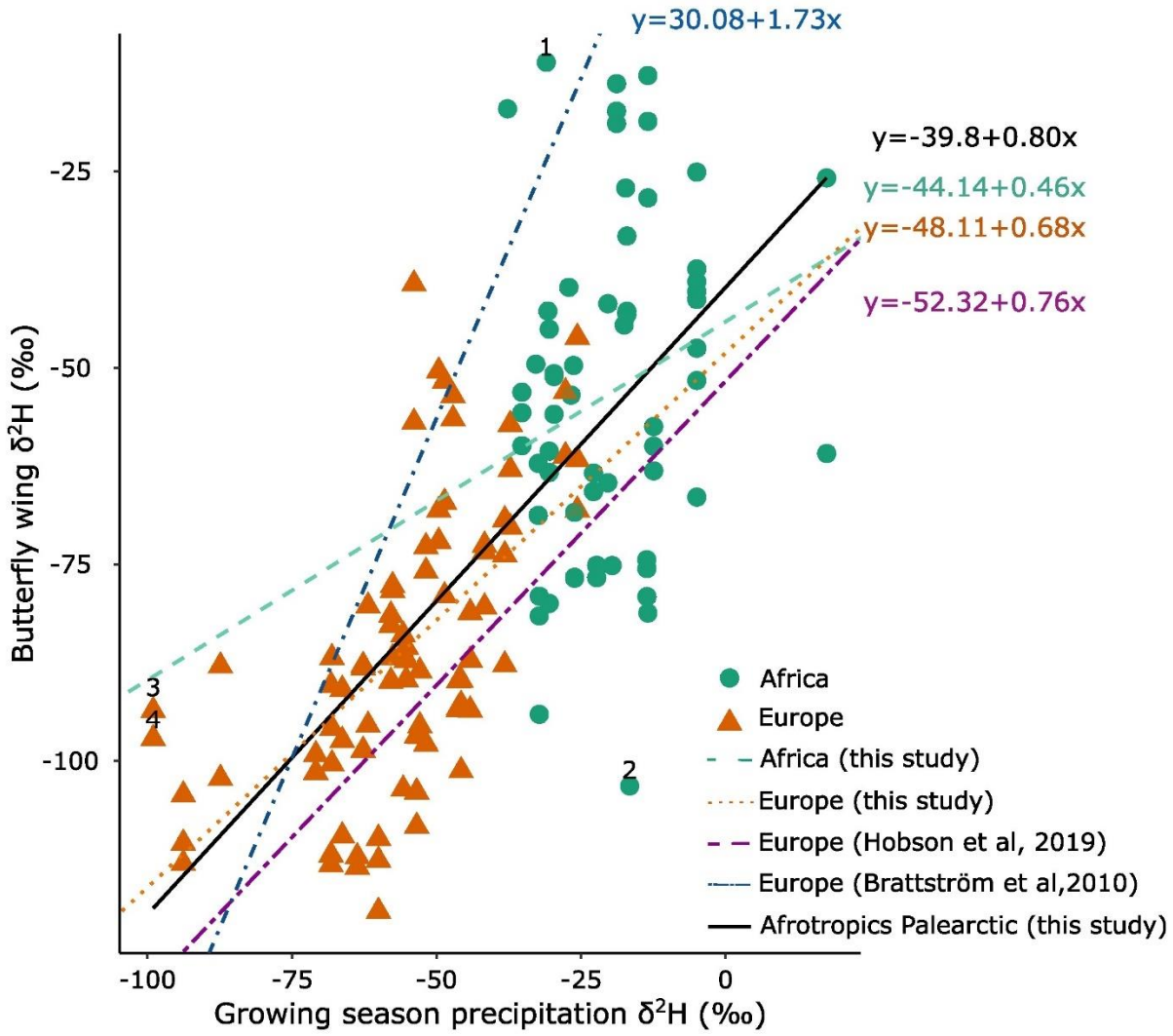

Figure 1.2. **Scatter plot between δ^2H_{wing} and δ^2H_{GSP}**. Linear regression for the Afro-Palearctic (entire study area from this study) (in black), Africa (this study) (in green) and Europe (this study) (in orange) are shown, as well as the three associated calibrating equations. Linear regression lines and equations of two additional studies of Brattström et al., (2010) (in blue) and Hobson et al., (2019) (in purple) were added for comparison. Samples numbered 1 and 2 are analytical outliers and were removed from our dataset. Samples numbered 3 and 4 are considered outliers only for Europe and were removed from the linear equation of Europe. Sample metadata is available in Table S1.2.

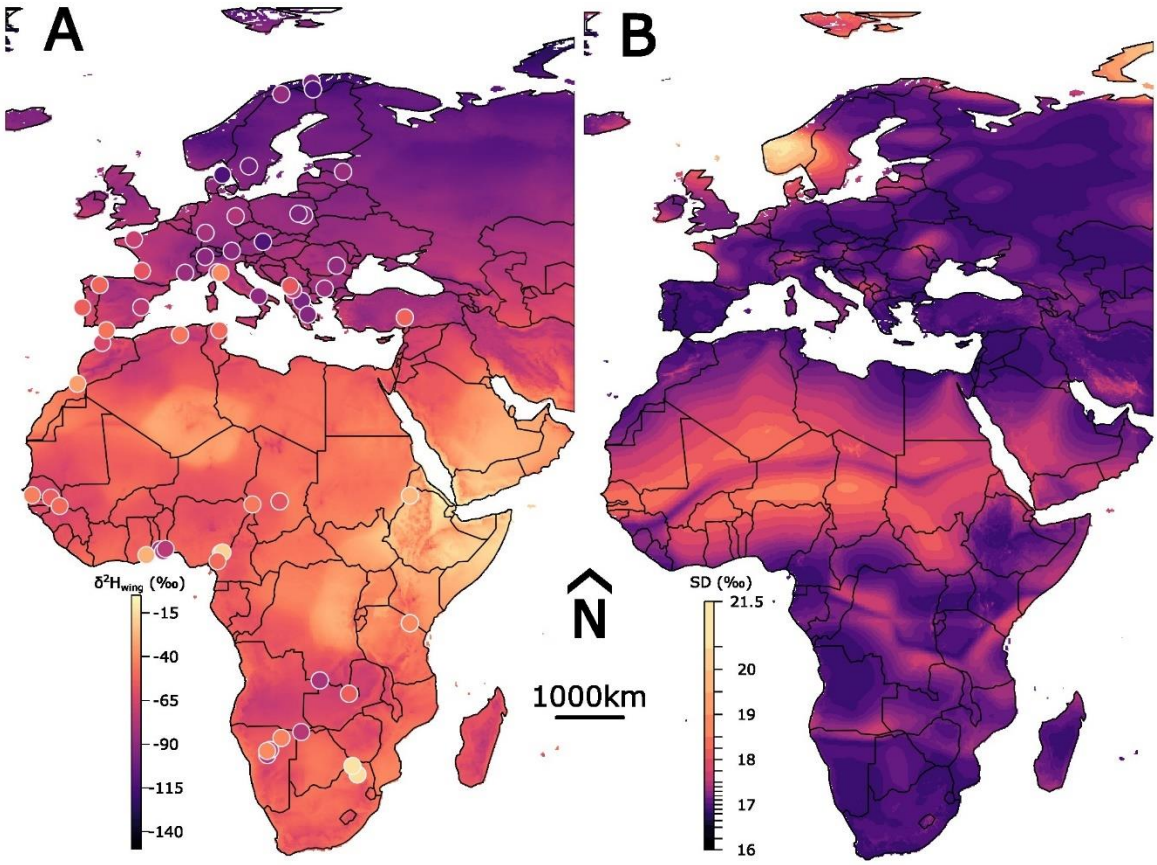

Figure 1.3. δ^2H_{wing} isoscape across the Afro-Palearctic range. A. Mean δ^2H_{wing} values with the location and mean δ^2H_{wing} values (43 sites). The isoscape was calibrated using the δ^2H_{GSP} from Bowen, Wassenaar & Hobson (2005) and the linear regression equation as shown in Fig. 1.2 using the *assignR* package. B. Standard-deviation of the δ^2H_{wing} values. Colorscale break points were selected to improve visualization and increase the contrast of the variations. Shapefile boundaries for figures A. and B. were obtained from the *rnaturalearth* package.

1.3.2 Factors of hydrogen isoscape uncertainty

1.3.2.1 Intra-site δ^2H_{wing} variance

The intra-site standard deviation did not exhibit spatial autocorrelation (Moran's I = −0.1; p = 0.34). Among the tested climatic and environmental variables, and after accounting for collinearity, only two variables, relative humidity (t-statistics; p-value=0.09) and mean EVI (t-statistics; p-value=0.03) of the month preceding the capture date were identified as significant predictors of intra-site δ^2H_{wing} variance at p-value=0.1 (Fig. 1.4 and R Script 1). The resulting

multivariate linear model explained only 12% of the total intra-site variance. Sites with lower relative humidity had higher intra-site δ^2H_{wing} variance (Fig. 1.4a and R Script 1). Sites with lower EVI had higher intra-site δ^2H_{wing} variance (Fig. 1.4 and R Script 1).

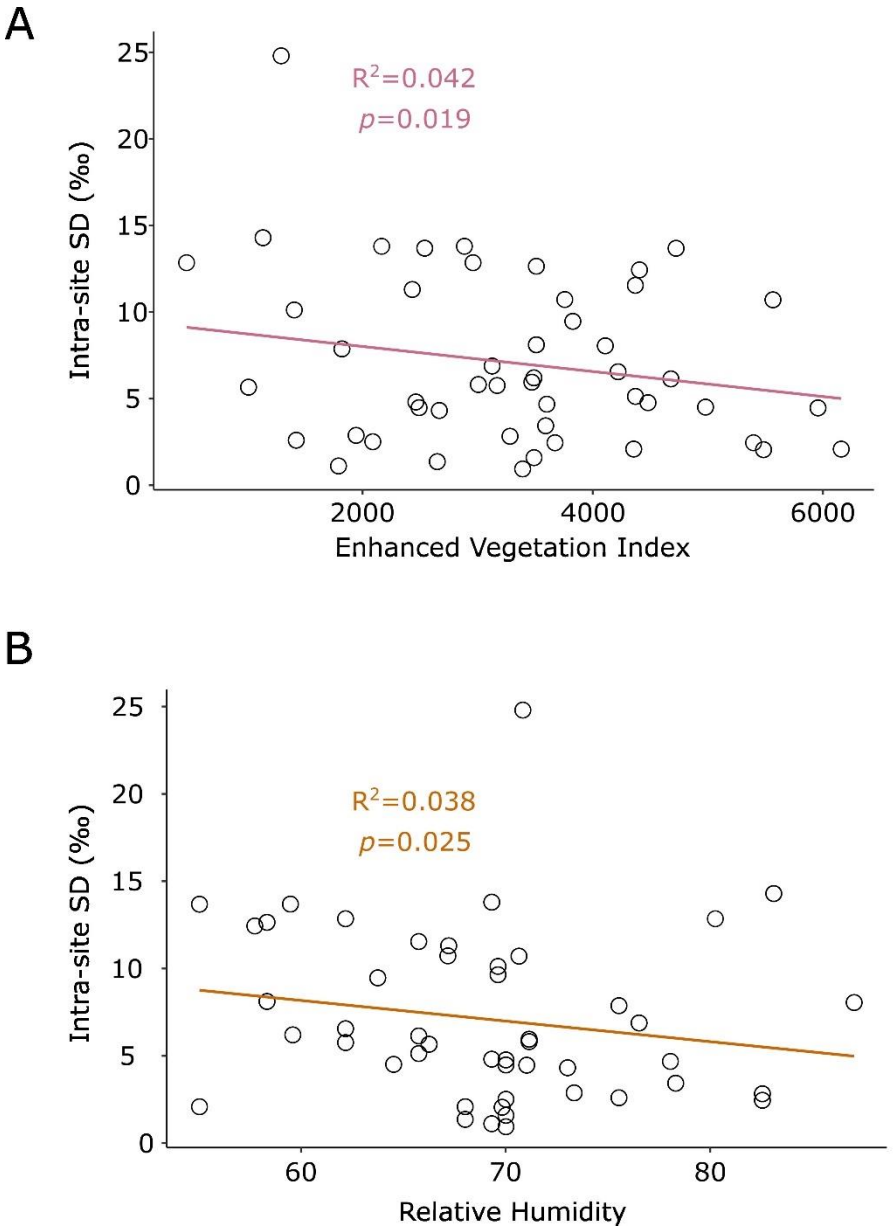

Figure 1.4. Controls of intra-site δ^2H_{wing} variance. Linear regression between intra-site δ^2H_{wing} standard deviation (‰) and A. enhanced vegetation index (EVI) mean value for the month preceding sampling, B. relative humidity mean value for the month preceding sampling. Both are calculated as the mean values within a 1 km buffer around the sampling site. Note that the r^2 and p-values of these monovariate linear regression are illustrative and differ from those discussed in the text and that originates from the multivariate linear regression model which account for multicolinearity.

1.3.2.2 Model residuals from the δ^2H wing-precipitation relationship

The model residuals did not exhibit spatial autocorrelation (Moran's I = −0.04; p = 0.66). After accounting for collinearity and pseudo-replication of samples collected at the same site, we fit a multivariate linear mixed model (with site as a random effect) to predict residuals. Significant predictors included the number of wet days of the month preceding sampling, vapor pressure of the month preceding sampling, relative humidity anomaly of the month preceding sampling and elevation. Sites with lower wet days and lower relative humidity anomalies (i.e, where negative relative humidity anomalies corresponds to dryer conditions than usual) had higher negative model residuals (Fig. 1.5), while sites with higher elevation were associated with higher more positive model residuals (Fig. 1.5 and R Script 1). The interaction between predictors demonstrated that the fixed effect explains 41.3% of the total residual variance. The relative humidity anomaly of the month preceding sampling was a significant predictor only when associated with the number of wet days preceding sampling. After accounting for both the fixed effects and the random effects, the remaining unexplained variation in the δ^2H_{wing} was 8.6‰.

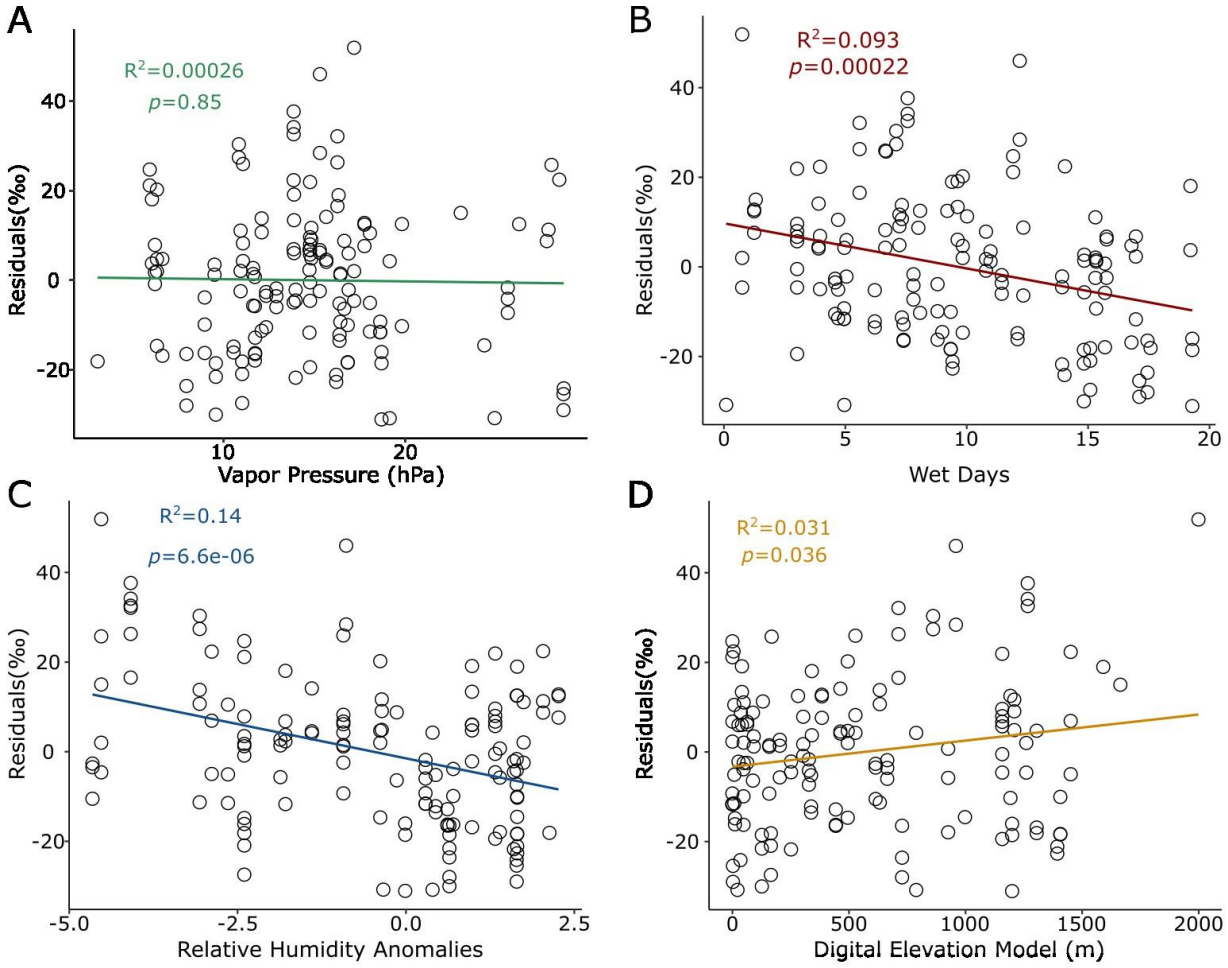

Figure 1.5. Controls of δ^2H_{wing} model residuals. Linear regression between δ^2H_{wing} model residuals (‰) and A. vapor pressure (hPa) of the month preceding sampling. B. wet days (precipitation > 0.01 mm) count per month from the month preceding sampling. C. relative humidity anomalies from the month prior to sampling with humidity anomaly, defined as a deviation from expected values in relative humidity from a multi-year averaged dataset. D. the minimum elevation (m) of the sample site within a buffer area of 1 km. Note that the r^2 and p-values of these monovariate linear regressions are only illustrative and differ from those discussed in the text and that originates from the multivariate linear mixed model which account for multicolinearity and pseudoreplication.

1.3.2.3 Multivariate linear mixed model predicting δ^2H_{wing} values

After accounting for collinearity and pseudo-replication of sample collected at the same site, we fit a multivariate linear mixed model (with site as a random effect) to predict δ^2H_{wing} values. Significant predictors included δ^2H_{GSP} values (t-statistics; p-value=$6.7x10^{-12}$) (Fig. 1.2), vapor pressure of the month preceding sampling (t-statistics; p-value=0.05), relative humidity

anomaly of the month preceding sampling (t-statistics; p-value=0.001) and elevation (t-statistics; p-value=0.04). The fixed effects explained close to 58% of the variance (vs. 48% when using only δ^2H_{GSP} values as predictor in the same mixed model). δ^2H_{wing} values were positively correlated with δ^2H_{GSP} values, vapor pressure of the month preceding sampling and elevation and negatively correlated with relative humidity anomaly (Fig. 1.6). An increase in vapor pressure during the month preceding sampling was found to be positively correlated with the δ^2H_{wing} values (Fig. 1.6a). Elevation was also found to have a positive association with the δ^2H_{wing} values (Fig. 1.6d). Number of wet days and the relative humidity anomaly of the month preceding sampling are negatively correlated with δ^2H_{wing} values (Fig. 1.6b and 1.6c).

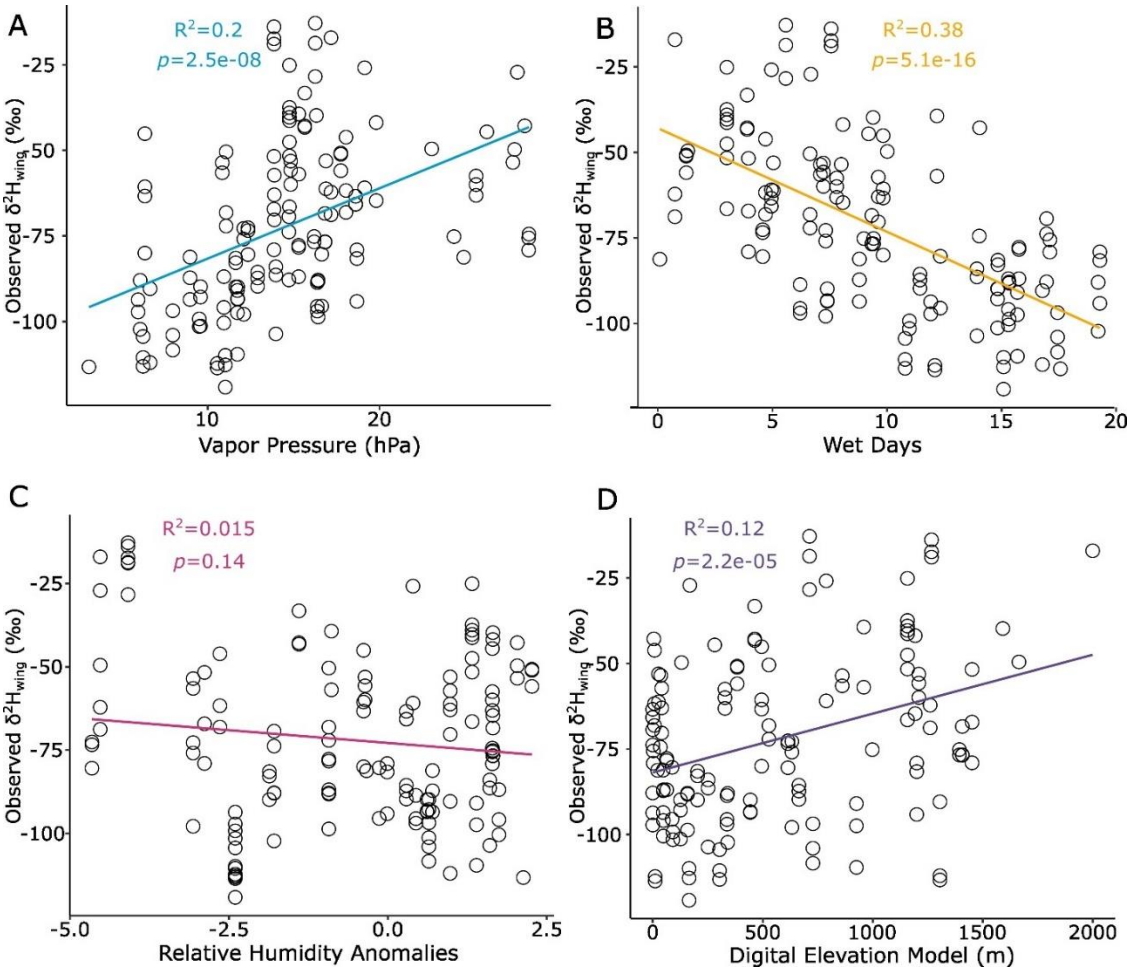

Figure 1.6. Model predictors of δ^2H_{wing} values. Linear regression between observed δ^2H_{wing} (‰) and A. vapor pressure (hPa). B. number of wet days (precipitation > 0.01 mm) count per month from the month preceding sampling. C. relative humidity anomalies from the month prior to sampling with humidity anomaly, defined as a deviation from expected values in relative humidity from a multi-year averaged dataset. D. the minimum elevation (m) of the sample site in a buffer area of 1 km. Note that the r^2 and p-values of these monovariate linear regressions are only illustrative and differ from those discussed in the text and that originates from the multivariate linear mixed model which account for multicolinearity and pseudoreplication.

1.4 Discussion

1.4.1 Known-origin dataset and hydrogen isoscape

1.4.1.1 Isoscape for the whole Afro-tropics Palearctic range

Our results confirm a strong positive relationship between δ^2H_{wing} values and δ^2H_{GSP} values at known-origin sites across the Afro-Palearctic range ($\delta^2H_{wing}= -39.80 + 0.80$ x δ^2H_{GSP}, $r^2=0.53$, n=142). This work represents the first large-scale effort to sample known-origin insects across the whole Afro-Palearctic range and to incorporate samples from the Afro-tropics improving the accuracy of the transfer function equation between known-origin δ^2H_{wing} and precipitation δ^2H isoscape (Contina et al., 2022). This dataset is also the first to analyze δ^2H_{wing} values for tropical climate increasing the coverage of existing known-origin insect δ^2H_{wing} datasets from boreal and temperate regions including United Kingdom and Ireland (Newton, 2021), Europe (Brattström et al., 2010), New Zealand and Australia (Holder et al., 2014), China (Qin and Shi, 2020) and North America (Hobson et al., 2019, 2012b). To date, the primary isoscape used to track migratory insects for the Afro-Palearctic range (Stefanescu et al., 2017; Talavera et al., 2018) was based on the known-origin dataset obtained from a few sampling sites in Europe (Brattström et al., 2010). This dataset had a limited geographic distribution and relied on a single species collected within a narrow time period. The calibration line obtained from this dataset was not appropriate for Africa and could have led to overestimation of up-to 40‰ in that region which is close to the whole range of δ^2H_{wing} across Europe (Fig. 1.2). The known-origin dataset collected in this study incorporates a multi-species collection over a broad temporal range making it more applicable to trace lepidopteran migratory insects across the entire Afro-Palearctic range. Despite the heterogeneous nature of the known-origin dataset collected in this study, the relationship between tissue and precipitation remains strong (Fig. 1.2). The resulting isoscape shows gradients in δ^2H values between the Palearctic realms and the Afro-tropic realms (Fig. 1.3) and will allow geographic assignments of migratory insect individuals moving North-South between these distant regions. The isoscape would also be applicable to trace the one-way dispersal and population connectivity of invasive insect pests (Dargent et al., 2023).

The average uncertainty (17.3‰) obtained from the calibrated δ^2H_{wing} isoscape is higher than previous δ^2H_{wing} isoscapes (i.e., Hobson et al. (2019): 8.4‰; Brattström et al. (2010): 7.9‰).

This higher uncertainty can be explained by the large temporal range of our sampling covering 12 years and different seasons and the incorporation of multiple species. This is quite different from the known-origin datasets of Hobson et al. (2019) and Brattström et al. (2010) which use a single species, year and season to produce their calibration. While we attempted to minimize this uncertainty by sampling closely related species, sampling from different months certainly introduces variance in the δ^2H_{wing} values as evidenced by the 20‰ amplitude observed for Red Admiral butterflies (*Vanessa atalanta*) at the same site for different sampling months (Brattström et al., 2010). In our case, the time of sampling follows the plant growing season across the range and the expected spatiotemporal distribution of an insect migratory cycle from the Afro-tropics to Europe during the winter and spring and from Europe to the Afro-tropics during the summer and fall. The sampling also covers multiple years, and therefore temporal variance likely contributes to a significant portion of the observed residuals. Using multiple species of butterflies as done in our sampling strategy might also contribute to additional δ^2H_{wing} variance due to distinct larval diet (e.g., trees vs. ephemeral plants), length of larval development or larval habitats (e.g., wetlands vs. drylands). While this isoscape has a higher uncertainty than those constructed using known-origin dataset with a single species and a single season, it is more broadly applicable to multiple herbivorous lepidopteran insect species across the whole Afro-Palearctic range and across annual multi-generational migratory cycle.

1.4.1.2 Isoscape for the Palearctic

When using only known-origin samples from the Palearctic the transfer function equation (δ^2H_{wing}= –42.80+0.79 x δ^2H_{GSP}, r^2=0.39, n=80) differs from those found in similar temperate regions in North America (δ^2H_{wing} = –55.32 +0.76 x δ^2H_{GSP}, r^2=0.68, n=150) (Hobson et al., 2019) and Europe (δ^2H_{wing} = 30.08+1.73 x, r^2=0.74, n=179) (Brattström et al., 2010). Similarly, the mean uncertainty of 14.6‰ is less than that of the isoscape across the whole Afro-Palearctic range but more than the uncertainty found in previous studies for similar regions (8.4‰, Hobson et al., (2019); 7.9‰, Brattström et al., (2010)). The slope of the equation from our European known-origin dataset is similar to that of Hobson et al. (2019) but the intercept and uncertainty are higher which would lead to distinct and less specific geographic assignments. The equation found in this study differs drastically from Brattström et al. (2010). While the predicted δ^2H_{wing} values are relatively similar in the boreal realm they diverge rapidly when moving south (Fig.

1.2). Brattström et al. (2010) equation is based on seven sites in Sweden but only one site on the Island of Capri (Italy) for the Mediterranean realm. The known-origin dataset collected in our study covers the Palearctic realm extensively including multiple sample sites from Mediterranean regions at different time of the year. Considering the scarcity of Mediterranean samples in Brattström et al. (2010), the different transfer functions are not totally surprising as simulation exercises performed by Contina et al. (2022) showed that lack of sampling of isotope extremes of the range could lead to large difference in calibration lines. The newly developed isoscape is therefore better calibrated across the Palearctic but will also have a higher uncertainty leading to less specific geographic assignments. This new isoscape could be useful to trace regional dispersal or migration of insects across the western Palearctic, including both bidirectional migration and one-way dispersive behavior. For example, the isoscape would be applicable to trace forest pest dispersal of moths within European forests (e.g., Bras et al., 2019; Chapman et al., 2012; Muñoz-Adalia and Colinas, 2020). It would also be applicable to trace north-south migration routes and connectivity between Mediterranean, temperate and boreal realms (e.g., Chapman et al., 2015; Hawkes et al., 2022).

1.4.1.3 Isoscape for the Afro-tropics

When considering only known-origin samples from the Afrotropics realm, the correlation between the δ^2H_{wing} values and δ^2H_{GSP} values is very weak ($\delta^2H_{wing} = -44.14+0.46 \times \delta^2H_{GSP}$, $r^2=0.07$, n=60). The resulting isoscape displays very high average uncertainty 19.6‰ and limited spatial variations (Fig. 1.3) limiting its usefulness for provenance within the Afro-tropics. This finding is in-line with other known-origin dataset of birds collected across the Afro-tropics and other tropical regions which showed high δ^2H_{wing} variability but limited correlation with δ^2H_{GSP} (Gutiérrez-Expósito et al., 2015; Hobson et al., 2012c; Seifert et al., 2018). δ^2H_{GSP} values display a limited range across the Afro-tropics. The lack of correlation with δ^2H_{GSP} values in the Afro-tropics likely arise from distinct seasonality and climate regimes, different length and season of the larval stage in different sections of the range, differences in species and hydrophysiology of host plants, systematic variations in the heterogeneity of water sources in different regions, and distinct mechanisms for the cycling of water between precipitation and larvae (Brattström et al., 2010; Hobson, 2008; Magozzi et al., 2020). It is well-known that tropical climates differ fundamentally from temperate climates with stochastic inter-annual (e.g., drought vs. wet years)

and intra-annual variations (wet and dry season) that may lead to large deviations of annual or seasonal δ^2H values in precipitation from long-term averaged isotopic values in precipitation (Vander Zanden et al., 2014). The use of the δ^2H_{GSP} isoscape as the reference model (where the GSP is defined as all the months with an average temperature above 0°C) is probably not ideal for tropical regions. Tropical climates have temperature above 0°C all year long but plants only grow during the wet season. Rainfall patterns and vegetation growth in many regions of Africa are highly seasonal with varying timing and duration of the wet season across the continent. However, using month-specific precipitation isoscapes associated with the month or the month preceding sampling did not improve the strength of the transfer function (Fig. S1.7). This observation suggests that a significant portion of the residual variance in the wing-precipitation relationship in the Afro-tropics is associated with the limited accuracy of the growing season precipitation isoscape in these regions (Bowen et al., 2005). There are only 44 GNIP (Global Network of Isotopes in Precipitation) stations, and these are not evenly distributed across the continent compared to other regions in the world (Bowen et al., 2005; Gutiérrez-Expósito et al., 2015; Kaseke et al., 2016). Global precipitation isoscapes are known to have limited predictive power in the tropics (Reichlin et al., 2013; Seifert et al., 2018). There are often obvious mismatches between observed δ^2H values and predicted δ^2H values in precipitation when precipitation isoscapes are downscaled in data deficient regions such as Africa, Asia or South America (Kaseke et al., 2016).

Considering the high uncertainty of the isoscape across the Afro-tropics, hydrogen isotopes will not provide specific geographic assignments in this region relative to the Palearctic or other regions with stronger relationship with δ^2H_{GSP}. Other complementary isotopes such as sulfur and strontium isotopes with potentially large variations in Africa (Bataille et al., 2020; Brlík et al., 2022; Janzen et al., 2020) could help improve resolution of geographic assignments in future ecological studies (Crowley et al., 2021; Hobson et al., 2012c; Reich et al., 2021). Beyond this, improving the specificity of hydrogen as a provenance tracer across the Afro-tropics would require a considerable decrease of the uncertainty of the isoscapes. As a first step in this direction, we investigated the controls of δ^2H_{wing} isoscape uncertainty.

1.4.2 Controls of hydrogen isoscape uncertainty and future improvements

1.4.2.1 Intra-site variance

In our study, we quantified intra-site variance by collecting at least three individuals per known-origin site and found an average standard deviation of 7.1‰ with large spatial disparities. Some of this intra-site variance might be due to slight difference in geographic origin of the collected specimen. While the specimens were collected at the same location at their adult stage, their site of larval development might have been different. However, most of the sampled species were non-migratory and had narrow home range (<5 km). These individuals were therefore unlikely to have moved long distances. Considering that climate and environmental statistics at buffer of 1 and 5 km showed similar relationships, local microclimate heterogeneity or adult mobility are unlikely to be dominant controls of this intra-site standard deviation. To better understand the underlying controls of this intra-site variance, we tested its relationship with climatic and environmental variables. We identified two significant predictors of intra-site variance including EVI and relative humidity of the month preceding sampling but the resulting model only explained 15% of the total variance (Fig. 1.4). EVI is a direct measure of the biophysical characteristics of land surfaces related to vegetation structure, composition, distribution and diversity of different taxa with high EVI reflecting healthy and dense vegetation and low EVI reflecting sparse, unhealthy and water stress vegetation (Tuanmu and Jetz, 2015). The negative correlation of intra-site δ^2H_{wing} variance with EVI suggests that isotopic variations are greater in local populations living in habitats less favorable to plant growth (i.e., dryer climates). Similarly, the negative correlation of intra-site variance and relative humidity of the month prior to sampling is likely a function of the higher evaporation rate occurring in low relative humidity conditions. When evaporation and its associated fractionation increase, then the likelihood of observing more variable δ^2H values increase (Telmet and Veizer, 2001). The remaining intra-site variance is likely associated with analytical uncertainty, with climate heterogeneity and with the inherent variability of biological samples (Magozzi et al., 2020). Isotopic data from known-origin samples commonly show high levels of variation even among conspecific individuals living at a common site (Magozzi et al., 2020). Those variations are likely due to slight differences related to different dietary choices, or distinct conditions of synthesis (Magozzi et al., 2019). This high intra-site δ^2H_{wing} variance of close to 8‰ provides a

minimal uncertainty limit of hydrogen δ^2H_{wing} isoscape that limits the potential of hydrogen isotopes for insect provenance applications.

1.4.2.2 Residuals in tissue-precipitation relationship

We found that vapor pressure, wet days count, and relative humidity anomaly (Fig. 1.5) explain a large part of the wing-precipitation model residual variance. More positive δ^2H_{wing} residuals (i.e., modeled δ^2H_{wing} values underestimate observed δ^2H_{wing} values) are generally associated with fewer wet days (Fig. 1.5b), lower vapor pressure (Fig. 1.5a), and more negative relative humidity anomalies in the month preceding sampling (Fig. 1.5c). Those variables indicate more arid and dryer conditions for the month preceding sampling. In those climatic conditions, evaporation rates are likely higher than usual and lead to strong evaporation losses between precipitation and soil water, soil water and plant, and plant and insect leading to incrementally fractionated hydrogen with more evaporation losses (Bowen et al., 2019). Consequently, specimens collected after dry months are more likely to have higher δ^2H_{wing} values reflecting the higher cumulative evaporation losses. Besides fractionation associated with evaporation losses, more wet days in the month preceding sampling could lead to more Rayleigh fractionation rainout effect leading rainfall to become more depleted in heavy isotopes than typical precipitation (Hollins et al., 2018). Therefore, if the sampling of known-origin butterflies occurs after a wetter month than usual, then it is possible that local precipitation for that month is more depleted in heavy isotopes than usual, which would explain the more negative residuals with more wet days (Fig. 1.5c).

More positive δ^2H_{wing} residuals were also observed in sites with higher elevation (Fig. 1.5d). We suggest that more positive residuals at higher altitudes are caused by faster evaporation rate at higher altitudes due to lower atmospheric pressure and more windy conditions in those environments (Smith and Donahue, 1991). The δ^2H_{GSP} values only consider precipitation processes and do not account for subsequent isotopic fractionation occurring in soils, plants and insect tissues. As a result, higher evaporation rates at higher altitudes will lead to soil water and plant water to be more enriched in heavy isotopes relative to precipitation and this signal will be transmitted to the insect wing growing in those regions. Conversely, at lower elevation, surface water might preferentially come from higher elevation zones with lower δ^2H values potentially explaining the negative residuals in those regions (Bedaso and Wu, 2021). Another alternative

hypothesis is that the modeled δ^2H_{GSP} have systematic biases associated with altitude particularly across regions with a very low density of GNIP stations like Africa. West et al., (2014) reported that δ^2H_{GSP} values were lower than those observed in precipitation and groundwater across South Africa. The inaccuracy of the δ^2H_{GSP} predictions is propagated to the predicted δ^2H_{wing} values explaining the positive residuals in those high elevation regions. The potential inaccuracies of the precipitation isoscape in high elevation regions underlines the need to improve the density of monitoring isotopic stations in those hydrologically complex regions.

Together those climatic and environmental variables explained the majority of the residuals. However, the intra-site variance remained high and difficult to explained as evidenced by both the high average intra-site standard deviation 7.1‰ and the high random effect of this mixed model of 9.2‰ per site. This result demonstrates that, when removing for intra-site variance, the majority of the residual variance can be explained by the environmental and climatic conditions at the sampling site. Depending on the ecological application, a potential solution to improve the specificity of δ^2H geolocation for insect migration in the Afro-tropics is to incorporate high-resolution monthly climatic and environmental data in the modeling framework to limit the influence of year-specific variability in δ^2H variations in precipitation and plant (Vander Zanden et al., 2014). However, the strong positive correlation between residuals and observed δ^2H_{wing} values (Fig. 1.5a) demonstrates that other systematic controls of δ^2H_{wing} variations have not yet been identified.

1.4.2.3 Implications for building insect isoscapes

This work produced a robust and broadly applicable isoscape to trace the dispersal of herbivorous lepidopterans across the Afro-Palearctic range, with a focus on butterflies. This isoscape will be useful to studies that are focused on tracing the long-distance migration or one-way dispersal of insect species at the trans-continental scale. For example, the distinct δ^2H_{wing} of the Afrotropics and Palearctic realms allows identifying trans-continental migrants between these regions. This isoscape, developed using multiple species collected at different times, is also useful to monitor the origin of individuals across a multi-generational migratory cycle where specific locations might gather multiple arrivals of migrants through time. However, this work also underlined the high uncertainty of the isoscape resulting from this broad sampling strategy and the application to distinct species and time should be approached with caution. When

sampling across multiple months and years, most of Africa display similar δ^2H_{wing} values and hydrogen isotopes would not be sufficient to infer regional origin of individuals dispersing throughout this realm. To enhance the specificity of geographic assignments in regions with similar δ^2H_{wing}, other isotopes such as strontium (Crowley et al., 2021; Reich et al., 2021) and sulfur isotopes (Bataille et al., 2021; Brlík et al., 2022) could be combined with hydrogen. The geology of Africa is very heterogeneous, and, on average, very old, leading to a large spread of strontium isotope ratios (Bataille et al., 2020; Janzen et al., 2020). In addition, sulfur isotope variations display strong east–west and coast-to-inland isotopic gradients across the Afro-tropics complementing hydrogen isotopes in geographic assignments (Brlík et al., 2022).

Another potential solution to improve the specificity of geographic assignments derived from hydrogen isotopes would be to develop species- and time-specific isoscapes. If the research question focuses on the dispersal of individuals from a given species at a given season and year (Dargent et al., 2023), then it should be possible to recalibrate the relationship between δ^2H_{wing} and δ^2H in precipitation. Using year-specific and/or monthly precipitation isoscapes instead of averaged precipitation surfaces, might help produce time-specific isoscapes that are more representative of the species and its period of larval growth (Vander Zanden et al., 2014). This is especially relevant in areas with stochastic inter-annual (e.g., drought vs. wet years) and intra-annual (e.g., seasonality in precipitation, high relative humidity vs. low relative humidity) climate variations which may produce large deviations between δ^2H in precipitation during the larval growth stage and the long-term averaged isotopic values (Vander Zanden et al., 2014). However, in regions with high evaporation rates, multiple episodes of isotopic fractionations might occur between precipitation and incorporation of hydrogen into the insect wing, blurring the relationship between δ^2H in precipitation and the insect wing. In this setting, leveraging high resolution spatiotemporal environmental and climatic data of the month preceding sampling could be an efficient approach to recalibrate proper tissue-specific isoscapes while accounting for both stochastic inter-annual (e.g., drought vs. wet years) and intra-annual (e.g., seasonality in precipitation, high relative humidity vs. low relative humidity) variations of δ^2H precipitation and post-precipitation fractionation processes. Using our known-origin dataset, we showed that with a mixed model incorporating δ^2H_{GSP} values, the number of wet days, the relative humidity anomaly and the mean vapor pressure of the month preceding sampling and elevation, we could

predict δ^2H_{wing} values with a much higher accuracy than with δ^2H_{GSP} values alone (Fig. 1.6). While we could not apply this model spatially because our known-origin sample set was sampled across multiple months and years, it demonstrates the possibility to improve tissue-specific isoscape accuracy. This type of time-specific isoscape would have a much lower spatial uncertainty than those produced using multi-year and multi-species calibration data (e.g., Hobson et al., 2019) and should help improve proveniencing in the Afro-tropics. However, these isoscapes can only be used to investigate the target species at the calibrated period and range (Contina et al., 2022) or they will produce biased or over-confident interpretations.

1.5 Conclusion

We have presented a novel tissue-specific butterfly wing hydrogen isoscape for the Afro-Palearctic region that can be used to investigate the connectivity and multigenerational migration cycle of terrestrial herbivorous insect populations. We demonstrated that while this isoscape has a large uncertainty, it is likely a conservative estimate of uncertainty when using it as a baseline for broad scale insect migratory cycle studies. By investigating the sources of uncertainty, we showed that climatic conditions for the month preceding sampling as well as elevation heterogeneity influenced the model uncertainty. In specific studies with well-constrained species and season, high resolution spatiotemporal climatic data can be leveraged to improve δ^2H_{wing} isoscapes.

Our isoscape should provide a well-calibrated baseline with appropriate uncertainty quantification for species focusing on lepidopteran species. However, as the isoscape was calibrated on closely related butterfly species feeding on non-vascular plants, it would be important to verify the validity of the isoscape on other lepidopteran species with distinct larval behavior such as those species feeding on vascular plants. Our study underlines some of the key intrinsic limitations of using hydrogen isotopes as an insect geolocation tool particularly in tropical regions where predicted δ^2H_{wing} are uncertain. In those regions, coupling hydrogen with other isotope systems such as strontium and sulfur will be essential to enhance geolocation specificity.

1.6 References

Alquezar, R., Costa, F.J. V, Sena-Souza, J.P., Nardoto, G.B., Hobson, K.A., 2022. A feather hydrogen (δ 2 H) isoscape for Brazil. PLoS One 1–19. https://doi.org/10.1371/journal.pone.0271573

Bataille, C.P., Crowley, B.E., Wooller, M.J., Bowen, G.J., 2020. Advances in global bioavailable strontium isoscapes. Palaeogeogr. Palaeoclimatol. Palaeoecol. 555, 109849. https://doi.org/10.1016/j.palaeo.2020.109849

Bataille, C.P., Jaouen, K., Milano, S., Trost, M., Steinbrenner, S., Crubézy, É., Colleter, R., 2021. Triple sulfur-oxygen-strontium isotopes probabilistic geographic assignment of archaeological remains using a novel sulfur isoscape of western Europe. PLoS One 16, 1–21. https://doi.org/10.1371/journal.pone.0250383

Bates, D., Mächler, M., Bolker, B.M., Walker, S.C., 2015. Fitting linear mixed-effects models using lme4. J. Stat. Softw. 67. https://doi.org/10.18637/jss.v067.i01

Bedaso, Z., Wu, S.Y., 2021. Linking precipitation and groundwater isotopes in Ethiopia - Implications from local meteoric water lines and isoscapes. J. Hydrol. 596, 126074. https://doi.org/10.1016/j.jhydrol.2021.126074

Borisov, S.N., Iakovlev, I.K., Borisov, A.S., Ganin, M.Y., Tiunov, A. V., 2020. Seasonal migrations of pantala flavescens (Odonata: Libellulidae) in middle asia and understanding of the migration model in the afro-asian region using stable isotopes of hydrogen. Insects 11, 1–12. https://doi.org/10.3390/insects11120890

Bowen, G.., 2023. The Online Isotopes in Precipitation Calculator, version 3.1 [WWW Document]. URL https://wateriso.utah.edu/waterisotopes/pages/data_access/oipc.html (accessed 8.9.23).

Bowen, G.J., Cai, Z., Fiorella, R.P., Putman, A.L., 2019. Isotopes in the water cycle: Regional- to global-scale patterns and applications. Annu. Rev. Earth Planet. Sci. 47, 453–479. https://doi.org/10.1146/annurev-earth-053018-060220

Bowen, G.J., Revenaugh, J., 2003. Interpolating the isotopic composition of modern meteoric precipitation. Water Resour. Res. 39, 1–13. https://doi.org/10.1029/2003WR002086

Bowen, G.J., Wassenaar, L.I., Hobson, K.A., 2005. Global application of stable hydrogen and oxygen isotopes to wildlife forensics. Oecologia 143, 337–348. https://doi.org/10.1007/s00442-004-1813-y

Bowen, G.J., West, J.B., 2008. Isotope Landscapes for Terrestrial Migration Research. Terr. Ecol. 2, 79–105. https://doi.org/10.1016/S1936-7961(07)00004-8

Bras, A., Avtzis, D.N., Kenis, M., Li, H., Vétek, G., Bernard, A., Courtin, C., Rousselet, J., Roques, A., Auger-Rozenberg, M.A., 2019. A complex invasion story underlies the fast spread of the invasive box tree moth (Cydalima perspectalis) across Europe. J. Pest Sci. (2004). 92, 1187–1202. https://doi.org/10.1007/s10340-019-01111-x

Brattström, O., Bensch, S., Wassenaar, L.I., Hobson, K.A., Åkesson, S., 2010. Understanding the migration ecology of European red admirals Vanessa atalanta using stable hydrogen isotopes. Ecography (Cop.). 33, 720–729. https://doi.org/10.1111/j.1600-0587.2009.05748.x

Brlík, V., Procházka, P., Hansson, B., Stricker, C.A., Yohannes, E., Powell, R.L., Wunder, M.B., 2022. Animal tracing with sulfur isotopes: Spatial segregation and climate variability in Africa likely contribute to population trends of a migratory songbird. J. Anim. Ecol. https://doi.org/10.1111/1365-2656.13848

Bugoni, L., McGill, R.A.R., Furness, R.W., 2008. Effects of preservation methods on stable isotope signatures in bird tissues. Rapid Commun. Mass Spectrom. 22, 2457–2462. https://doi.org/10.1002/rcm.3633

Chapman, J.W., Bell, J.R., Burgin, L.E., Reynolds, D.R., Pettersson, L.B., Hill, J.K., Bonsall, M.B., Thomas, J.A., 2012. Seasonal migration to high latitudes results in major reproductive

benefits in an insect. Proc. Natl. Acad. Sci. U. S. A. 109, 14924–14929. https://doi.org/10.1073/pnas.1207255109

Chapman, J.W., Reynolds, D.R., Wilson, K., 2015. Long-range seasonal migration in insects: Mechanisms, evolutionary drivers and ecological consequences. Ecol. Lett. 18, 287–302. https://doi.org/10.1111/ele.12407

Clem, C.S., Hobson, K.A., Harmon-Threatt, A.N., 2022. Do Nearctic hover flies (Diptera: Syrphidae) engage in long-distance migration? An assessment of evidence and mechanisms. Ecol. Monogr. 92, 1–20. https://doi.org/10.1002/ecm.1542

Contina, A., Magozzi, S., Vander Zanden, H.B., Bowen, G.J., Wunder, M.B., 2022. Optimizing stable isotope sampling design in terrestrial movement ecology research. Methods Ecol. Evol. 13, 1237–1249. https://doi.org/10.1111/2041-210X.13840

Coplen, T.B., 2011. Guidelines and recommended terms for expression of stable-isotope-ratio and gas-ratio measurement results. Rapid Commun. Mass Spectrom. 25, 2538–2560. https://doi.org/10.1002/rcm.5129

Coplen, T.B., Qi, H., 2016. A revision in hydrogen isotopic composition of USGS42 and USGS43 human-hair stable isotopic reference materials for forensic science. Forensic Sci. Int. 266, 222–225. https://doi.org/10.1016/j.forsciint.2016.05.029

Crowley, B.E., Bataille, C.P., Haak, B.A., Sommer, K.M., 2021. Identifying nesting grounds for juvenile migratory birds with dual isotope: an initial test using North American raptors. Ecosphere 12. https://doi.org/10.1002/ecs2.3765

Dargent, F., Candau, J.-N., Studens, K., Perrault, K.H., Reich, M.S., Bataille, C.P., 2023. Characterizing eastern spruce budworm's large-scale dispersal events through flight behavior and stable isotope analyses. Front. Ecol. Evol. 11, 1–14. https://doi.org/10.3389/fevo.2023.1060982

Didan, K., 2015. MOD13C2 MODIS/Terra Vegetation Indices Monthly L3 Global 0.05Deg CMG V006 [WWW Document]. https://doi.org/10.5067/MODIS/MOD13C2.006

Ehleringer, J.R., Bowen, G.J., Chesson, L.A., West, A.G., Podlesak, D.W., Cerling, T.E., 2008. Hydrogen and oxygen isotope ratios in human hair are related to geography. Proc. Natl. Acad. Sci. U. S. A. 105, 2788–2793. https://doi.org/10.1073/pnas.0712228105

Feng, X., Porporato, A., Rodriguez-Iturbe, I., 2013. Changes in rainfall seasonality in the tropics. Nat. Clim. Chang. 3, 811–815. https://doi.org/10.1038/nclimate1907

Flockhart, D.T., Wassenaar, L.I., Martin, T.G., Hobson, K.A., Wunder, M.B., Norris, D.R., 2013. Tracking multi-generational colonization of the breeding grounds by monarch butterflies in eastern North America. Proc. R. Soc. B Biol. Sci. 280. https://doi.org/10.1098/rspb.2013.1087

Flockhart, T.T., Brower, L.P., Ramirez, M.I., Hobson, K.A., Wassenaar, L.I., Altizer, S., Norris, D.R., 2017. Regional climate on the breeding grounds predicts variation in the natal origin of monarch butterflies overwintering in Mexico over 38 years. Glob. Chang. Biol. 23, 2565–2576. https://doi.org/10.1111/gcb.13589

Fraser, I., Meier-Augenstein, W., Kalin, R.M., 2008. Stable isotope analysis of human hair and nail samples: The effects of storage on samples. J. Forensic Sci. 53, 95–99. https://doi.org/10.1111/j.1556-4029.2007.00607.x

García-Berro, A., Talla, V., Vila, R., Wai, H.K., Shipilina, D., Chan, K.G., Pierce, N.E., Backström, N., Talavera, G., 2023. Migratory behaviour is positively associated with genetic diversity in butterflies. Mol. Ecol. 32, 560–574. https://doi.org/10.1111/mec.16770

Gutiérrez-Expósito, C., Ramírez, F., Afán, I., Forero, M.G., Hobson, K.A., 2015. Toward a deuterium feather isoscape for sub-saharan Africa: Progress, challenges and the path ahead. PLoS One 10, 1–12. https://doi.org/10.1371/journal.pone.0135938

Hallworth, M.T., Marra, P.P., McFarland, K.P., Zahendra, S., Studds, C.E., 2018. Tracking dragons: Stable isotopes reveal the annual cycle of a long-distance migratory insect. Biol. Lett. 14. https://doi.org/10.1098/rsbl.2018.0741

Harris, I., Osborn, T.J., Jones, P., Lister, D., 2020. Version 4 of the CRU TS monthly high-resolution gridded multivariate climate dataset. Sci. Data 7, 1–18. https://doi.org/10.1038/s41597-020-0453-3

Hawkes, W.L.S., Walliker, E., Gao, B., Forster, O., Lacey, K., Doyle, T., Massy, R., Roberts, N.W., Reynolds, D.R., Özden, Ö., Chapman, J.W., Wotton, K.R., 2022. Huge spring migrations of insects from the Middle East to Europe: quantifying the migratory assemblage and ecosystem services. Ecography (Cop.). 2022, 1–15. https://doi.org/10.1111/ecog.06288

Hersbach, H., Bell, B., Berrisford, P., Hirahara, S., Horányi, A., Muñoz-Sabater, J., Nicolas, J., Peubey, C., Radu, R., Schepers, D., Simmons, A., Soci, C., Abdalla, S., Abellan, X., Balsamo, G., Bechtold, P., Biavati, G., Bidlot, J., Bonavita, M., De Chiara, G., Dahlgren, P., Dee, D., Diamantakis, M., Dragani, R., Flemming, J., Forbes, R., Fuentes, M., Geer, A., Haimberger, L., Healy, S., Hogan, R.J., Hólm, E., Janisková, M., Keeley, S., Laloyaux, P., Lopez, P., Lupu, C., Radnoti, G., de Rosnay, P., Rozum, I., Vamborg, F., Villaume, S., Thépaut, J.N., 2020. The ERA5 global reanalysis. Q. J. R. Meteorol. Soc. 146, 1999–2049. https://doi.org/10.1002/qj.3803

Hobson, K.A., 2008. Applying Isotopic Methods to Tracking Animal Movements. Terr. Ecol. https://doi.org/10.1016/S1936-7961(07)00003-6

Hobson, K.A., Anderson, R.C., Soto, D.X., Wassenaar, L.I., 2012a. Isotopic Evidence That Dragonflies (Pantala flavescens) Migrating through the Maldives Come from the Northern Indian Subcontinent. PLoS One 7, 9–12. https://doi.org/10.1371/journal.pone.0052594

Hobson, K.A., Barnett-Johnson, R., Cerling, T., 2010. Using isoscapes to track animal migration. Isoscapes Underst. movement, pattern, Process Earth through Isot. Mapp. 273–298. https://doi.org/10.1007/978-90-481-3354-3_13

Hobson, K.A., Doward, K., Kardynal, K.J., Mcneil, J.N., 2018. Inferring origins of migrating insects using isoscapes: a case study using the true armyworm, Mythimna unipuncta, in North America. Ecol. Entomol. 43, 332–341. https://doi.org/10.1111/een.12505

Hobson, K.A., Kardynal, K.J., Koehler, G., 2019. Expanding the isotopic toolbox to track monarch butterfly (Danaus plexippus) origins and migration: On the utility of stable oxygen isotope (δ18O) measurements. Front. Ecol. Evol. 7, 1–8. https://doi.org/10.3389/fevo.2019.00224

Hobson, K.A., Kusack, J.W., Mora-Alvarez, B.X., 2021. Origins of six species of butterflies migrating through northeastern mexico: New insights from stable isotope (δ2h) analyses and a call for documenting butterfly migrations. Diversity 13, 1–13. https://doi.org/10.3390/d13030102

Hobson, K.A., Soto, D.X., Paulson, D.R., Wassenaar, L.I., Matthews, J.H., 2012b. A dragonfly (δ2h) isoscape for North America: A new tool for determining natal origins of migratory aquatic emergent insects. Methods Ecol. Evol. 3, 766–772. https://doi.org/10.1111/j.2041-210X.2012.00202.x

Hobson, K.A., Van Wilgenburg, S.L., Wassenaar, L.I., Powell, R.L., Still, C.J., Craine, J.M., 2012c. A multi-isotope (δ 13 C, δ 15 N, δ 2 H) feather isoscape to assign Afrotropical migrant birds to origins. Ecosphere 3, art44. https://doi.org/10.1890/es12-00018.1

Hobson, K.A., Wassenaar, L.I., Taylor, O.R., 1999. Stable isotopes (δD and δ13C) are geographic indicators of natal origins of monarch butterflies in eastern North America. Oecologia 120, 397–404. https://doi.org/10.1007/s004420050872

Holder, P.W., Armstrong, K., Van Hale, R., Millet, M.A., Frew, R., Clough, T.J., Baker, J.A., 2014. Isotopes and trace elements as natal origin markers of Helicoverpa armigera - An experimental model for biosecurity pests. PLoS One 9, 1–13. https://doi.org/10.1371/journal.pone.0092384

Hollins, S.E., Hughes, C.E., Crawford, J., Cendón, D.I., Meredith, K.M., 2018. Rainfall isotope variations over the Australian continent – Implications for hydrology and isoscape applications. Sci. Total Environ. 645, 630–645. https://doi.org/10.1016/j.scitotenv.2018.07.082

Hu, G., Lim, K.S., Horvitz, N., Clark, S.J., Reynolds, D.R., Sapir, N., Chapman, J.W., 2016. Mass seasonal bioflows of high-flying insect migrants. Science (80-.). 354, 1584–1587. https://doi.org/10.1126/science.aah4379

Janzen, A., Bataille, C., Copeland, S.R., Quinn, R.L., Ambrose, S.H., Reed, D., Hamilton, M., Grimes, V., Richards, M.P., le Roux, P., Roberts, P., 2020. Spatial variation in bioavailable strontium isotope ratios (87Sr/86Sr) in Kenya and northern Tanzania: Implications for ecology, paleoanthropology, and archaeology. Palaeogeogr. Palaeoclimatol. Palaeoecol. 560, 109957. https://doi.org/10.1016/j.palaeo.2020.109957

Kaseke, K.F., Wang, L., Wanke, H., Turewicz, V., Koeniger, P., 2016. An analysis of precipitation isotope distributions across Namibia using historical data. PLoS One 11, 1–19. https://doi.org/10.1371/journal.pone.0154598

Komsta, L., 2022. Package "outliers": Tests for Outliers.

Lindroos, E.E., Bataille, C.P., Holder, P.W., Talavera, G., Reich, M.S., 2023. Temporal stability of δ2H in insect tissues: Implications for isotope-based geographic assignments. Front. Ecol. Evol. 11, 1–12. https://doi.org/10.3389/fevo.2023.1060836

Ma, C., Vander Zanden, H.B., Wunder, M.B., Bowen, G.J., 2020. assignR: An r package for isotope-based geographic assignment. Methods Ecol. Evol. 11, 996–1001. https://doi.org/10.1111/2041-210X.13426

Magozzi, S., Vander Zanden, H.B., Wunder, M.B., Bowen, G.J., 2019. Mechanistic model predicts tissue–environment relationships and trophic shifts in animal hydrogen and oxygen isotope ratios. Oecologia 191, 777–789. https://doi.org/10.1007/s00442-019-04532-8

Magozzi, S., Vander Zanden, H.B., Wunder, M.B., Trueman, C.N., Pinney, K., Peers, D., Dennison, P.E., Horns, J.J., Şekercioğlu, Ç.H., Bowen, G.J., 2020. Combining Models of Environment, Behavior, and Physiology to Predict Tissue Hydrogen and Oxygen Isotope Variance Among Individual Terrestrial Animals. Front. Ecol. Evol. 8, 1–17. https://doi.org/10.3389/fevo.2020.536109

Marx, M., Schumm, Y.R., Kardynal, K.J., Hobson, K.A., Rocha, G., Zehtindjiev, P., Bakaloudis, D., Metzger, B., Cecere, J.G., Spina, F., Cianchetti-Benedetti, M., Frahnert, S., Voigt, C.C., Lormée, H., Eraud, C., Quillfeldt, P., 2022. Feather stable isotopes (δ^{2}Hf and δ^{13}Cf) identify the Sub-Saharan wintering grounds of turtle doves from Europe. Eur. J. Wildl. Res. 68. https://doi.org/10.1007/s10344-022-01567-w

Muñoz-Adalia, E.J., Colinas, C., 2020. The invasive moth Paysandisia archon in Europe: Biology and control options. J. Appl. Entomol. 144, 341–350. https://doi.org/10.1111/jen.12746

Naimi, B., Hamm, N.A.S., Groen, T.A., Skidmore, A.K., Toxopeus, A.G., 2014. Where is positional uncertainty a problem for species distribution modelling? Ecography (Cop.). 37, 191–203. https://doi.org/10.1111/j.1600-0587.2013.00205.x

NASA JPL, 2020. NASADEM Merged DEM Global 1 arc second V001 | NASA Open Data Portal [WWW Document]. URL https://data.nasa.gov/dataset/NASADEM-Merged-DEM-Global-1-arc-second-V001/dqg3-mwid/data (accessed 5.3.23).

Newton, J., 2021. An insect isoscape of UK and Ireland. Rapid Commun. Mass Spectrom. 35, 1–8. https://doi.org/10.1002/rcm.9126

Qin, Z., Shi, J., 2020. Feasibility of species origin traceability by hydrogen stable isotopes: Sample case of lymantria dispar l. (lepidoptera: Erebidae). Forests 11, 1–10. https://doi.org/10.3390/f11111209

Quinby, B.M., Creighton, J.C., Flaherty, E.A., 2020. Stable isotope ecology in insects: a review. Ecol. Entomol. 45, 1231–1246. https://doi.org/10.1111/een.12934

R Core Team, 2023. R: A Language and Environment for Statistical Computing [WWW Document]. URL https://www.r-project.org/ (accessed 5.6.23).

RDocumentation, 2009. Cook’s Distances function - RDocumentation [WWW Document]. URL https://www.rdocumentation.org/packages/car/versions/1.2-16/topics/Cook’s Distances (accessed 5.27.23).

Reich, M.S., Flockhart, D.T.T., Norris, D.R., Hu, L., Bataille, C.P., 2021. Continuous-surface geographic assignment of migratory animals using strontium isotopes: A case study with monarch butterflies. Methods Ecol. Evol. 2021, 1–13. https://doi.org/10.1111/2041-210X.13707

Reichlin, T.S., Hobson, K.A., Van Wilgenburg, S.L., Schaub, M., Wassenaar, L.I., Martín-Vivaldi, M., Arlettaz, R., Jenni, L., 2013. Conservation through connectivity: Can isotopic gradients in Africa reveal winter quarters of a migratory bird? Oecologia 171, 591–600. https://doi.org/10.1007/s00442-012-2418-5

Rubenstein, D.R., Hobson, K.A., 2004. From birds to butterflies: Animal movement patterns and stable isotopes. Trends Ecol. Evol. 19, 256–263. https://doi.org/10.1016/j.tree.2004.03.017

Satterfield, D.A., Sillett, T.S., Chapman, J.W., Altizer, S., Marra, P.P., 2020. Seasonal insect migrations: massive, influential, and overlooked. Front. Ecol. Environ. 18, 335–344. https://doi.org/10.1002/fee.2217

Seifert, N., Ambrosini, R., Bontempo, L., Camin, F., Liechti, F., Rubolini, D., Scandolara, C., Saino, N., Hahn, S., 2018. Matching geographical assignment by stable isotopes with African non-breeding sites of barn swallows Hirundo rustica tracked by geolocation. PLoS One 13, 1–16. https://doi.org/10.1371/journal.pone.0202025

Smith, W.K., Donahue, R.A., 1991. Simulated influence of altitude on photosynthetic CO2 uptake potential in plants. Plant. Cell Environ. 14, 133–136. https://doi.org/10.1111/j.1365-3040.1991.tb01380.x

Soto, D.X., Koehler, G., Wassenaar, L.I., Hobson, K.A., 2017. Re-evaluation of the hydrogen stable isotopic composition of keratin calibration standards for wildlife and forensic science applications. Rapid Commun. Mass Spectrom. 31, 1193–1203. https://doi.org/10.1002/rcm.7893

Stefanescu, C., Páramo, F., Åkesson, S., Alarcón, M., Ávila, A., Brereton, T., Carnicer, J., Cassar, L.F., Fox, R., Heliölä, J., Hill, J.K., Hirneisen, N., Kjellén, N., Kühn, E., Kuussaari, M., Leskinen, M., Liechti, F., Musche, M., Regan, E.C., Reynolds, D.R., Roy, D.B., Ryrholm, N., Schmaljohann, H., Settele, J., Thomas, C.D., van Swaay, C., Chapman, J.W., 2013. Multi-

generational long-distance migration of insects: Studying the painted lady butterfly in the Western Palaearctic. Ecography (Cop.). 36, 474–486. https://doi.org/10.1111/j.1600-0587.2012.07738.x

Stefanescu, C., Puig-Montserrat, X., Samraoui, B., Izquierdo, R., Ubach, A., Arrizabalaga, A., 2017. Back to Africa: autumn migration of the painted lady butterfly Vanessa cardui is timed to coincide with an increase in resource availability. Ecol. Entomol. 42, 737–747. https://doi.org/10.1111/een.12442

Stefanescu, C., Soto, D.X., Talavera, G., Vila, R., Hobson, K.A., 2016. Long-distance autumn migration across the Sahara by painted lady butterflies: Exploiting resource pulses in the tropical savannah. Biol. Lett. 12, 6–9. https://doi.org/10.1098/rsbl.2016.0561

Suchan, T., Talavera, G., Sáez, L., Ronikier, M., Vila, R., 2019. Pollen metabarcoding as a tool for tracking long-distance insect migrations. Mol. Ecol. Resour. 19, 149–162. https://doi.org/10.1111/1755-0998.12948

Talavera, G., Bataille, C., Benyamini, D., Gascoigne-Pees, M., Vila, R., 2018. Round-trip across the Sahara: Afrotropical Painted Lady butterflies recolonize the Mediterranean in early spring. Biol. Lett. 14. https://doi.org/10.1098/rsbl.2018.0274

Talavera, G., García-Berro, A., N K Talla, V., Bahleman, F., Kébé, K., 2023. The Afrotropical breeding grounds of the Palearctic-African migratory painted lady butterflies (Vanessa cardui). Proc. Natl. Acad. Sci. 120, 10. https://doi.org/10.1073/pnas

Telmet, K., Veizer, J., 2001. Erratum: Isotopic constraints on the transpiration, evaporation, energy, and gross primary production budgets of a large boreal watershed: Ottawa River Basin, Canada" (Global Biogeochemical Cycles). Global Biogeochem. Cycles 15, 1035–1036. https://doi.org/10.1029/2001GB001820

Terzer, S., Wassenaar, L.I., Araguás-Araguás, L.J., Aggarwal, P.K., 2013. Global isoscapes for δ18O and δ2H in precipitation: Improved prediction using regionalized climatic regression models. Hydrol. Earth Syst. Sci. 17, 4713–4728. https://doi.org/10.5194/hess-17-4713-2013

Torniainen, J., Mikonranta, L., 2018. The origins of northern European Autographa gamma individuals evaluated using hydrogen stable isotopes. Ecol. Entomol. 43, 699–702. https://doi.org/10.1111/een.12635

Tuanmu, M.N., Jetz, W., 2015. A global, remote sensing-based characterization of terrestrial habitat heterogeneity for biodiversity and ecosystem modelling. Glob. Ecol. Biogeogr. 24, 1329–1339. https://doi.org/10.1111/geb.12365

Vander Zanden, H.B., Wunder, M.B., Hobson, K.A., Van Wilgenburg, S.L., Wassenaar, L.I., Welker, J.M., Bowen, G.J., 2014. Contrasting assignment of migratory organisms to geographic origins using long-term versus year-specific precipitation isotope maps. Methods Ecol. Evol. 5, 891–900. https://doi.org/10.1111/2041-210X.12229

Vickery, J.A., Mallord, J.W., Adams, W.M., Beresford, A.E., Both, C., Cresswell, W., Diop, N., Ewing, S.R., Gregory, R.D., Morrison, C.A., Sanderson, F.J., Thorup, K., Van Wijk, R.E., Hewson, C.M., 2023. The conservation of Afro-Palaearctic migrants: What we are learning and what we need to know? Ibis (Lond. 1859). https://doi.org/10.1111/ibi.13171

Wassenaar, L.I., Hobson, K.A., 2003. Comparative equilibration and online technique for determination of non-exchangeable hydrogen of keratins for use in animal migration studies. Isotopes Environ. Health Stud. 39, 211–217. https://doi.org/10.1080/1025601031000096781

Wassenaar, L.I., Hobson, K.A., 1998. Natal origins of migratory monarch butterflies at wintering colonies in Mexico: New isotopic evidence. Proc. Natl. Acad. Sci. U. S. A. 95, 15436–15439. https://doi.org/10.1073/pnas.95.26.15436

West, A.G., February, E.C., Bowen, G.J., 2014. Spatial analysis of hydrogen and oxygen stable isotopes (“isoscapes”) in ground water and tap water across South Africa. J. Geochemical Explor. 145, 213–222. https://doi.org/10.1016/j.gexplo.2014.06.009

Wunder, M.B., Kester, C.L., Knopf, F.L., Rye, R.O., 2005. A test of geographic assignment using isotope tracers in feathers of known origin. Oecologia 144, 607–617. https://doi.org/10.1007/s00442-005-0071-y

Yamanaka, T., Makino, Y., Wakiyama, Y., Kishi, K., Maruyama, K., Kano, M., Ma, W., Suzuki, K., 2015. How reliable are modeled precipitation isoscapes over a high-relief mountainous region? Hydrol. Res. Lett. 9, 118–124. https://doi.org/10.3178/hrl.9.118

Zeng, J., Liu, Y., Zhang, H., Liu, J., Jiang, Y., Wyckhuys, K.A.G., Wu, K., 2020. Global warming modifies long-distance migration of an agricultural insect pest. J. Pest Sci. (2004). 93, 569–581. https://doi.org/10.1007/s10340-019-01187-5

Zomer, R.J., Xu, J., Trabucco, A., 2022. Version 3 of the Global Aridity Index and Potential Evapotranspiration Database. Sci. Data 9, 1–15. https://doi.org/10.1038/s41597-022-01493-1

Chapter 2: Trans-Saharan migratory patterns in *Vanessa cardui*: evidence for moderate migratory connectivity and a southward leapfrog migration

In preparation for *iScience*

Authors: Megan S. Reich[1]*, Sana Ghouri[1]*, Gerard Talavera[2], Samantha Zabudsky[3], Lihai Hu[3], Daria Shipilina[4], Roger Vila[5], Dino J. Martins[6], Steve C. Collins[7], Ivy Ng'iru[8], Clément Bataille[1,3]

[1]Department of Biology, University of Ottawa, Ontario, Canada

[2]Institut Botànic de Barcelona (IBB), CSIC-Ajuntament de Barcelona, Barcelona, 08038 Catalonia, Spain

[3]Department of Earth and Environmental Sciences, University of Ottawa, Ontario, Canada

[4] Department of Ecology and Genetics, Program of Evolutionary Biology, Uppsala University, Uppsala, Sweden

[5]Institut de Biologia Evolutiva, CSIC-UPF, Barcelona, 08003 Catalonia, Spain

[6]Institut Botànic de Barcelona, Consejo Superior de Investigaciones Científicas and Ajuntament de Barcelona, Barcelona, Catalonia 08038, Spain

[7]African Butterfly Research Institute, Nairobi, Kenya

[8]Mpala Research Centre, Nanyuki 555-10400, Kenya

Author Contributions

Megan S. Reich: Conceptualization; Isotope analysis, Data analysis, Data interpretation, Writing - original draft

Sana Ghouri: Modeling of strontium isoscape, Isotope analysis, Writing – strontium isoscape and supplementary material, Writing - review & editing

Gerard Talavera: Conceptualization, Resources, Writing - review & editing, Supervision

Samantha Zabudsky: Isotope analysis

Lihai Hu: Isotope analysis

Daria Shipilina, Roger Vila, Dino J. Martins, Steve C. Collins & Ivy Ng'iru: Resources

Clément Bataille: Conceptualization, Modeling of strontium isoscape, Writing – review & editing, Supervision

2.0 Summary

Some insects, such as the painted lady butterfly *Vanessa cardui*, exhibit complex annual migration cycles spanning multiple generations, often transversing inhospitable habitat like seas and deserts. Understanding insect migratory connectivity and patterns across barriers is essential for characterizing population dynamics and predicting the impacts of global change on insect-mediated ecosystem services. Here, we use isotope geolocation, combining hydrogen and strontium isotopes, to estimate the natal origin of painted ladies captured north and south of the Sahara during spring and autumn. Our findings reveal moderate migratory connectivity characterized by a broad front, parallel migration across the Sahara. We also report evidence of a leapfrog migration in painted lady butterflies, wherein early autumn migrants from higher latitudes cover greater distances southward than their late autumn counterparts. This work represents a major advancement in our understanding of insect migration patterns, especially in the eastern Sahara, where empirical studies have been scarce.

2.1 Introduction

Multigenerational migrations equip insects with the capacity to swiftly respond to seasonal environmental changes, yet this very trait also renders them vulnerable to certain challenges. Unlike migratory vertebrates, which typically complete round-trip migrations between overwintering and breeding grounds within a single generation, insects have shorter lifespans and require several generations to complete their annual migration cycle, with each generation completing a single segment of the overall cycle (Chapman et al., 2015). The spatial extent of suitable climatic and biotic conditions, largely determined by host plant availability, can change drastically throughout the year, prompting each generation to embark on naïve migratory journeys in search of suitable habitat (Chowdhury et al., 2021). However, many individual insects do not survive the journey, while others conclude their journeys in unsuitable habitats that cannot sustain the next generation, potentially leading to local extirpation or population bottlenecks. Fortunately, the suitable habitat of migratory insects tends to be broad, with reticular migratory patterns that provide redundancy and compensate for the impact of local bottlenecks (García-Berro et al., 2023). While these reticular patterns are generally thought to enhance the resilience of populations to environmental perturbation (Gao et al., 2020; Gilroy et al., 2016),

global climate change and habitat degradation are large-scale changes influencing the population dynamics and migratory patterns of some migratory species. For example, the monarch butterfly *Danaus plexippus* population in North America seems to be declining, with changing spring weather conditions playing an important role in the decline (Zylstra et al., 2021). Similarly, outbreaks of desert locust *Schistocerca gregaria* are influenced by the increasing frequency of extreme weather events (Salih et al., 2020), and changes to monsoon patterns are affecting the migration patterns of the brown planthopper *Nilaparvata lugens*, a devastating agricultural pest (Lv et al., 2023). Delineating predictable spatiotemporal linkages of insects across their migratory range is an imperative first-step for predicting insect population dynamics and understanding how they will respond to global change.

Understanding migratory patterns and connectivity across natural barriers, such as seas and deserts, may be particularly important for insect population dynamics. Migratory journeys across barriers can be especially perilous and large-scale losses can lead to population bottlenecks (Klaassen et al., 2014; Lok et al., 2015). The Sahara is the world's third-largest desert and, for the migratory animals that traverse it, it constitutes at least a thousand kilometer journey through unsuitable habitat. The migratory connectivity of many bird species in the Palearctic-Afrotropical migration system has been well-explored (e.g., Fattorini et al., 2023; Guilherme et al., 2023). In general, birds seem to migrate in relatively straight trajectories across the Sahara along seasonally-changing, but distinctive, flyways (e.g., Åkesson et al., 2016; Jiguet et al., 2019). These studies gave scientists the baseline information needed to detect that many of these bird species are facing population declines and propose international conservation action (Jiguet et al., 2019b; Marcacci et al., 2023; Sanderson et al., 2006; Vickery et al., 2014), thus illustrating that understanding migratory connectivity across biogeographic barriers and geopolitical borders is important. In general, insect migration remains understudied compared to research on migratory birds and mammals (Satterfield et al., 2020). While there are growing indications that many insect species undertake trans-Saharan journeys, empirical evidence remains limited. The irregular migrations of a well-studied Saharan insect, the desert locust, tend to originate from recessive zones within the Sahara itself, rather than crossing it (Meynard et al., 2017; Pedgley et al., 1995). As a result, the annual migrations of the painted lady butterfly *Vanessa cardui* stand out as the primary example of trans-Saharan insect migration.

Over the past decade, regular seasonal migrations of the painted lady butterfly across the Sahara have been verified using a variety of techniques, including field observations, monitoring stations, isotope geolocation, ecological niche modeling, and pollen metabarcoding analysis (Menchetti et al., 2019; Stefanescu et al., 2016; Talavera et al., 2023, 2018; Talavera and Vila, 2017). The Afro-Palearctic population of painted lady butterflies undergoes an annual migratory cycle spanning 8 to 10 overlapping generations (Talavera and Vila, 2017). Painted lady adults live for about 3 to 6 weeks, mating multiple times during this period and laying up to over 1000 eggs that develop into adults over 23 to 45 days, depending on environmental conditions (Stefanescu et al., 2021, 2013; Talavera and Vila, 2017). Thus, the offspring of a single female can depart in several migratory waves, intermingling with older generations. These painted ladies migrate as far north as Scandinavia during the summer, travel south to regions on both sides of the Sahara for the European winter (i.e., North Africa and sub-Saharan Africa), and then return to Europe in the spring (Stefanescu et al., 2016; Talavera et al., 2023, 2018). This recurring migration across the Sahara offers a unique opportunity to study insect migratory connectivity between well-differentiated faunistic regions and across a natural barrier.

There are multiple reasons why insect migration is understudied. For one, the multi-generational migration cycle adds a layer of complexity to the study of insect migration, demanding investigation of each segment of the annual migration cycle. Moreover, understanding insect migratory patterns requires addressing both its spatial and temporal dimensions. Thus, large-scale collaborations are essential for investigating the international and intercontinental migrations of insects (e.g., Diffendorfer et al., 2023; Talavera et al., 2023). Another reason why insect migration is understudied is that insects are difficult to track with traditional techniques, like biologger technology (e.g., radiotelemetry, light loggers) because of their small size, large population sizes, and short lifespans. Instead, intrinsic biomarkers, such as isotopes, have become quintessential tools for studying insect migration. Local isotopic signatures are incorporated into developing tissues as the larval insect feeds (Hobson et al., 1999) and, after metamorphosis, these local isotopic signatures are largely preserved in the wings (Lindroos et al., 2023). Thus, the isotopic signature of a migrant butterfly's wing can be measured and compared to a spatial model of isotopic variation to estimate the individual butterfly's natal origin (i.e., isotope-based geographic assignment). Hydrogen isotope values (δ^2H) have been used for insect geolocation for over twenty years (Hobson et al., 1999; Wassenaar and Hobson, 1998) and, due

to global precipitation patterns, often act as a crude proxy for the latitude of origin (Bowen et al., 2005). However, δ^2H-based geographic assignment rarely provides adequate longitudinal resolution. Strontium isotope ratios ($^{87}Sr/^{86}Sr$) have recently been used for the geolocation of insects and have the potential to provide increased longitudinal resolution (Reich et al., 2021), showing that it is important to further develop technologies to advance our understanding of migratory insect population dynamics and multi-generational migratory connectivity.

Here, we investigate the spatiotemporal trans-Saharan migratory connectivity and patterns of the painted lady butterfly using δ^2H and $^{87}Sr/^{86}Sr$-based geographic assignment. Through a large, international collaboration led by the Painted Lady Migration Network, a global citizen science effort, 118 painted lady samples were opportunistically collected from many sites south and north of the Sahara and the Arabian Desert, an extension of the Sahara, so that the migratory patterns along the length of the geographic barriers could be compared. Applying dual δ^2H and $^{87}Sr/^{86}Sr$ for continuous-surface isotope-based geographic assignment requires a reliable spatial model of isotopic variation across the landscape (i.e., an isoscape). A new hydrogen isoscape was recently calibrated for butterfly wings for the Afro-Palearctic region (Ghouri et al., 2023), but a robust bioavailable strontium isoscape of this region did not exist. We compiled bioavailable $^{87}Sr/^{86}Sr$ data from the literature and completed this database with additional analysis of $^{87}Sr/^{86}Sr$ ratios in plants from 45 sites. We used this database and a spatial interpolation ensemble machine-learning framework to develop a $^{87}Sr/^{86}Sr$ isoscape across the study area. Using the isoscapes, we estimated the natal origin of the collected painted lady butterflies, then estimated migration distance and direction of travel. Those isotope-based metrics allowed us to discuss the connectivity and migratory patterns of painted ladies across the Sahara and Arabian Desert.

2.2 Methods

2.2.1 Painted lady sample collection

Two different waves of painted ladies are thought to cross the Sahara, the first migrating south in the autumn, and the second migrating north in the late winter and early spring (Stefanescu et al., 2016; Talavera et al., 2018; Talavera and Vila, 2017). However, painted ladies have overlapping generations and thus trans-Saharan migrants do not necessarily migrate at the

same time; instead, painted ladies seem to arrive on the far side of the Sahara over a period of weeks or months, the local-scale destinations of which vary between years (García-Berro et al., 2023). To investigate the migratory connectivity of painted lady butterflies, 118 samples were opportunistically collected from south and north of the Sahara from a range of dates to give us the best chance of collecting trans-Saharan migrants (Fig. 2.1).

2.2.2 Hydrogen isotope analysis

Of the 118 samples, the δ^2H of 69 samples have already been reported in the literature (Stefanescu et al., 2016; Talavera et al., 2018; Reich et al., *in prep*.). However, some of these samples were analyzed at the University of Utah and the Stable Isotope Hydrology and Ecology Laboratory of Environment Canada using older standard δ^2H values (ORX: -35.4‰; DS: -172.7‰ and KHS: -54.1‰; CBS: -197‰, respectively). To ensure that these measurements were compatible with the hydrogen isoscape (Ghouri et al., 2023), and with the other samples analyzed in this study, the δ^2H values were converted back to international standard scale, Vienna Standard Mean Ocean Water - Standard Light Antarctic Precipitation (VSMOW-SLAP), using the *reftrans* function in the *assignR* package in R (Ma et al., 2020; Magozzi et al., 2021).

The δ^2H values of the remaining 49 samples were measured at the Ján Veizer Stable Isotope Laboratory at the University of Ottawa, Canada. Prior to δ^2H analysis, a forewing from each butterfly was soaked, with agitation, in three successive baths (1h, 30min, 10min) of 2:1 chloroform: methanol solution to remove surficial dust and lipids, which are known to introduce error into δ^2H measurements (Hobson et al., 2017; Paritte and Kelly, 2009), then dried in the laboratory oven at 50°C for over 24 hours. Samples were cut, avoiding large wing veins, from the wing to reduce intra-individual variation from pigmentation (Hobson et al., 2017) and wing veins (Lindroos et al., 2023). Samples were then weighed (0.150mg ± mg) into silver capsules and loaded into a zero-blank autosampler (Thermo, Germany). All measurements were taken using high temperature (1400°C) flash pyrolysis (TCEA, Thermo Finnigan, Germany) with a helium carrier passed through a chromium-filled reactor and, after separation, introduced via a Conflow IV interface (Thermo Finnigan, Germany) into a Delta V Plus IRMS (Thermo Finnigan, Germany). Two different analytical methods were used. The first 25 samples were subjected to the equilibration approach with dual waters, following the methodology outlined in (Meier-

Augenstein et al., 2011). The more common non-exchangeable δ^2H values of the final 13 samples were determined using a comparative equilibrium approach described in Bataille et al. (2022). To maintain uniformity and ensure consistency across these analytical protocols, we selected 20 samples for duplicate analysis, using both protocols (comparative equilibrium and equilibration with dual waters). Through this comparative analysis, a calibration equation was developed between the two methods (Figure S2.8) and used to ensure all δ^2H values were on the same scale. All data are reported based on a three-point calibration using: CBS (caribou hoof; -157 ± 0.9‰; (Soto et al., 2017)), KHS (kudu horn; -35.3 ± 1.1‰; (Soto et al., 2017)), and USGS43 (human hair; -44.4 ± 2.0‰; (Coplen and Qi, 2016)). To assess the quality of the measurements, one keratin reference standard, USGS42 (human hair; measured: -75.3 ± 0.5‰, n=4; standard: -72.9 ± 2.2‰ (Coplen and Qi, 2016)), as well as two in-house chitin standards, ground and homogenised *Lymantria dispar dispar* L. (measured: -64.4 ± 1.8‰, n=6; long-term average: -64 ± 0.8‰) and Alfa Aesar chitin (measured: -22.8 ± 0.7‰, n=4; long-term average: -22 ± 1.2‰), were measured as internal standards. Based on within-run replicates of the internal standards and repeated sample measurements, precision of all measurements are estimated to be about ± 2‰. All reported δ^2H values are normalized to the VSMOW-SLAP standard scale.

2.2.3 Strontium isotope analysis

Of the 118 samples, the strontium isotope ratios ($^{87}Sr/^{86}Sr$) of 18 samples have already been reported in the literature (Reich et al., *in prep*.). The $^{87}Sr/^{86}Sr$ analyses for the remaining samples were performed in three analytical batches at different facilities. To prepare the first batch of 25 samples, a single forewing was washed in a 2:1 v/v chloroform:methanol solution in three successive washes, each lasting 1 hour, 30 minutes, and 5 minutes, respectively, to remove surficial dust. The wings were then digested at 120°C for 48 hours on a hot plate using a mixture of H_2O_2 and concentrated distilled nitric acid. The first batch was measured at the Queen's Facility for Isotope Research at Queen's University, Canada in January 2019 using a Neptune™ multi-collector inductively coupled plasma mass spectrometer (MC-ICP-MS; ThermoScientific, Bremen, Germany). The reproducibility of the $^{87}Sr/^{86}Sr$ measurement was 0.71020 ± 0.00006 (1 SD, n = 4) for 1 ppb NIST SRM987.

To prepare the second and third batch for $^{87}Sr/^{86}Sr$ analysis, a single forewing from each butterfly was cleaned using pressurized nitrogen gas for 2 min. at 10 psi to remove any surface contaminants (e.g., dust; (Reich et al., 2021)). The wings were then digested using microwave digestion (Anton Paar Multiwave 7000; Austria) in 1 mL concentrated nitric acid (16M; distilled TraceMetal™ Grade; Fisher Chemical, Canada). The separation of Sr was processed using a protocol, as described in Hu et al. (2020). The remaining steps, including temperature adjustment and duration, aliquot preparation, and analysis for Sr content via inductively coupled plasma mass spectrometry (ICP-MS; Agilent 8800 ICP-QQQ, Agilent Technologies Inc., CA, USA), were consistent with the procedures outlined in Reich et al. (2023). Calibration standards were prepared using single-element certified standards obtained from SCP Science (Montreal, Canada). After separation, eluates were dried and re-dissolved in 200 µL 2% v/v HNO_3 for $^{87}Sr/^{86}Sr$ analysis. The second batch (n = 17) was measured at GEOTOP-UQAM in Montreal, Canada in July 2021 with a Nu-Plasma II MC-ICP-MS (Nu Instruments) coupled to a desolvating nebulizer (Aridus II, CETAC Technologies). The reproducibility of the $^{87}Sr/^{86}Sr$ measurement was 0.71022 ± 0.00006 (n = 6) for 5 ppb NIST SRM987 and 0.71022 ± 0.00002 (n = 14) for 25 ppb NIST SRM987. An in-house pure Sr standard also had high reproducibility (0.70815 ± 0.00002, n = 4). The third batch (n = 85 plus the 18 samples presented in (Reich et al., *in prep*.) was measured at the Pacific Centre for Isotopic and Geochemical Research at the University of British Columbia, Canada in December 2021 using a Nu-Plasma II MC-ICP-MS (Nu Instruments) coupled to a desolvating nebulizer (Aridus II, CETAC Technologies). The reproducibility of the $^{87}Sr/^{86}Sr$ measurement for 5 ppb NIST SRM987 was 0.71025 ± 0.00009 (n = 138) and 0.71019 ± 0.00011 (n = 48) for 1.4 ppb NIST SRM987. A matrix-matched chitin internal standard, 5 ppb Alfa Aesar chitin, was also used (0.713959 ± 0.00009; n=3). Procedural blanks were negligible.

Instrumental mass fractionation was corrected by normalizing $^{86}Sr/^{88}Sr$ to 0.1194 using the exponential law (Moore et al., 1982). The isotopes ^{84}Sr, ^{86}Sr, and ^{87}Sr have isobaric interferences from ^{84}Kr, ^{86}Kr, and ^{87}Rb respectively, and, in all cases, were corrected for using the ^{85}Rb and ^{83}Kr signals.

2.2.4 Bioavailable strontium isoscape for the Afro-Palearctic

We compiled 8,755 bioavailable $^{87}Sr/^{86}Sr$ measurements from Europe, the Middle East, and Africa from 308 literature studies, and contributed an additional 45 new plant $^{87}Sr/^{86}Sr$ measurements from Africa (Table S2.1). We built upon the global compilation of Bataille et al. (2020) selecting samples from the Afro-Palearctic region in that initial database. Our updated compilation encompasses 35 more studies specific to the Afro-Palearctic range compared to Bataille et al. (2020), and we included a substantial 3,260 more samples from this same region than were present in the previous dataset by actively searching for recently published or unpublished studies with bioavailable $^{87}Sr/^{86}Sr$ ratios. While the coverage is greatly improved, the sampling density varies across the study area with a higher density of bioavailable $^{87}Sr/^{86}Sr$ data in Europe (Fig. S2.1). The compiled metadata are identical to Bataille et al. (2020) (Table S2.1). In the majority of cases, geographic coordinates were reported by the authors in the publication. When geographic coordinates were not included, we used Google Earth to georeferenced geographic information for each sample by using locality names and/or maps. The method of georeferencing and its associated uncertainty are reported in our metadata. When needed, authors were contacted for clarification purposes regarding sample locality. We converted all data to decimal degrees for consistency.

Using the compilation from the literature, we identified critical spatial data gaps within the Afro-Palearctic range and searched the digital collection of the *Institut Botànic de Barcelona* (IBB, CSIC) and identified plant samples with precise georeferencing, date of collection and taxa names that were located within the existing spatial data gaps in our study area (Table S2.2; Fig. S2.1). Sampling locations were selected to maximize geological variability over the study area. If possible, multiple samples were selected from each locality. We sampled ~1 g of each selected plant sample and cut them into small pieces. These samples were grouped into a total of 45 plant pools incorporating 2 to 5 plants based on their sample locations (Table S2.2). The majority of our plants are from the Asteraceae family with some exceptions from the Malvaceae and the Urticaceae families. The selected plants are from various taxa (mostly Asteracea family with some Malvacea and Urticacea) and were sampled in 12 countries from Africa between 2014 and 2021. We cleaned the plants to remove all surface mineral dust by placing the cut sample in

distilled deionized (DDI) water into the ultrasonic bath for 15 minutes. The plants were then rinsed another 2 times with DDI water and finally with ultrapure deionized H_2O (18.2 MΩ·cm @ 25 °C). Plants were then dried in the oven at 70 °C. We then digested those plants using microwave digestion, analyzed their Sr concentrations, isolated their Sr, and determined their $^{87}Sr/^{86}Sr$ ratios using preparation protocols and analytical approaches identical to those described for the painted ladies. All our plant samples underwent $^{87}Sr/^{86}Sr$ analysis at the Pacific Centre for Isotopic and Geochemical Research at the University of British Columbia, where a Nu-Plasma II high-resolution multi-collector inductively coupled plasma mass spectrometer (MC-ICP-MS; Nu Instruments) coupled to a desolvating nebulizer (Aridus IITM, CETAC Technologies) was employed.

2.2.4.1 Auxiliary variables for the regression models

We assembled a catalog of 28 environmental and climatic geospatial data known to influence bioavailable $^{87}Sr/^{86}Sr$ variation according to Capo et al. (1998) and Bataille et al. (2020). We used the same ensemble of variables as in Bataille et al. (2020) to represent geology, soil properties, relief, climate, and agricultural activity (Table S2.2). However, to better account for the different sources of atmospheric deposition that could impact bioavailable $^{87}Sr/^{86}Sr$ including volcanic ash (Serna et al., 2020), aerosols (Bataille et al., 2013) and anthropogenic deposition (Capo et al. 1998), we introduced new atmospheric deposition variables (Table S2). We reprojected and resampled each of the geospatial dataset (Table S2.2) into WGS84-Eckert IV at 1 km resolution. Using the sample locations from our $^{87}Sr/^{86}Sr$ metadata compilation, we extracted the local pixel values for each of these 28 tested predictors.

2.2.4.2 Machine-learning regressions

We first predicted bioavailable $^{87}Sr/^{86}Sr$ data across the Afro-Palearctic region using random forest regression (RF) through the *caret* package (Kuhn, 2008) using Bataille et al. (2020)'s framework. We used the *VSURF* package (Variable Selection Using Random Forest) to optimize and identify the most important predictors (Genuer et al., 2015) and predicted bioavailable $^{87}Sr/^{86}Sr$ across the Afro-Palearctic using the selected predictors (Fig. S2.3, S2.4 and S2.5). We used the results of RF regression as a benchmark to identify predictors and interpret mechanistic controls of bioavailable $^{87}Sr/^{86}Sr$ ratios across the study area. We then advanced the

modeling framework of bioavailable $^{87}Sr/^{86}Sr$ ratios by applying a novel spatial interpolation ensemble machine-learning regression (EML) approach through the *landmap* package (Hengl et al., 2021). One of the known issues with RF is the absence of consideration of spatial dependence structure in the data. Several approaches have been proposed to solve this issue including adding "geographical features" such as buffer or oblique distances (Hengl T et al, 2022) or combining multi-scale RF models (Georganos et al., 2021). Another issue with RF is that when applied by itself, it can produce biased results due to the inherent limitations of the algorithm. Bataille et al. (2020) demonstrated how RF produced overly confident predictions and extrapolation in data poor regions. The spatial EML approach resolves these known issues. The *landmap* package (Hengl et al., 2021) has solved many of those challenges. The *landmap* framework accounts for spatial dependency by incorporating buffer distances around each point as covariates in the regression while keeping computational needs limited by using oblique distances and PCA to summarize those spatial dependencies. The modeling framework further accounts for spatial dependencies by applying a spatial cross-validation approach to account for geographic sampling biases. Additionally, EML combines a series of machine-learning algorithms limiting the biases of using a single algorithm (i.e., RF) while improving performance and robustness of the model. When applying the spatial interpolation EML, we used the same training set and predictors selected in the RF regression. We used the default setting to make predictions where the meta-learner is generated from the linear model from five independently fitted learners including RF, optimized distributed gradient boosting, support vector machines, neural network and Lasso and Elastic-Net Regularized Generalised Linear Models. We also used the default output including the mean prediction which represents the best unbiased estimate of bioavailable $^{87}Sr/^{86}Sr$ ratios and the prediction errors obtained as the lower and upper 67% quantile (~1 standard deviation on the Gaussian distribution) implemented via the *forestError* package (Lu & Hardin, 2021). We compared the result of this EML model to the RF results to demonstrate the ability of this approach to improve accuracy, robustness, and unbiasedness (Fig. S2.5 and S2.6).

2.2.5 Isotope-based geographic assignment

The natal origin of each of the painted lady samples was estimated using continuous-surface isotope-based geographic assignment via the *assignR* package (Ma et al., 2020) in R v4.1.0 (R Core Team, 2023). First, a growing-season amount-weighted precipitation isoscape, sourced from waterisotope.org, using the OIPC v3.2 from Bowen et al. (2005), was calibrated to butterfly wing tissue using the linear relationship between precipitation and a calibration dataset of residential butterflies from across Europe and Africa (Ghouri et al., 2023), resulting in a wing chitin hydrogen isoscape (δ^2H_{wing}= –39.80 + 0.80 x δ^2H_{GSP}, R^2=0.53). The isotopic signature of each unknown-origin painted lady was then compared, using a normal probability density function, to the butterfly wing tissue hydrogen isoscape and the aforementioned bioavailable strontium isoscape to estimate the probability that each pixel of the isoscapes was the natal origin. The resulting posterior probability surfaces were summarized into binary surfaces using a 2:1 odds ratio, where the top third of the probability distribution was re-coded as highly probable (i.e., 1) and the remaining pixels were re-coded as low probability (i.e., 0). Next, we screened for butterflies that had a high probability of originating from their capture location or had a minimum distance of less than 100 km. These butterflies are either (1) local or regional butterflies that have developed in the capture area, or (2) migrants from a far-off location that has the same isotopic signature as the capture.

After filtering out the putative locals, the migratory trajectories of 66 migrants were assessed. Binary surfaces were summed, then normalized by the number of individuals, resulting in maps representing the proportion of individuals with a high probability of originating from each pixel. A conservative estimate of migration distance, minimum distance, was measured as the shortest distance from the capture location to the highly probable area of natal origin. Finally, a modification of the *wDist* function of the *assignR* package was used to estimate the direction that was traveled using a distance-weighted probability density function.

2.3 Results and Discussion

2.3.1 Strontium isotope geolocation enables new ecological insights

2.3.1.1 Novel strontium isotope compilation for the Afro-Palearctic range

We developed a new bioavailable strontium isoscape for the geolocation of *V. cardui* butterflies in the Afro-Palearctic. The new isoscape relies on a newly compiled bioavailable $^{87}Sr/^{86}Sr$ data across this region, and the addition of 45 new plant $^{87}Sr/^{86}Sr$ measurements from Africa. Together the dataset greatly improves the number of samples available for the African continent relative to Bataille et al. (2020) (n = 1820 vs n = 939). However, the compiled dataset still displays significant geographic biases with more samples in the Palearctic regions (n = 6980) relative to Africa (n = 1820) (Figure S2.1). The dataset displayed a wide range of $^{87}Sr/^{86}Sr$ ratios spanning from 0.70250 to 0.82636 with bioavailable $^{87}Sr/^{86}Sr$ ratios ranging between 0.70403 to 0.78848 in Africa.

2.3.1.2 Selected predictors of the machine-learning regression

Fourteen dominant predictors were identified to predict bioavailable $^{87}Sr/^{86}Sr$ across the Afro-Palearctic range (Fig. S2.2). Those predictors are similar to those selected in previous efforts to map bioavailable $^{87}Sr/^{86}Sr$ in other study areas (e.g., Bataille et al., 2020, 2018; Janzen et al., 2020; Kramer et al., 2022; Reich et al., 2021). As in many other regions, geological variables, including the age of the underlying terranes or geological units and the predicted bedrock $^{87}Sr/^{86}Sr$ dominate reflecting the influence of age and lithology (Bataille and Bowen, 2012), with younger and more mafic geological units transmitting lower ratios to ecosystems than older more felsic units (Fig. S2.4B, S2.4I). Soil properties, notably pH and clay content (Fig. S2.4F, S2.4H), show strong relationship with bioavailable $^{87}Sr/^{86}Sr$ with higher soil pH and lower clay content usually correspond with lower bioavailable $^{87}Sr/^{86}Sr$ ratios because more alkaline soils often reflect carbonate-dominated underlying bedrock with lower $^{87}Sr/^{86}Sr$ ratios (Capo et al., 1998). As expected for this desert-dominated region, the deposition of dust aerosols is an important contributor to bioavailable $^{87}Sr/^{86}Sr$ with higher dust inputs corresponding to high bioavailable $^{87}Sr/^{86}Sr$ (Bataille et al., 2020; Janzen et al., 2020). Higher sea salt aerosol deposition leads to bioavailable $^{87}Sr/^{86}Sr$ ratios to converge towards the seawater ratios of 0.7092

(Bataille et al., 2020). Interestingly, several of the newly incorporated atmospheric deposition variables were selected as important predictors of bioavailable $^{87}Sr/^{86}Sr$ (Fig. S2.3A) and reflect the key inputs of black carbon (Capo et al., 1998; Hartman and Richards, 2014) and volcanic ash (Serna et al., 2020) on soils.

2.3.1.3 Improved modeling approach to map bioavailable Sr across the Afro Palearctic range

The n-fold cross validation of the spatial interpolation ensemble machine learning (EML) demonstrated slightly superior performance to the typical random forest (RF) regression framework (Bataille et al., 2020, 2018) (RSME=0.0029; $R^2 = 0.74$ vs. RMSE=0.0031 and $R^2 = 0.73$). The EML isoscape is largely dominated by RF (highest absolute t-value < 2x10-16), but also relies on gradient boosting (t-value = 0.04), support vector machine (t-value = 0.02) and generalized linear model (t-value = 0.04). Overall, the use of multiple learners, leads to moderate performance improvements but enhances the robustness of the resulting model (Hengl et al., 2021). As expected from the dominance of RF in the EML predictions, the EML isoscape showed patterns very similar to the RF-based model with ratios ranging from 0.70366 to 0.77394 with the highest $^{87}Sr/^{86}Sr$ ratios in cratonic areas of Africa and lowest $^{87}Sr/^{86}Sr$ ratios along the basaltic African rift region (Fig. S2.5A, S2.6A). The difference between spatial interpolation EML and RF-based modeling was more significant when comparing the spatially explicit uncertainty maps with the EML isoscape displaying more normally distributed and lower average uncertainty (0.00347 vs. 0.00448) (Fig. S2.5B, S2.6B). The EML isoscape algorithm incorporates spatial dependencies and uses an unbiased spatial cross-validation approach leading to more robust uncertainty estimates (Hengl et al., 2021). However, this approach is best applied for local to regional bioavailable $^{87}Sr/^{86}Sr$ predictions as computational time becomes prohibitive for dataset with thousands of bioavailable $^{87}Sr/^{86}Sr$ (Hengl et al., 2021). Additionally, the EML framework lacks direct interpretability (i.e., absence of partial dependence plots or importance of predictors), so we still recommend to use the RF-based modeling approach as a basis to select predictors and discuss bioavailable $^{87}Sr/^{86}Sr$ patterns before using the spatial interpolation EML to produce the most accurate and unbiased $^{87}Sr/^{86}Sr$ isoscape. The novel isoscape is applicable to geolocate migratory painted ladies across the Palearctic-Afrotropical range, but, more broadly, it

provides a ground-breaking tool to investigate the mobility of other terrestrial insects, migratory animals (e.g., migratory megafauna, birds or early hominids) (Copeland et al., 2011), archeological humans (e.g., enslaved Africans) (Wang et al., 2023) and modern humans human remains (Degryse et al., 2012; Pye, 2004), tissues and manufactured substrates across Africa (e.g., drugs, ivory, wood) (van der Merwe et al., 1990).

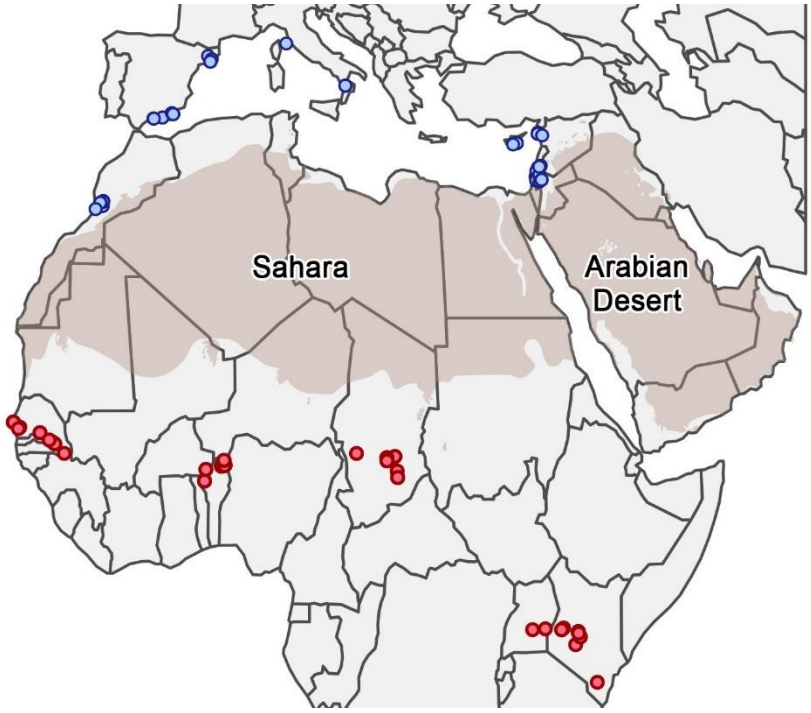

Figure 2.1. Collection sites for painted ladies butterflies (n = 118). Butterflies were collected north of the Sahara, encompassing regions in Morocco, Spain, Cyprus, Italy, Israel, Jordan, and Syria, during the months of January and April in 2012, 2016, 2017, and 2019 (Table S2.4). These butterflies represent northward-migrating painted ladies, based on our current understanding of seasonal patterns of suitable habitat (Menchetti et al., 2019; Talavera et al., 2023, 2018). To portray southward-migrating butterflies, samples were collected south of the Sahara, at multiple sites in Senegal, Benin, Chad, Uganda, and Kenya, spanning the months of August through December in 2014, 2017, 2018, and 2019. Desert shapefiles were sourced from Dinerstein et al. (2017).

As a prerequisite to assess the connectivity of migratory individuals across the Sahara, we used dual δ^2H and $^{87}Sr/^{86}Sr$-based geographic assignments to assess the natal origin of all the collected specimens. Our sampling strategy was crafted to capture migrants from both sides of the Sahara; however, we were only able to confidently classify 56% of the 118 samples as migratory (i.e., having traveled > 100 km). The remaining samples had dual isotopic signatures similar enough

to their capture location that we could not rule out a local origin (Fig. S2.9). It is possible that these individuals are also migrants, but from regions of natal origin with similar isotopic signatures as their capture locations. Those individuals had isotopic signatures that are highly redundant on the Afro Palearctic range, with $^{87}Sr/^{86}Sr$ ratios ~0.709 ± 0.001 common in most regions with marine sediments (Reich et al., 2021), and δ^2H values typical of warm wet climates of the Afrotropical regions (Ghouri et al., 2023). Alternatively, these individuals might have been collected later in the season and represent the locally-sourced offspring of migrants. In this study we are interested in migratory individuals, therefore we took the most conservative approach and excluded these potentially local individuals from further analyses of migratory connectivity.

2.3.2 Moderate migratory connectivity across the Sahara and Arabian Desert

Migratory connectivity refers to the degree to which individuals from one area of the migratory range migrate exclusively to another area without mixing with other individuals from elsewhere, with strong connectivity indicating a low amount of mixing (Gao et al., 2020; Webster et al., 2002). This term is often used to qualify the migratory patterns of birds, which often show strong connectivity and a discrete spatial structure in migratory trajectories across the Afro-Palearctic region (Gao et al., 2020). However, certain bird species exhibit moderate migratory connectivity, which is marked by spatial overlap in the breeding range (e.g., Finch et al., 2015; Koleček et al., 2016). In contrast, insects, due to their multi-generational, reticular migration patterns, typically display weaker migratory connectivity compared to birds (Gao et al., 2020; García-Berro et al., 2023).

In contrast to this general trend, painted ladies showed moderate migratory connectivity, characterized by a predominant latitudinal, rather than longitudinal, movement pattern, suggesting a parallel migration across the desert (Fig. 2.2). Individuals collected in the easternmost regions were estimated to migrate north from East Africa or the southern Arabian Peninsula in the spring (Fig. 2.2B) and south from the northern Arabian Peninsula when collected in the autumn (Fig. 2.2D). While this migratory pattern has long been suspected, empirical evidence has been absent until now (e.g., Larsen, 1975). For the westernmost butterflies, the most probable regions of origin exhibited less cohesiveness than in their eastern counterparts due to the broader range of sampling locations and times, resulting in a wider range

of isotopic signatures. During the autumn, many of the westernmost individuals showed estimates of natal origin in temperate Europe (Fig. 2.2C). Conversely, in the spring, individuals from the westernmost regions exhibited broader posterior probability surfaces, suggesting a natal origin ranging from northwestern Africa to as far east as the Arabian Peninsula (Fig. 2.2A). Our hypothesis is that the most likely origin for these butterflies lies directly south of their capture locations in the Western Sahara and the Canary Islands (Fig. 2.2A). This is supported by the presence of abundant banana pollen on one of these individuals (16C413); banana plants are present in the Canary Islands but not in the Arabian Peninsula (Gorki et al., *in review*). Furthermore, historical observations, recent ecological niche models, and monitoring data also suggest that the Western Sahara and the Canary Islands offer highly suitable breeding conditions for painted ladies from December through to February (Stefanescu et al., 2012; Talavera et al., 2023). We conclude that the westernmost butterflies primarily undertake migrations through regions spanning from western Europe to the west and central Sahel, encompassing the western Sahara and Canary Islands (Fig. 2.2A, 2.2C), and easternmost butterflies migrate through areas between the Eastern Mediterranean and East Africa, including the Arabian Peninsula (Fig. 2.2B, 2.2D).

Strong migratory connectivity can lead to adaptation and genetic differentiation between populations (Webster et al., 2002). Trans-Saharan migrations in birds often show longitudinal migratory divides, where adaptive populations follow western, eastern and, occasionally, central flyways (e.g., Åkesson et al., 2016; Briedis et al., 2020; Marx et al., 2016). However, the likelihood of discovering an adaptive longitudinal migratory divide among populations of painted ladies in the Afro-Palearctic region is remote, as is shown by the mounting evidence of inter-continental panmixia and shared demographic history (García-Berro et al., 2023; Reich et al., *in prep*; Suchan et al., *in review*). The migratory connectivity of painted ladies appears to be weaker than that observed in a few other migratory insect species, such as the fall armyworm moth *Spodoptera frugiperda* and the monarch butterfly (Gao et al., 2020). In these species, well-defined migration routes exist between discrete breeding grounds, separated by a geographic barrier oriented in a north-south direction (i.e., the Appalachian Mountains and Rocky Mountains) (Tessnow et al., 2023). In contrast, painted ladies breed across virtually the entire longitudinal expanse of Africa, with no significant geographical gaps of unsuitable habitat (Menchetti et al 2019; Talavera et al, 2023). We anticipate that expanding sampling efforts to

include more butterflies in Central Africa and the Central Mediterranean would reveal a continuum of predominantly north-south movement along the Sahara resulting in a broad front migration pattern with minimal longitudinal crossover (Fig. 2.2E). Instead of indicating adaptation to distinct migratory routes, the moderate migratory connectivity observed across the Sahara is likely a behavioral response aimed at minimizing migratory costs, as butterflies that migrate shorter distances directly across the Sahara may experience higher survival rates (Somveille et al., 2019).

While our data primarily supports the prevalence of latitudinal migratory trajectories, we do not rule out the possibility of some longitudinal movements. A closer examination of the posterior probability surfaces for individual butterflies reveals that many individuals are probably not following straight-line paths, and there may be variation in origin and migration routes even among individuals collected at the same site (Supplemental information). It is likely that environmental conditions along the migration path, such as prevailing wind direction (see Hu et al., 2021), affect the energetic costs associated with different routes and alter flight trajectories (Fattorini et al., 2023). An example of longitudinal movement is the individual collected in Italy, which displayed natal origins far to the east in the Arabian Peninsula (Fig. 2.2B). This specimen was collected in April 2019 (Fig. 2.3C), a year marked by an outbreak of painted lady butterflies, attributed to anomalous vegetation growth in the Arabian Peninsula (Gorki et al., *in review*; Hawkes et al., 2022; López-Mañas et al., 2022), that likely facilitated the spread of individuals from the hotspot to other parts of the range, extending as far west as Italy. Thus, long-distance longitudinal movements between the westernmost and easternmost Sahara can occur, but are presumably rare occurrences. The distribution of painted ladies in the Palearctic region extends from Portugal to Japan and the extent of connections between Europe and Africa with Asia are poorly understood. The migratory patterns of the easternmost butterflies in our study highlight the potential role of the Arabian Peninsula as a crucial stepping-stone connecting Europe, Africa, and Asia (Fig. 2.2B, 2.2D) (Larsen, 1984). Subsequent research should delve into whether the observed scarcity of longitudinal movements spans the Palearctic region and whether it results in genetic differentiation, which could be achieved by examining east-west patterns of genetic isolation by distance.

Migratory connectivity has been appraised in only a few insect species, but has important conservation implications. In species with weak migratory connectivity, local population bottlenecks can be mitigated through a compensatory demographic model (García-Berro et al., 2023). In contrast, species with stronger migratory connectivity may be more vulnerable to adverse environmental changes in specific sections of their range (Webster et al., 2002). The population of monarch butterflies in North America serves as a good example of this phenomenon. Although it comprises a single, panmictic population, monarch butterflies show relatively strong migratory connectivity between the western and eastern sides of the Rocky Mountains, with minimal crossover between these regions (Gao et al., 2020). Monarchs west of the Rockies are at high risk of local extirpation, likely due to environmental changes in that region (Pelton et al., 2019). The strong migratory connectivity of the species largely prevents the larger census size east of the Rockies from bolstering the western numbers (but see Vandenbosch, 2007). Historically, the Afro-Palearctic population of painted ladies has demonstrated demographic stability, albeit with large population fluctuations due to outbreak dynamics (García-Berro et al., 2023). However, in the context of global change, which can influence the climate and weather events on a broad scale, conservation practitioners should remain cognizant that moderate connectivity may reduce the compensatory abilities of the reticular migration pattern, especially along the longitudinal edges of the geographic range (Taylor and Norris, 2010). This is particularly pertinent during January and February, when occupancy and spatial extent are at their lowest (Talavera et al., 2023). Future studies quantifying the temporal and spatial migratory connectivity over each segment of the annual migration cycle are essential for a comprehensive assessment of the compensatory abilities within painted lady migration patterns (Knight et al., 2021), and how they may be influenced by anthropogenic climate change and habitat degradation.

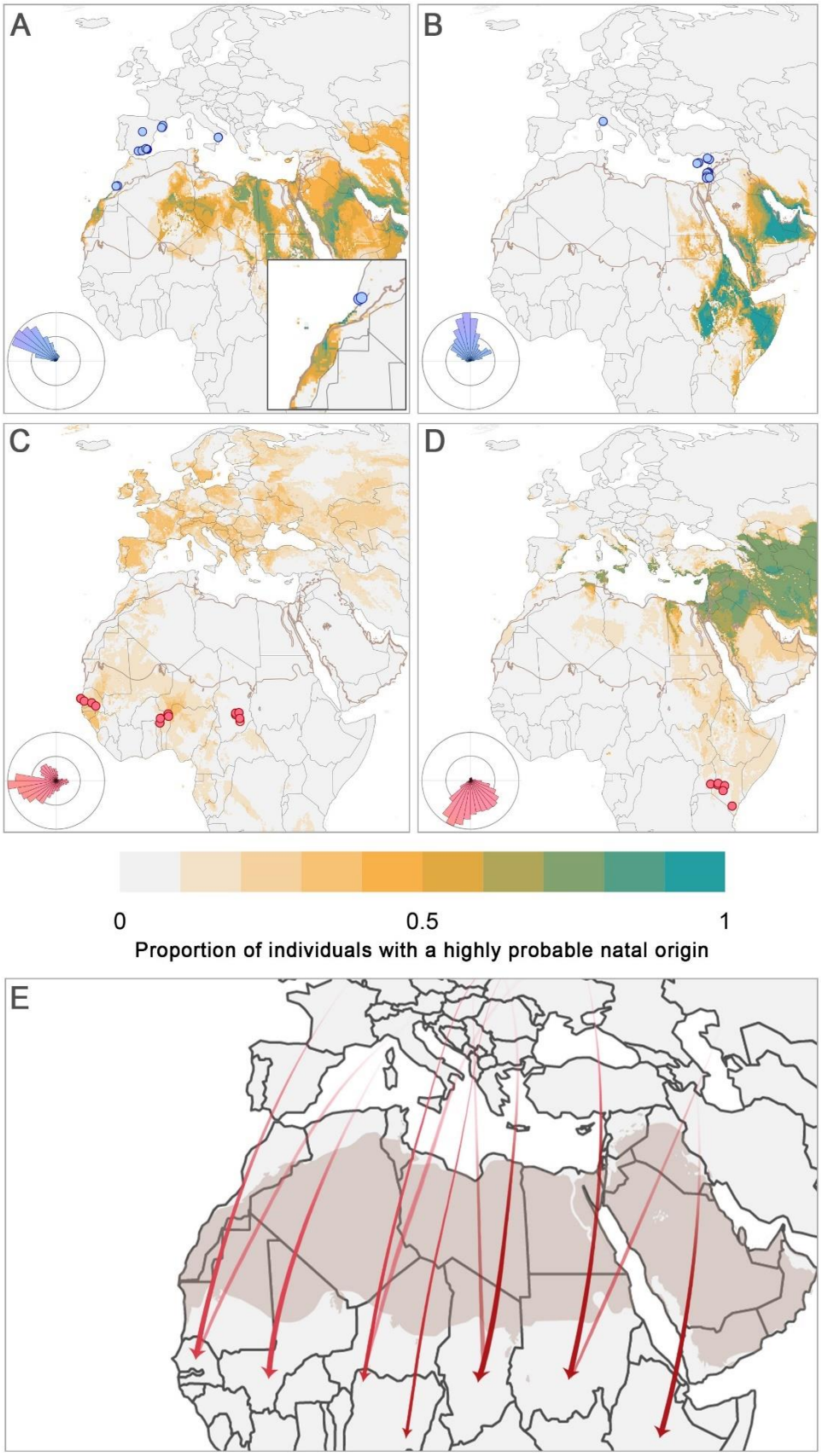
A
B
C
D
0
0.5
1
Proportion of individuals with a highly probable natal origin
E

Figure 2.2. Summarized posterior probability surfaces from δ^2H and $^{87}Sr/^{86}Sr$-based geographic assignment, illustrating the proportion of migratory individuals with a high probable natal origin at a given location, as defined by the 2:1 odds ratio. Teal areas indicate high cohesion in the estimated area of natal origin. The inset rose plots depict the combined probability-weighted estimates of the direction from the estimated natal origin to the capture location. Red (south of the Sahara) and blue (north of the Sahara) circles represent butterflies that were captured from (A) northwest of the Sahara in the late winter/early spring (n = 17), (B) northeast of the Sahara in the late winter/spring. Included is a long-distance migrant from Italy that clustered with the northeast captures (n = 15); (C) southwest of the Sahara in the autumn (n = 26), and (D) southeast of the Sahara in the late autumn (n = 8). (E) An illustration of the hypothesized broad front migration pattern with moderate migratory connectivity across the Sahara.

2.3.3 Northward progression

Our findings provide strong support for long-distance trans-Mediterranean and trans-Saharan migrations during the southward segment of the migratory cycle (Fig. 2.3H). These extensive migrations likely occur at high altitude (Stefanescu et al., 2013), and bear a striking resemblance to the long-distance autumn migrations of the overwintering generation of monarch butterflies (Reppert and de Roode, 2018). In contrast, during the spring, monarchs are known to gradually recolonize the USA and Canada in a northward progression over several generations, each covering short distances (Flockhart et al., 2013). Interestingly, our findings suggest a similar migratory behavior in painted ladies, with most spring migrants journeying shorter distances (Fig. 2.2A, 2.2B, 2.3H). Although our sampling was not sufficient to fully reconstruct the migratory connectivity across the Sahara on the northward segment of the migratory cycle, our results imply that most painted ladies migrating north from sub-Saharan Africa likely undertake shorter journeys to breed in northern Africa, with their offspring subsequently moving into Europe in a gradual northward progression. This reinforces the importance of North Africa as the primary source for spring migrants to Europe (Stefanescu et al., 2011). The similarities in seasonal differences in migratory patterns between painted ladies and monarch butterflies suggests the presence of conserved seasonal environmental cues, such as temperature, photoperiod, and host plant development (Goehring and Oberhauser, 2002), influencing the behavior of both species.

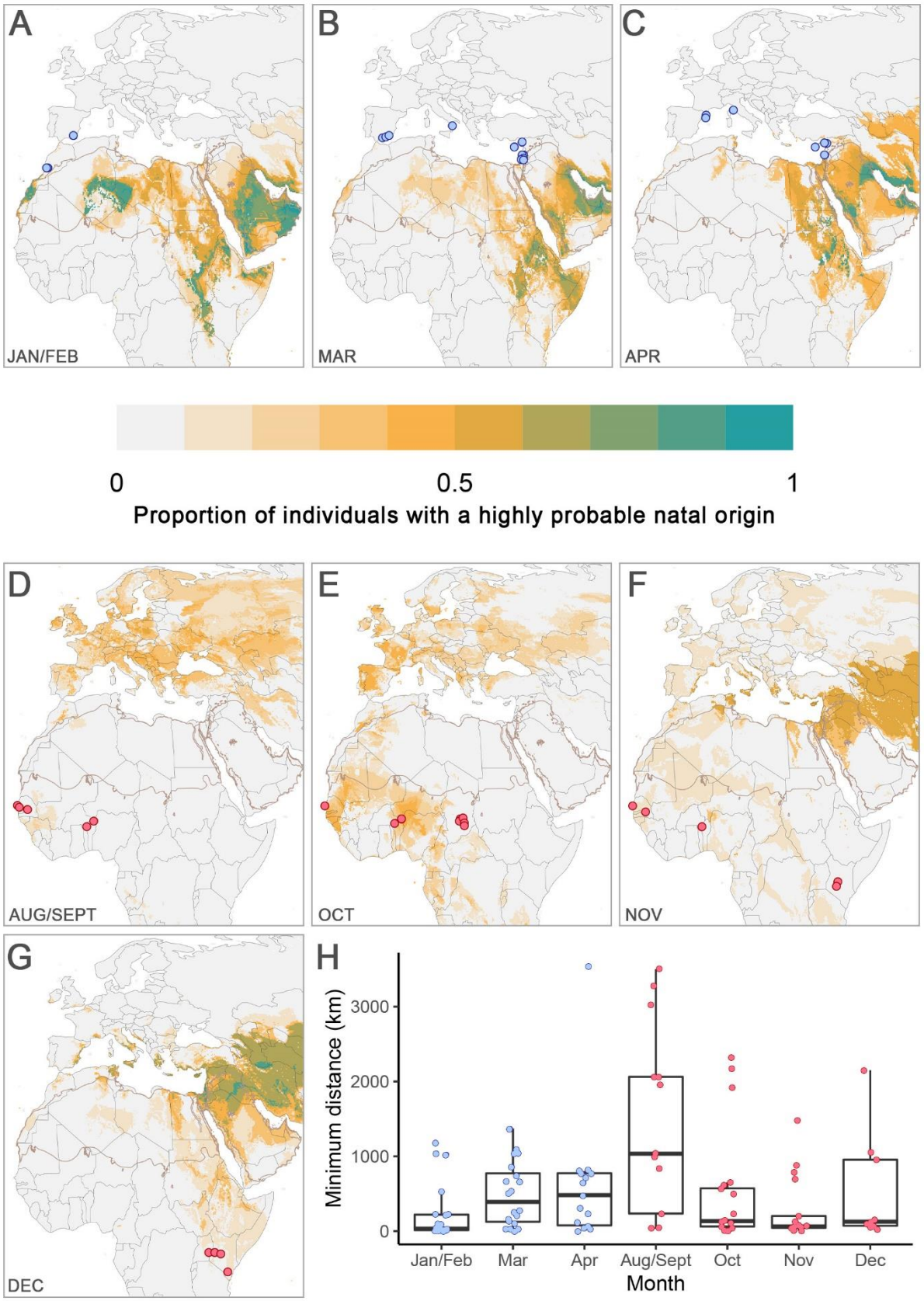
A
JAN/FEB
B
MAR
C
APR
0
0.5
1
Proportion of individuals with a highly probable natal origin
D
AUG/SEPT
E
OCT
F
NOV
G
DEC
H
Minimum distance (km)
3000
2000
1000
0
Jan/Feb
Mar
Apr
Aug/Sept
Oct
Nov
Dec
Month

Figure 2.3. Summarized posterior probability surfaces from δ^2H and $^{87}Sr/^{86}Sr$-based geographic assignment, illustrating the proportion of migratory individuals with a high probable natal origin at a given location, as defined by the 2:1 odds ratio, organized by month. Red (south of the Sahara) and blue (north of the Sahara) circles represent individuals captured during (A) January (n = 1) and February (n = 6) from Spain and Morocco, (B) March from Spain, Italy, Cyprus, Israel, Jordan, and Syria (n = 15), (C) April from Spain, Italy, Cyprus, Israel and Syria (n = 10), (D) August (n = 1) and September (n = 8) from Benin and Senegal, (E) October from Senegal, Benin and Chad (n = 14), (F) November from Senegal, Benin, and Kenya (n = 5), and (G) December captured from Uganda and Kenya (n = 6). (H) Minimum migratory distance (km) estimates for all painted lady samples (n = 118).

2.3.4 Southward generational temporal leapfrog migration

Leapfrog migration is used to describe a migration pattern commonly found in vertebrates wherein individuals that breed further north migrate beyond other groups to locations further south. Here, we describe a leapfrog migration for one of the migratory segments of the annual migration cycle of painted lady butterflies (Fig. 2.4B). Isotope-based geographic assignment has helped identify similar leapfrog migration patterns in birds (e.g., Nelson et al., 2015), but this is some of the first convincing evidence of a leapfrog migration in butterflies (but see Hobson et al., 2021). We identified the presence of many long-distance migrants, up to over 3,500 km, from northern and central Europe to West Africa from August through to November (Fig. 2.3D, 2.3E, 2.3F). In October and November, other painted ladies are migrating shorter distances from central and southern Europe to the circum-Mediterranean region (Reich et al., *in prep.*; Gorki et al., *in review*). In other words, in autumn, butterflies bred in northern Europe migrate further south than butterflies bred in southern Europe, suggesting a leapfrog migration pattern in the western Afro-Palearctic (Fig. 2.4B).

Temporal migration patterns are likely to be the primary driver of the putative leapfrog migration in painted ladies. We detect a temporal shift in origin in the long-distance migrants from temperate Europe to the Sahel, with δ^2H values, a rough proxy for latitude of origin, showing an increase over time; thus, the earliest arrivals to West Africa seem to originate from more northern latitudes (Fig. 2.4A). No genetic differentiation has been found between the painted ladies involved in this generational leapfrog migration in the western Afro-Palearctic, pointing to behavioral plasticity as the main mechanism by which painted ladies are cued to fly short or long

distances (Reich et al., *in prep*). Strong environmental cues in northern Europe (e.g., Scandinavia), such as photoperiod, temperature, and host plant phenology, change earlier in the autumn (i.e., September), and could prompt migratory behavior (Goehring and Oberhauser, 2002; Guerra and Reppert, 2013). However, the circum-Mediterranean region is not suitable breeding habitat in September (Talavera et al., 2023), so painted ladies reaching this region must continue further south to suitable breeding grounds in the Sahel (Fig. 2.3D, 2.4B). In October and November, both the circum-Mediterranean region and Sahel are highly suitable breeding habitat, and so painted ladies of progressively more southern origin can migrate either short or long distances (Fig. 2.3E, 2.3F). Similar temporal shifts in δ^2H values were recently detected in *D. gilippus* and attributed to a leapfrog migration pattern, although a short-distance migratory group was not identified in the study (Hobson et al., 2021). Although there are likely additional costs associated with the long-distance migration from northern Europe to the Sahel, such as decreased survival during migration (Newton, 2007), they may be overshadowed by the benefits of being the first arrivals to the region, as has been suggested for birds (Morrison et al., 2019), including a release from parasites, high abundance of larval host plants, and reduced competition.

The broad spatiotemporal coverage of our sampling on the western side of the range, particularly for the early autumn, facilitated the identification of this leapfrog migration. In contrast, we only have samples from November and December for the easternmost samples, limiting our ability to identify early autumn long-distance movements in that part of the range (Fig. 2.3F, 2.3G). However, even with these limitations, we were able to detect long-distance migrations from the Eastern Mediterranean to Kenya in November and December, providing the first empirical evidence of direct migration from the eastern Palearctic to eastern tropical Africa (Fig. 2.3F, 2.3G). Short-distance migrations from the Ethiopian Highlands to Kenya in December were also detected (Fig. 2.3G), and were likely the offspring of southward migrants to Ethiopia in October and November, although they could also be sourced from refuge individuals from areas with year-round suitability in the highlands and coastal areas (Menchetti et al., 2019; Talavera et al., 2023; Talavera and Vila, 2017). Those observations also suggest the possibility of leapfrog migration in the east but additional studies with higher spatiotemporal sampling in central and eastern Africa will be required to confirm this hypothesis.

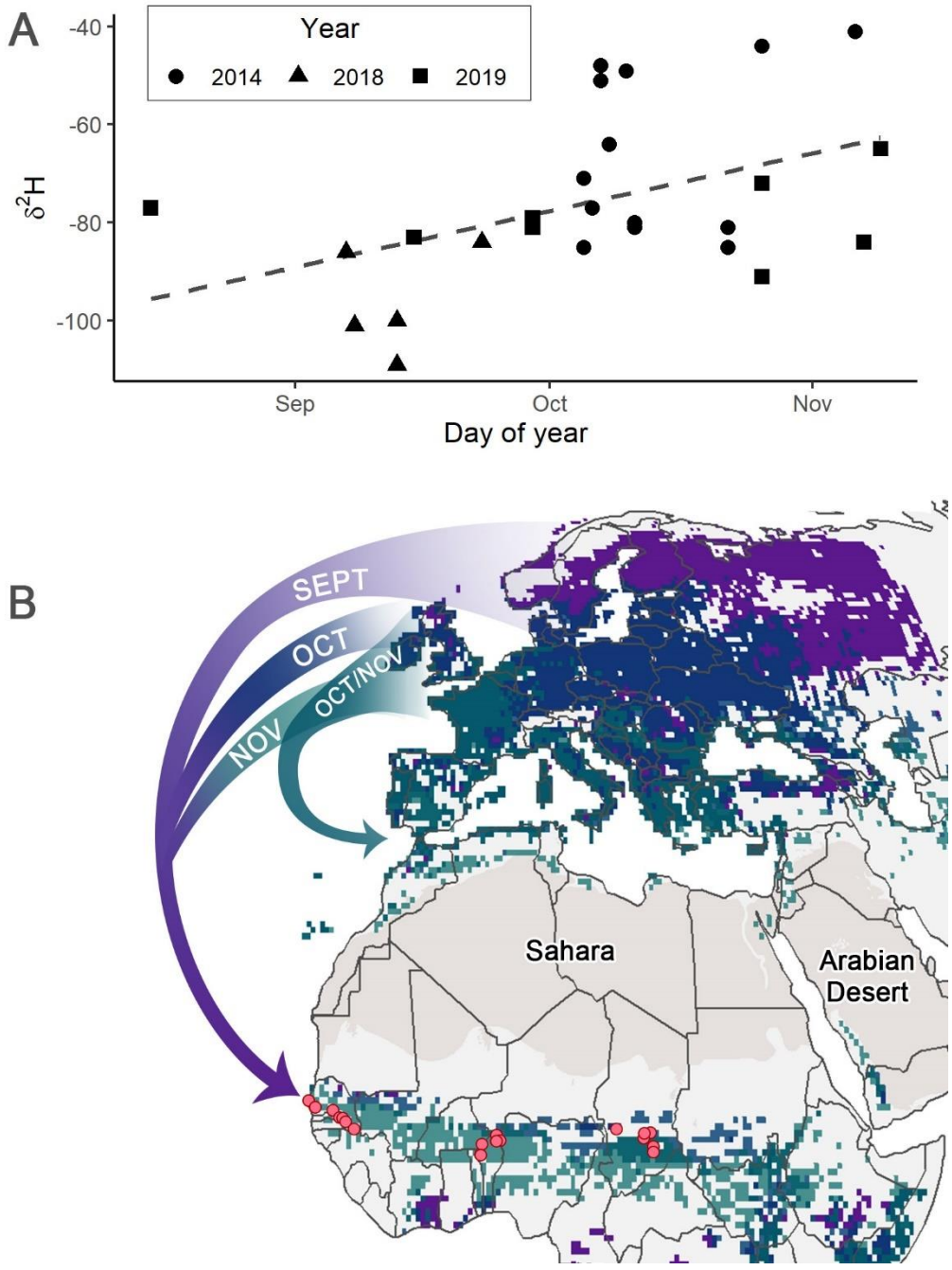

Figure 2.4. Leapfrog migration pattern in the southward trans-Saharan segment of the annual migratory cycle in the Afro-Palearctic. (A) Hydrogen isotope values (δ^2H) of migrants captured in Senegal, Benin, and Chad during the autumn (n = 44). The shape indicates the sampling year. (B) Conceptual model illustrating the proposed southward leapfrog migration. The map presents overlapping monthly representations of suitable breeding habitat (P > 95%) sourced from Talavera et al. (2023). In September, painted ladies originating from suitable habitat (indicated in purple) migrate to sub-Saharan Africa. In October (suitable habitat indicated by blue) and November (turquoise), painted ladies from progressively southern locations migrate to either the circum-Mediterranean region or sub-Saharan Africa.

2.4 Conclusion

2.4.1 Future work

Although we have elucidated many characteristics of the broad-scale migration patterns of painted lady butterflies across the Sahara, many other questions regarding the ecology and behavioral adaptations of insects navigating this challenging terrain persist. These questions encompass the environmental cues that prompt them to either embark on desert crossings or halt their migration, and how they might adjust their physiology, flight altitude or diurnal migration timing to successfully traverse this region. Many trans-Saharan migratory birds have been observed changing their behavior while crossing the desert (Jiguet et al., 2019a; Schmaljohann et al., 2007). For example, numerous songbirds switch from migrating during the day to migrating at night and resting in the shade of sand dunes or rocks during the day (Biebach et al., 1986). Moreover, a knowledge gap remains concerning the fuel usage and recharge strategies of painted ladies. Little is known about whether they exploit floral and water resources in oases, wadi, and mountain ranges, such as the Ahaggar and Tibesti Mountains. Subsequent research should also investigate the impact of migratory painted ladies on the delicate ecosystems of desert regions, the Sahel, and the sub-Saharan savanna (e.g., Pittaway, 1981; Stefanescu and Paramo, 2010; Talavera and Vila, 2017). Studies should also delve into co-migration and the predator-prey dynamics between migratory birds and bats with migratory insects (e.g., Cohen and Satterfield, 2020; Hawkes et al., 2023). Given anthropogenic climate change and widespread habitat degradation, delineating insect migratory patterns and connectivity becomes critically important. This understanding will help prevent the loss of essential ecosystem services by providing vital insights for conservation action, as well as pest management strategies in agriculture and forestry.

2.4.2 Limitations of the study

While isotope-based estimates of natal origin allowed us to explore the trans-Saharan migratory patterns and migratory connectivity of painted lady butterflies in remarkable detail, some caveats remain. The combination of δ^2H and ^{87}Sr/^{86}Sr for geographic assignment provided

more specific estimates of natal origin than using a single isotope. However, even in the best-case scenario, the estimated area of natal origin remained extensive, averaging approximately 5 million km^2, equivalent to half the size of Europe. Some individuals exhibited particularly broad estimated areas of natal origin due to the redundancy of certain isotopic signatures across the landscape. These fewer specific estimates of natal origin can potentially introduce inaccuracies in downstream metrics, such as estimates of migration distance (Hallworth et al., 2018). In contrast to the findings of Talavera et al (2018), which relied solely on δ^2H, our approach combining δ^2H and $^{87}Sr/^{86}Sr$ was unable to detect definitive trans-Saharan migrants north of the Sahara (Figure 2.3). Nevertheless, we propose that northward movements from sub-Saharan Africa are still likely to occur, given the comparatively large number of painted ladies present in sub-Saharan Africa from December to February (Talavera et al., 2023). To complete the northward migration and connectivity model of painted ladies across the Sahara, future research should concentrate on sampling during late winter (e.g., February, March) and in locations closer to the northern edge of the Sahara (e.g., Tunisia, Libya) to capture northward trans-Saharan migrants. Future effort should also focus on enhancing estimates of natal origin by combining isotope-based geographic assignment with other techniques, including ecological niche modeling, pollen metabarcoding analysis, wind trajectory modeling and the incorporation of additional isotopes.

2.5 Supplementary Information

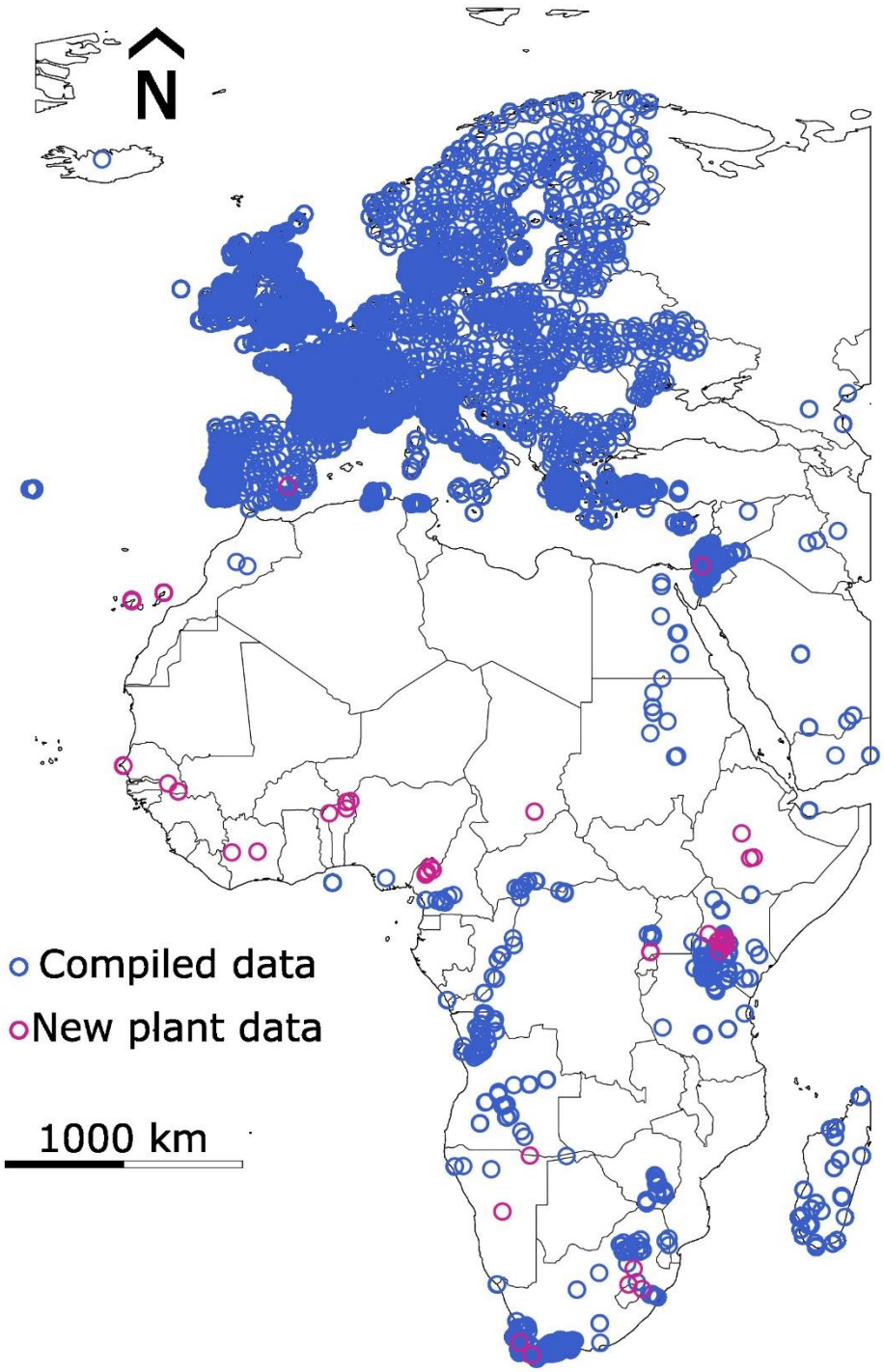

Figure S2.1. Geographic distribution of bioavailable $^{87}Sr/^{86}Sr$ data compilation across the Afro-Palearctic range. Compiled data from existing literature is depicted in blue, while pink represents newly collected plant sample data from this study (Table S2.2). The shapefile for country boundaries was obtained from *rnaturalearth* package.

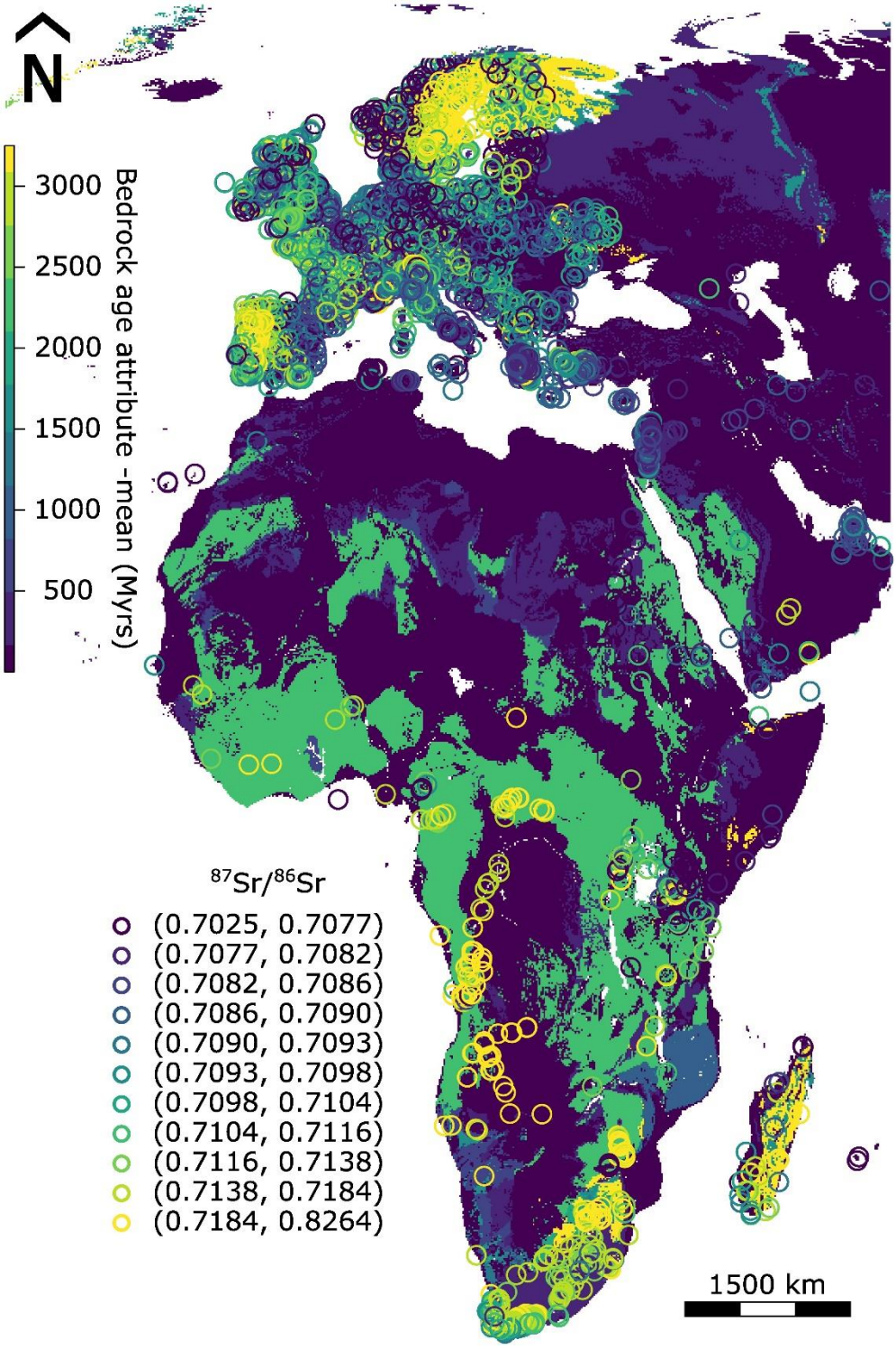

Figure S2.2. Spatial Distribution of $^{87}Sr/^{86}Sr$ ratios in the Afro-Palearctic Range from Table S2.1 overlaid on bedrock age (Myrs). Bedrock age offers a geological context, while points denote $^{87}Sr/^{86}Sr$ ratios, reflecting isotopic variation in the Afro-Palearctic region. The color-coded points represent distinct strontium isotope categories.

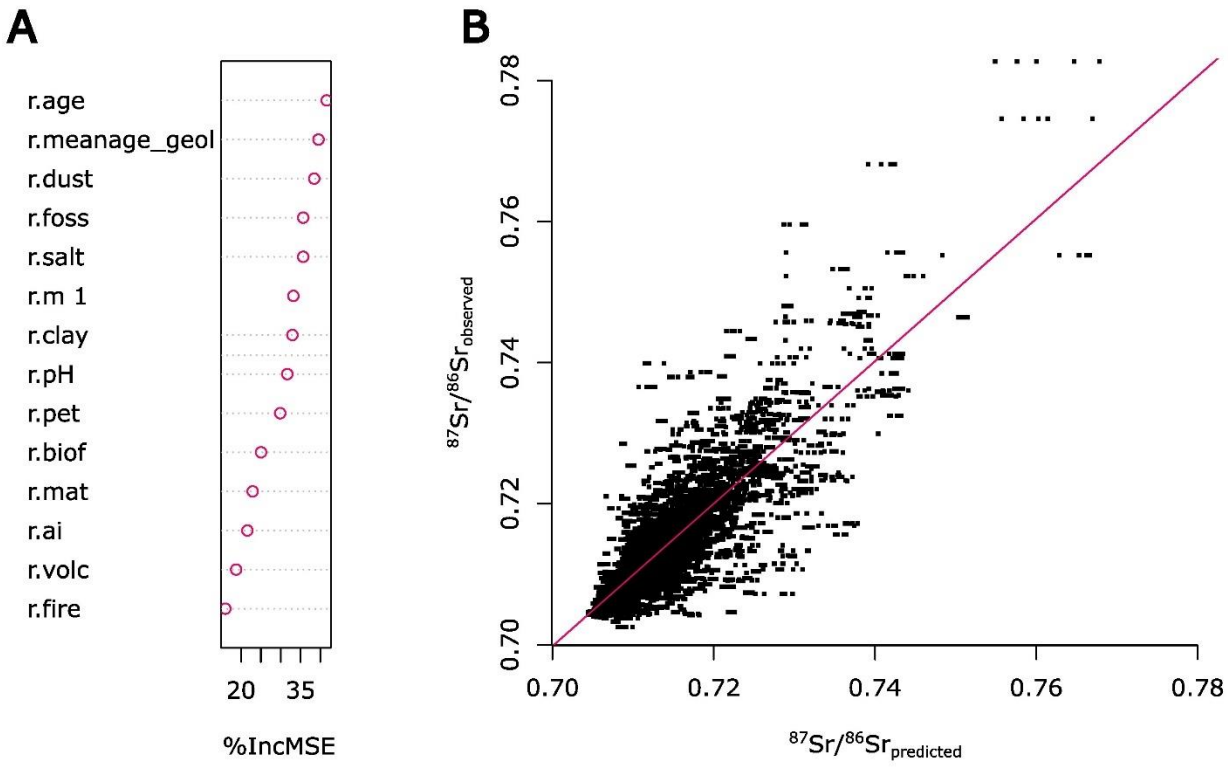

Figure S2.3. Random forest regression model for the bioavailable $^{87}Sr/^{86}Sr$ dataset A) Variable importance plot after selection of predictors by VSURF with %IncMSE as the evaluation standard. %IncMSE stands for increase in mean squared error percent and indicates that if a predictor variable is more important, the model's mean squared error of prediction will increase when the variable is taken out of the model. As a result, the variable's importance is directly proportional to the value of %IncMSE. The description and unit of each selected predictors is described in Table S3; B) N-fold cross-validation results with best fit linear model (pink line) for the random forest regression model

Table S2.2. | List of 28 geological, climatic, environmental, and anthropogenic geospatial data used as auxiliary variables in the random forest regression and in the spatial interpolation ensemble machine learning to create our regional bioavailable $^{87}Sr/^{86}Sr$ isoscape for the Afro-Palearctic range based on Bataille et al. 2020.

Variable ID	Description	Source of data
r.age	Terrane age attribute (Myrs)	(Mooney et al., 1998)
r.ai	Global Aridity Index *Aridity Index*= Mean annual precipitation÷ *Mean annual evapotranspiration*	(Trabuco & Zomer, 2019)
r.bulk	Bulk density of the fine earth fraction (kg/m^3)	(Hengl et al., 2021)
r.cec	Cation Exchange Capacity (cmol+ /kg)	(Hengl et al., 2021)
r.clay	Clay (weight %)	(Hengl et al., 2021)
r.biof	Biofuels (Black Carbon) ($kg/m^2/s$)	(Chien et al., 2016)
r.biog	Primary biogenic deposition ($kg/m^2/s$)	(Chien et al., 2016; Brahney et al., 2015)
r.wet	Wet dust deposition ($kg/m^2/s$)	(Chien et al., 2016)
r.foss	Fossil Fuel (Black Carbon) ($kg/m^2/s$)	(Chien et al., 2016)
r.dry	Dry dust deposition ($kg/m^2/s$)	(Chien et al., 2016; Brahney et al., 2015)
r.dust	Multi-models average of dust deposition ($g/m^2/year$)	(Chien et al., 2016; Brahney et al., 2015)
r.dust20	Dust deposition ($kg/m^2/s$)	(Chien et al., 2016)
r.fire	Black carbon deposition ($kg/m^2/s$)	(Chien et al., 2016)
r.volc	Volcanos (S) ($kg/m^2/s$)	(Brahney et al., 2015)
r.elevation	Hole-filled Digital Elevation Model	(Jarvis et al., 2008)
r.GUM	Unconsolidated sediment map	(Börker et al., 2018)
r.bouger	WGM2012_Bouguer Mean	(Balmino et al., 2012)
r.m1	Median bedrock model ($^{87}Sr/^{86}Sr$)	(Bataille et al., 2014)

r.mat	Mean annual temperature (°C)	(Harris et al., 2020)
r.map	Mean annual precipitation (mm/yr)	(Harris et al., 2020)
r.maxage_geol	GLiM age attribute – maximum (Myrs)	(Hartmann and Moosdorf, 2012; Bataille et al, 2020)
r.meanage_geol	GLiM age attribute – mean (Myrs)	(Hartmann and Moosdorf, 2012; Bataille et al, 2020)
r.minage_geol	GLiM age attribute – minimum (Myrs)	(Hartmann and Moosdorf, 2012; Bataille et al, 2020)
r.pet	Global Potential Evapo-Transpiration (mm day^{-1})	(Trabuco & Zomer, 2019)
r.ph	Soil pH in H_2O solution (x10)	(Hengl et al., 2021)
r.salt	Simulation of sea salt aerosol deposition (g/m^2/year)	(Chien et al., 2016)
r.srsrq1	Quartile 1 bedrock model ($^{87}Sr/^{86}Sr$)	(Bataille et al., 2014)
r.srsrq3	Quartile 3 bedrock model ($^{87}Sr/^{86}Sr$)	(Bataille et al., 2014)

Table S2.3. | Newly generated $^{87}Sr/^{86}Sr$ ratio of plants sampled in various localities across Africa for this study with the country of collection, locality name of collection, the $^{87}Sr/^{86}Sr$ ratio and it's associated uncertainty, and the geographic coordinates of latitude and longitude (Decimal Degree)

Sample ID	Country	Locality	$^{87}Sr/^{86}Sr$	Latitude (DD)	Longitude (DD)	$^{87}Sr/^{86}Sr$ error (2SD)
SG01	Cameroon	Mount Bamboutos	0.7079988	5.72	10.15	0.00006
SG02	Cameroon	Santa	0.7105366	5.84	10.16	0.00006
SG03	Cameroon	Santa	0.7100263	5.84	10.16	0.00006
SG04	Senegal	Kedogou	0.7182688	12.55	-12.19	0.00006
SG06	Ethiopia	Dodola	0.7082053	6.98	39.20	0.00006
SG07	Occupied Palestine	Zaak	0.7083495	31.41	34.87	0.00006
SG08	Spain	Jover, Santa Cruz de Tenerife	0.7078654	28.55	-16.37	0.00006
SG09	Spain	Vereda del Aire, Santa Cruz de Tenerife	0.7068648	28.47	-16.35	0.00006
SG10	Spain	Vereda del Aire, Santa Cruz de Tenerife	0.7067863	28.47	-16.35	0.00006
SG11	Spain	Lanzarote	0.70615355	29.16	-13.50	0.00006
SG12	Benin	Malanville	0.717046	11.74	3.28	0.00006
SG13	Benin	Toglou	0.7094487	14.71	-17.12	0.00006
SG14	Benin	Kandi	0.7108541	11.13	2.93	0.00006
SG15	Senegal	Kédougou	0.7161394	12.55	-12.19	0.00006
SG16	Ivory Coast		0.7273909	7.52	-5.07	0.00006
SG17	Ivory Coast		0.7380935	7.46	-7.38	0.00006
SG18	Chad	Zakouma National Park	0.7186733	10.87	19.82	0.00006
SG19	Benin	Tanguieta	0.7159909	10.73	1.38	0.00006
SG20	South Africa	Malmesbury Farm	0.71292185	-33.47	18.47	0.00006
SG21	South Africa	Western Cape	0.7105643	-34.52	19.56	0.00006
SG25	South Africa		0.7126712	-27.31	28.73	0.00006
SG26	South Africa		0.7133362	-28.64	28.27	0.00006
SG27	South Africa		0.7170605	-29.01	29.49	0.00006
SG28	Uganda		0.7267079	-0.86	30.25	0.00006
SG29	Uganda		0.729844	-0.85	30.23	0.00006
SG30	Kenya		0.7073782	-0.79	36.43	0.00006
SG31	Namibia	Rundu	0.7261313	-17.87	19.41	0.00006

SG31	Namibia	Daas Viljoen	0.7261313	-22.55	16.94	0.00006
SG32	Namibia	Dienoun Diala	0.7145887	13.21	-13.11	0.00006
SG33	Benin	Alibori River, W National Park	0.7129371	11.66	2.92	0.00006
SG34	Ethiopia	Adaba, Road Dodola to Dinsho	0.70584945	7.04	39.52	0.00006
SG35	Cameroon	Oku	0.7076261	9.05	38.44	0.00006
SG36	Cameroon		0.7129523	6.23	10.50	0.00006
SG37	Cameroon		0.70961225	6.00	10.67	0.00006
SG38	Cameroon		0.7067544	5.75	10.16	0.00006
SG39	Cameroon	Baraka (Mount Bamboutos)	0.7067752	5.61	10.04	0.00006
SG40	Uganda		0.72667155	-0.86	30.25	0.00006
SG41	Spain	Nerpio	0.7090214	38.07	-2.35	0.00006
SG42	Kenya	Nyeri	0.7054877	-0.36	37.00	0.00006
SG43	Kenya	Nyanyuki	0.7069037	0.03	37.06	0.00006
SG49	Kenya	Mpala Research Centre	0.7068935	0.35	36.89	0.00006
SG50	Kenya		0.7045672	-0.09	36.65	0.00006
SG51	Kenya		0.7046653	-0.09	36.65	0.00006
SG52	Kenya	Nyanyuki	0.7077665	0.04	36.30	0.00006
SG53	Kenya	Iten	0.7065008	0.64	35.46	0.00006

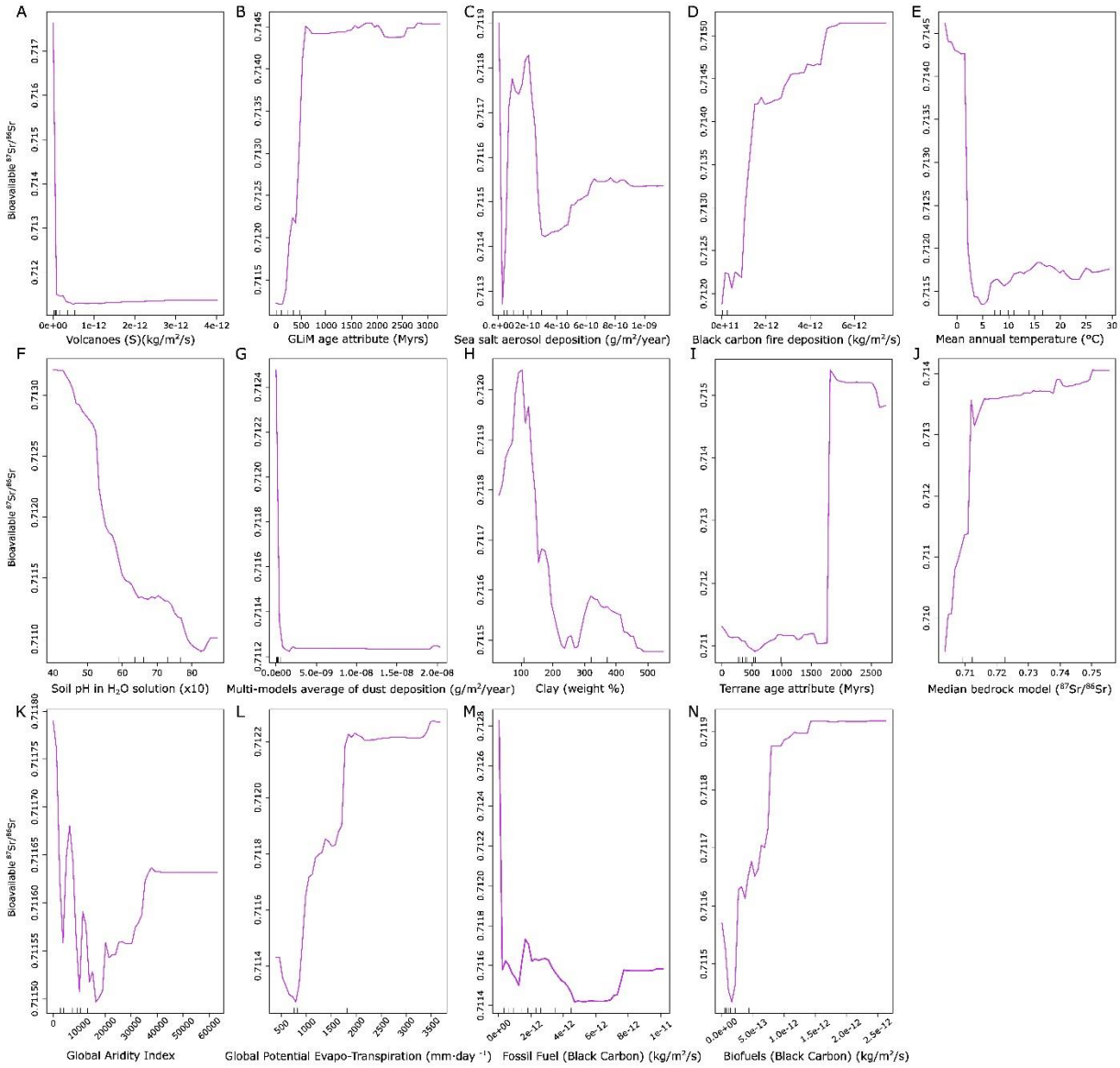

Figure S2.4. Partial dependence plots between predictors (x-axis) and predicted bioavailable $^{87}Sr/^{86}Sr$ (y-axis) from random forest regressions using the new compilation of bioavailable$^{87}Sr/^{86}Sr$ dataset. Refer to Table S2.2 for description and sources of each covariate. Hash marks along the x axis show covariate sample decile values.

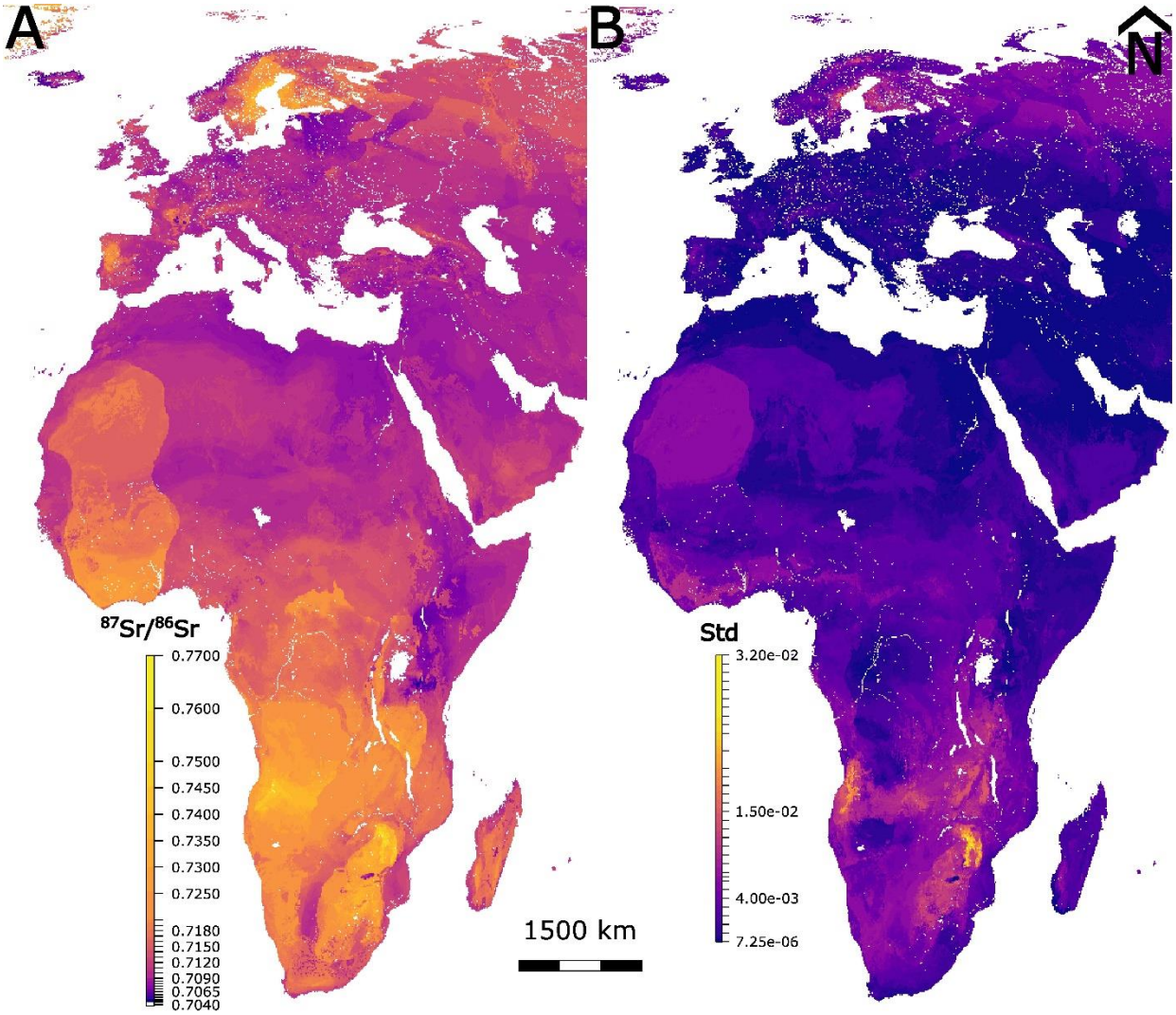

Figure S2.5. Predicted bioavailable $^{87}Sr/^{86}Sr$ isoscape across the Afro-Palearctic and its associated uncertainty generated using random forest regression. A) Mean bioavailable $^{87}Sr/^{86}Sr$ predictions; B) Standard-deviation of bioavailable $^{87}Sr/^{86}Sr$ predictions. Colorscale breakpoints were selected to improve visualization and increase contrast.

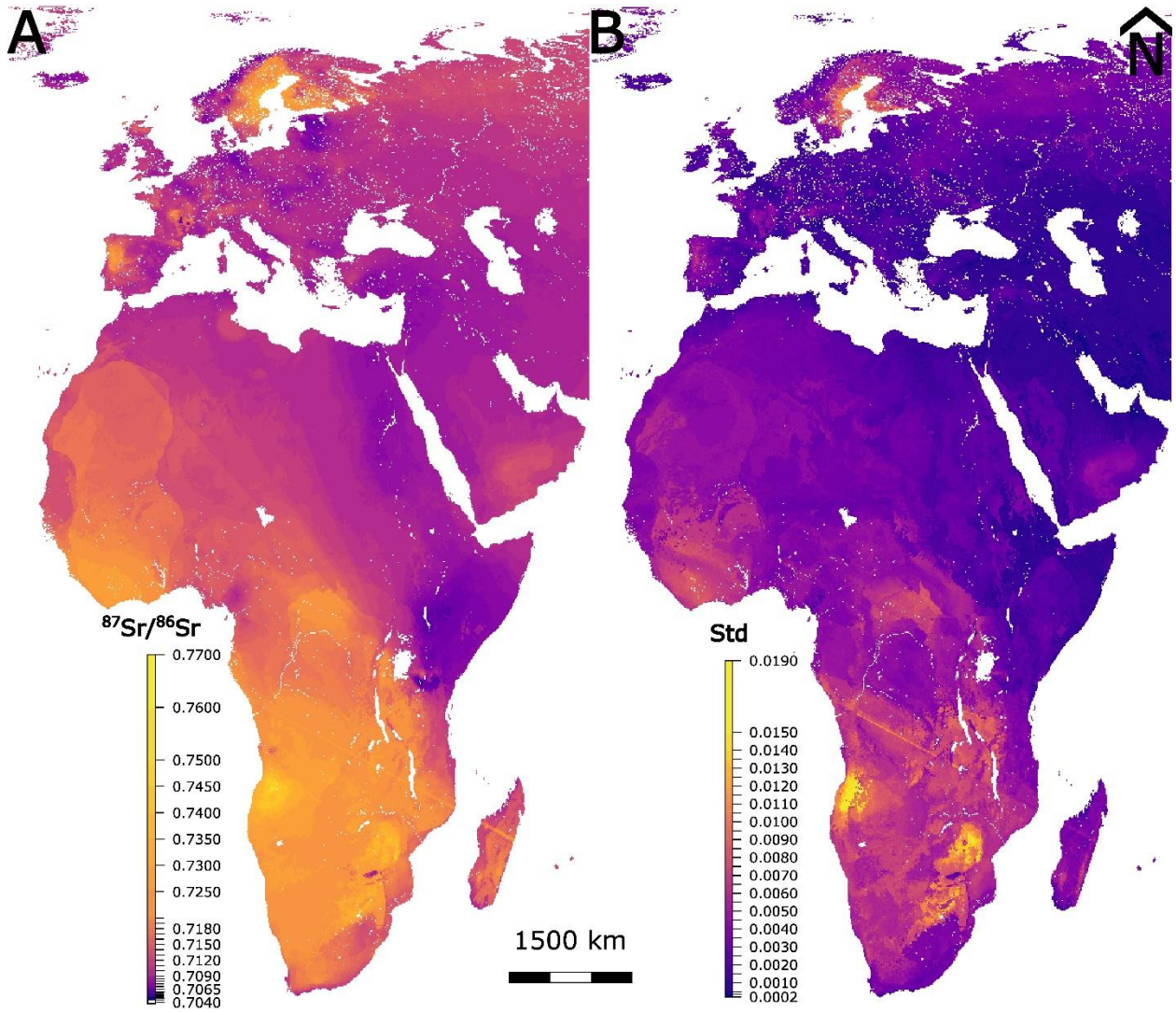

Figure S2.6. Predicted bioavailable $^{87}Sr/^{86}Sr$ isoscape across the Afro-Palearctic and its associated uncertainty generated using Ensemble machine learning. A) Mean bioavailable $^{87}Sr/^{86}Sr$ predictions; B) Standard-deviation of bioavailable $^{87}Sr/^{86}Sr$ predictions. Colorscale breakpoints were selected to improve visualization and increase contrast.

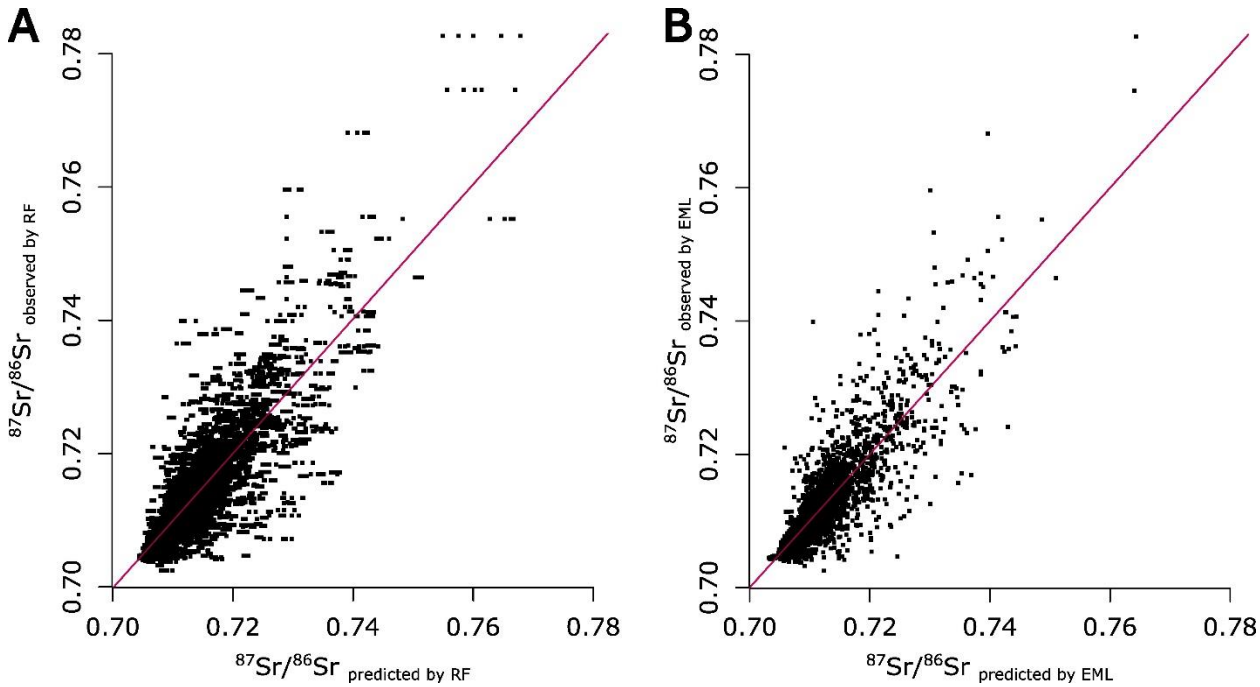

Figure S2.7. N-fold cross-validation results between observed bioavailable $^{87}Sr/^{86}Sr$ and predicted bioavailable $^{87}Sr/^{86}Sr$ A. by random forest regression model using the framework of Bataille et al. (2020); B. by spatial interpolation Ensemble machine learning model using the landmap package (Hengl et al. 2021). Pink lines represent the best fit linear model.

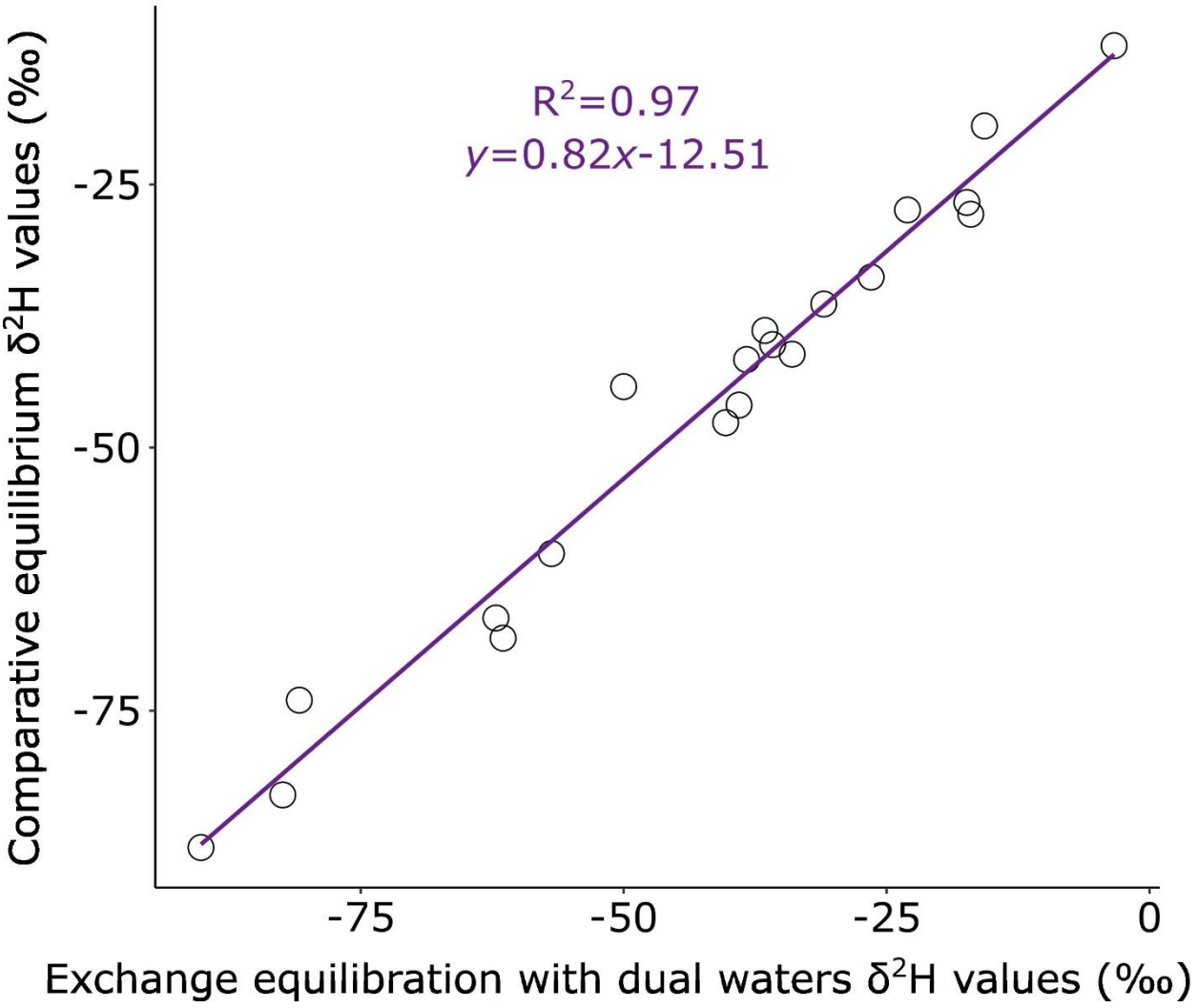

Figure S2.8. Scatterplot of twenty wing samples from a given site used for duplicate analysis using both the exchange equilibration with dual waters (%) and comparative equilibrium protocols (%). A linear model between δ^2H values resulting from this comparative analysis was developed. The following calibration equation was applied to correct all samples analysed by the exchange equilibration with dual waters method for consistency.

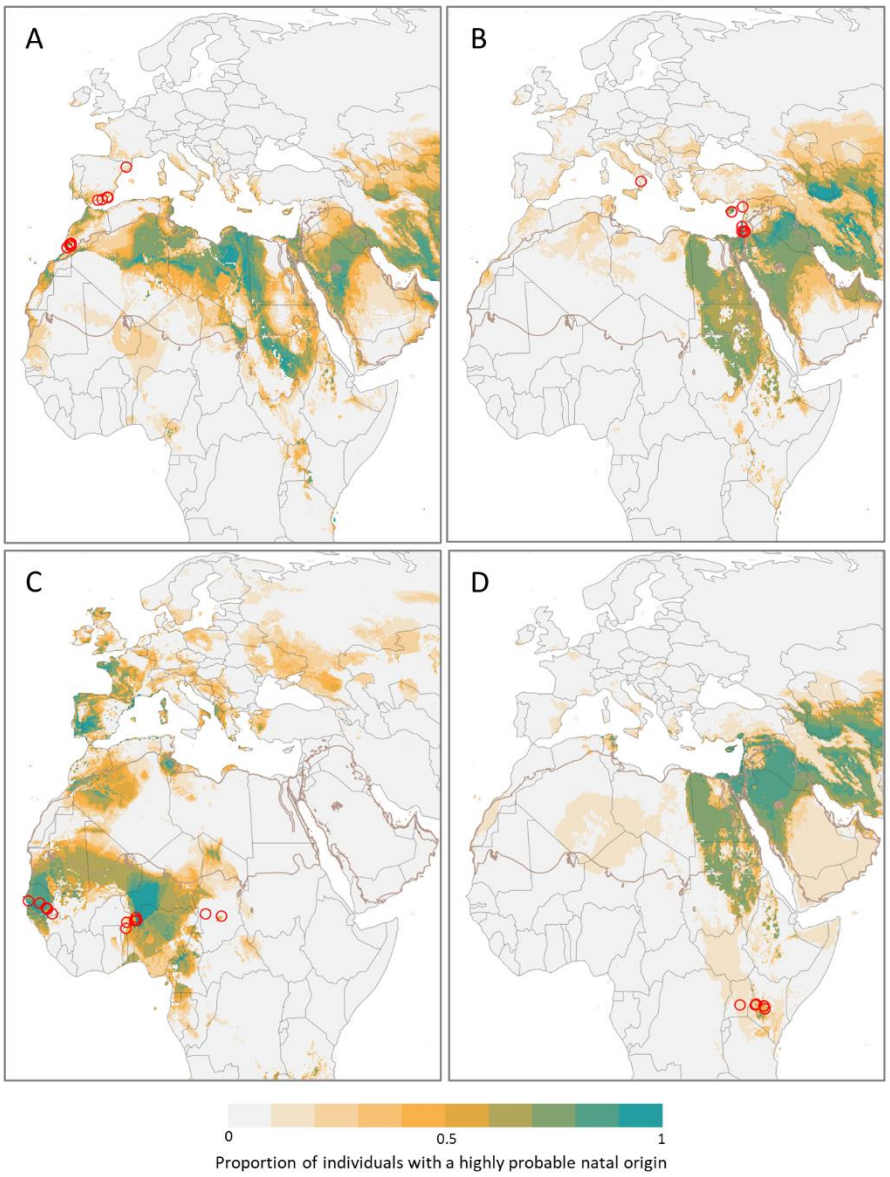

Figure S2.9. Estimated natal origins of painted ladies categorized as putative locals. (A) Captures from northwest of the Sahara in the late winter/early spring (n =18); (B) captures from northeast of the Sahara in the late winter/spring (n = 8); (C) captures from southwest of the Sahara in the autumn (n =18); (D) captures from southeast of the Sahara in the late autumn (n =8).

2.6 References

Åkesson, S., Bianco, G., Hedenstrom, A., 2016. Negotiating an ecological barrier: Crossing the Sahara in relation to winds by common swifts. *Philos. Trans. R. Soc. B Biol*. Sci. 371. https://doi.org/10.1098/rstb.2015.0393

Balmino, G., Vales, N., Bonvalot, S., Briais, A., 2012. Spherical harmonic modelling to ultra-high degree of Bouguer and isostatic anomalies. J. Geod. 86, 499–520. https://doi.org/10.1007/s00190-011-0533-4

Bataille, C.P., Ammer, S.T.M., Bhuiyan, S., Chartrand, M.M.G., St-Jean, G., Bowen, G.J., 2022. Multi-isotopes in human hair: A tool to initiate cross-border collaboration in international cold-cases. *PLoS One* 17, 1–21. https://doi.org/10.1371/journal.pone.0275902

Bataille, C.P., Bowen, G.J., 2012. Mapping $^{87}Sr/^{86}Sr$ variations in bedrock and water for large scale provenance studies. *Chem. Geol*. 304–305, 39–52. https://doi.org/10.1016/j.chemgeo.2012.01.028

Bataille, C.P., Brennan, S.R., Hartmann, J., Moosdorf, N., Wooller, M.J., Bowen, G.J., 2014. A geostatistical framework for predicting variations in strontium concentrations and isotope ratios in Alaskan rivers. *Chem. Geol*. 389, 1–15. https://doi.org/10.1016/j.chemgeo.2014.08.030

Bataille, C.P., Crowley, B.E., Wooller, M.J., Bowen, G.J., 2020. Advances in global bioavailable strontium isoscapes. *Palaeogeogr. Palaeoclimatol. Palaeoecol*. 555, 109849. https://doi.org/10.1016/j.palaeo.2020.109849

Bataille, C.P., von Holstein, I.C.C., Laffoon, J.E., Willmes, M., Liu, X.M., Davies, G.R., 2018. A bioavailable strontium isoscape for Western Europe: A machine learning approach. *PLoS One 13*, 1–28. https://doi.org/10.1371/journal.pone.0197386

Biebach, H., Friedrich, W., Heine, G., 1986. Interaction of bodymass, fat, foraging and stopover period in trans-Sahara migrating passerine birds. *Oecologia 69*, 370–379. https://doi.org/10.1007/BF00377059

Börker, J., Hartmann, J., Amann, T., Romero-Mujalli, G., 2018. Terrestrial sediments of the earth: Development of a global unconsolidated sediments map database (GUM). *Geochemistry, Geophys. Geosystems 19*, 997–1024. https://doi.org/10.1002/2017GC007273

Bowen, G.J., Wassenaar, L.I., Hobson, K.A., 2005. Global application of stable hydrogen and oxygen isotopes to wildlife forensics. *Oecologia 143*, 337–348. https://doi.org/10.1007/s00442-004-1813-y

Brahney, J., Ballantyne, A.P., Kociolek, P., Leavitt, P.R., Farmer, G.L., Neff, J.C., 2015. Ecological changes in two contrasting lakes associated with human activity and dust transport in western Wyoming. Limnol. *Oceanogr. 60*, 678–695. https://doi.org/10.1002/lno.10050

Briedis, M., Bauer, S., Adamík, P., Alves, J.A., Costa, J.S., Emmenegger, T., Gustafsson, L., Koleček, J., Krist, M., Liechti, F., Lisovski, S., Meier, C.M., Procházka, P., Hahn, S., 2020.

Broad-scale patterns of the Afro-Palaearctic landbird migration. *Glob. Ecol. Biogeogr. 29*, 722–735. https://doi.org/10.1111/geb.13063

Capo, R.C., Stewart, B.W., Chadwick, O.A., 1998. Strontium isotopes as tracers of ecosystem processes: Theory and methods. *Geoderma 82*, 197–225. https://doi.org/10.1016/S0016-7061(97)00102-X

Chapman, J.W., Reynolds, D.R., Wilson, K., 2015. Long-range seasonal migration in insects: Mechanisms, evolutionary drivers and ecological consequences. *Ecol. Lett. 18*, 287–302. https://doi.org/10.1111/ele.12407

Chien, C.-T., Mackey, K., Dutkiewicz, S., Mahowald, N., Prospero, J., Paytan, A., 2016. Effects of African dust deposition on phytoplankton in the western tropical Atlantic Ocean off Barbados. *Global Biogeochem. Cycles* 1199–1214. https://doi.org/10.1002/2015GB005334.Received

Chowdhury, S., Fuller, R.A., Dingle, H., Chapman, J.W., Zalucki, M.P., 2021. Migration in butterflies: a global overview. *Biol. Rev. 96*, 1462–1483. https://doi.org/10.1111/brv.12714

Cohen, E.B., Satterfield, D.A., 2020. 'Chancing on a spectacle:' co-occurring animal migrations and interspecific interactions. *Ecography (Cop.). 43*, 1657–1671. https://doi.org/10.1111/ecog.04958

Copeland, S.R., Sponheimer, M., De Ruiter, D.J., Lee-Thorp, J.A., Codron, D., Le Roux, P.J., Grimes, V., Richards, M.P., 2011. Strontium isotope evidence for landscape use by early hominins. *Nature 474*, 76–78. https://doi.org/10.1038/nature10149

Coplen, T.B., Qi, H., 2016. A revision in hydrogen isotopic composition of USGS42 and USGS43 human-hair stable isotopic reference materials for forensic science. *Forensic Sci. Int. 266*, 222–225. https://doi.org/10.1016/j.forsciint.2016.05.029

Degryse, P., De Muynck, D., Delporte, S., Boyen, S., Jadoul, L., De Winne, J., Ivaneanu, T., Vanhaecke, F., 2012. Strontium isotopic analysis as an experimental auxiliary technique in forensic identification of human remains. *Anal. Methods 4*, 2674–2679. https://doi.org/10.1039/c2ay25035g

Diffendorfer, J.E., Drum, R.G., Mitchell, G.W., Rendón-Salinas, E., Sánchez-Cordero, V., Semmens, D.J., Thogmartin, W.E., March, I.J., 2023. The benefits of big-team science for conservation: Lessons learned from trinational monarch butterfly collaborations. *Front. Environ. Sci. 11*. https://doi.org/10.3389/fenvs.2023.1079025

Dinerstein, E., Olson, D., Joshi, A., Vynne, C., Burgess, N.D., Wikramanayake, E., Hahn, N., Palminteri, S., Hedao, P., Noss, R., Hansen, M., Locke, H., Ellis, E.C., Jones, B., Barber, C.V., Hayes, R., Kormos, C., Martin, V., Crist, E., Sechrest, W., Price, L., Baillie, J.E.M., Weeden, D., Suckling, K., Davis, C., Sizer, N., Moore, R., Thau, D., Birch, T., Potapov, P., Turubanova, S., Tyukavina, A., de Souza, N., Pintea, L., Brito, J.C., Llewellyn, O.A., Miller, A.G., Patzelt, A., Ghazanfar, S.A., Timberlake, J., Klöser, H., Shennan-Farpón, Y., Kindt, R., Lillesø, J.-P.B., van Breugel, P., Graudal, L., Voge, M., Al-Shammari, K.F., Saleem, M., 2017. An Ecoregion-Based

Approach to Protecting Half the Terrestrial Realm. *Bioscience 67*, 534–545. https://doi.org/10.1093/biosci/bix014

Fattorini, N., Costanzo, A., Romano, A., Rubolini, D., Baillie, S., Bairlein, F., Spina, F., Ambrosini, R., 2023. Eco-evolutionary drivers of avian migratory connectivity. *Ecol. Lett. 26*, 1095–1107. https://doi.org/10.1111/ele.14223

Finch, T., Saunders, P., Avilés, J.M., Bermejo, A., Catry, I., de la Puente, J., Emmenegger, T., Mardega, I., Mayet, P., Parejo, D., Račinskis, E., Rodríguez-Ruiz, J., Sackl, P., Schwartz, T., Tiefenbach, M., Valera, F., Hewson, C., Franco, A., Butler, S.J., 2015. A pan-European, multipopulation assessment of migratory connectivity in a near-threatened migrant bird. *Divers. Distrib. 21*, 1051–1062. https://doi.org/10.1111/ddi.12345

Flockhart, D.T.T., Wassenaar, L.I., Martin, T.G., Hobson, K.A., Wunder, M.B., Norris, D.R., 2013. Tracking multi-generational colonization of the breeding grounds by monarch butterflies in eastern North America. *Proc. R. Soc. B Biol. Sci. 280*, 20131087. https://doi.org/10.1098/rspb.2013.1087

Gao, B., Hedlund, J., Reynolds, D.R., Zhai, B., Hu, G., Chapman, J.W., 2020. The 'migratory connectivity' concept, and its applicability to insect migrants. *Mov. Ecol. 8*, 1–13. https://doi.org/10.1186/s40462-020-00235-5

García-Berro, A., Talla, V., Vila, R., Wai, H.K., Shipilina, D., Chan, K.G., Pierce, N.E., Backström, N., Talavera, G., 2023. Migratory behaviour is positively associated with genetic diversity in butterflies. *Mol. Ecol. 32*, 560–574. https://doi.org/10.1111/mec.16770

Genuer, R., Poggi, J.M., Tuleau-Malot, C., 2015. VSURF: An R package for variable selection using random forests. *R J. 7*, 19–33. https://doi.org/10.32614/rj-2015-018

Georganos, S., Grippa, T., Niang Gadiaga, A., Linard, C., Lennert, M., Vanhuysse, S., Mboga, N., Wolff, E., Kalogirou, S., 2021. Geographical random forests: a spatial extension of the random forest algorithm to address spatial heterogeneity in remote sensing and population modelling. *Geocarto Int. 36,* 121–136. https://doi.org/10.1080/10106049.2019.1595177

Ghouri, S., Reich, M. S., Lopez-Mañas, R., Talavera, G., Bowen, G. J., Vila, R., K. Talla, V. N., Collins, S. C., Martins, D. J., & Bataille, C. P. (2024). A hydrogen isoscape for tracing the migration of herbivorous lepidopterans across the Afro-Palearctic range. Rapid Communications in Mass Spectrometry, 38(3), e9675. https://doi.org/10.1002/rcm.9675

Gilroy, J.J., Gill, J.A., Butchart, S.H.M., Jones, V.R., Franco, A.M.A., 2016. Migratory diversity predicts population declines in birds. *Ecol. Lett. 19*, 308–317. https://doi.org/10.1111/ele.12569

Goehring, L., Oberhauser, K.S., 2002. Effects of photoperiod, temperature, and host plant age on induction of reproductive diapause and development time in *Danaus plexippus*. *Ecol. Entomol. 27*, 674–685. https://doi.org/10.1046/j.1365-2311.2002.00454.x

Gorki, J. L., Sáez, L., López-Mañas, R., Menchetti, M., Shapoval, N., Andersen, A., Benyamini, D., Daniels, S., García-Berro, A., Reich, M. S., Scalercio, S., Toro-Delgado, E., Bataille, C. P.,

Domingo-Marimon, C., Vila, R., Suchan, T., Talavera, G. (*in review*). Pollen metabarcoding reveals the origin and multigenerational migratory pathway of an intercontinental-scale butterfly outbreak.

Guerra, P.A., Reppert, S.M., 2013. Coldness Triggers Northward Flight in Remigrant Monarch Butterflies. *Curr. Biol. 23*, 419–423. https://doi.org/10.1016/j.cub.2013.01.052

Guilherme, J.L., Jones, V.R., Catry, I., Beal, M., Dias, M.P., Oppel, S., Vickery, J.A., Hewson, C.M., Butchart, S.H.M., Rodrigues, A.S.L., 2023. Connectivity between countries established by landbirds and raptors migrating along the African–Eurasian flyway. *Conserv. Biol. 37*. https://doi.org/10.1111/cobi.14002

Hallworth, M.T., Marra, P.P., McFarland, K.P., Zahendra, S., Studds, C.E., 2018. Tracking dragons: Stable isotopes reveal the annual cycle of a long-distance migratory insect. *Biol. Lett. 14*. https://doi.org/10.1098/rsbl.2018.0741

Harris, I., Osborn, T.J., Jones, P., Lister, D., 2020. Version 4 of the CRU TS monthly high-resolution gridded multivariate climate dataset. *Sci. Data 7*, 1–18. https://doi.org/10.1038/s41597-020-0453-3

Hartman, G., Richards, M., 2014. Mapping and defining sources of variability in bioavailable strontium isotope ratios in the Eastern Mediterranean. *Geochim. Cosmochim. Acta 126*, 250–264. https://doi.org/10.1016/j.gca.2013.11.015

Hartmann, J., Moosdorf, N., 2012. The new global lithological map database GLiM: A representation of rock properties at the Earth surface. Geochemistry, *Geophys. Geosystems 13*. https://doi.org/10.1029/2012GC004370

Hawkes, W.L., Davies, K., Weston, S., Moyes, K., Chapman, J.W., Wotton, K.R., 2023. Bat activity correlated with migratory insect bioflows in the Pyrenees. R. Soc. *Open Sci. 10*. https://doi.org/10.1098/rsos.230151

Hawkes, W.L.S., Walliker, E., Gao, B., Forster, O., Lacey, K., Doyle, T., Massy, R., Roberts, N.W., Reynolds, D.R., Özden, Ö., Chapman, J.W., Wotton, K.R., 2022. Huge spring migrations of insects from the Middle East to Europe: quantifying the migratory assemblage and ecosystem services. *Ecography (Cop.)*. 2022, 1–15. https://doi.org/10.1111/ecog.06288

Hengl, T., 2021. *landmap*: Automated Spatial Prediction using Ensemble Machine Learning version 0.0.13 from CRAN [WWW Document]. URL https://rdrr.io/cran/landmap/ (accessed 8.18.23).

Hengl, T., Miller, M.A.E., Križan, J., Shepherd, K.D., Sila, A., Kilibarda, M., Antonijević, O., Glušica, L., Dobermann, A., Haefele, S.M., McGrath, S.P., Acquah, G.E., Collinson, J., Parente, L., Sheykhmousa, M., Saito, K., Johnson, J.M., Chamberlin, J., Silatsa, F.B.T., Yemefack, M., Wendt, J., MacMillan, R.A., Wheeler, I., Crouch, J., 2021. African soil properties and nutrients mapped at 30 m spatial resolution using two-scale ensemble machine learning. *Sci. Rep. 11*, 1–18. https://doi.org/10.1038/s41598-021-85639-y

Hengl, T., Nussbaum, M., Wright, M.N., Heuvelink, G.B.M., Gräler, B., 2018. Random forest as a generic framework for predictive modeling of spatial and spatio-temporal variables. *PeerJ 6*, e5518. https://doi.org/10.7717/peerj.5518

Hobson, K.A., Kusack, J.W., Mora-Alvarez, B.X., 2021. Origins of six species of butterflies migrating through northeastern mexico: New insights from stable isotope (δ2h) analyses and a call for documenting butterfly migrations. *Diversity 13*, 1–13. https://doi.org/10.3390/d13030102

Hobson, K.A., Plint, T., Serrano, E.G., Alvarez, X.M., Ramirez, I., Longstaffe, F.J., 2017. Within-wing isotopic (δ2H, δ13C, δ15N) variation of monarch butterflies: implications for studies of migratory origins and diet. *Anim. Migr. 4*. https://doi.org/10.1515/ami-2017-0002

Hobson, K.A., Wassenaar, L.I., Taylor, O.R., 1999. Stable isotopes (δD and δ13C) are geographic indicators of natal origins of monarch butterflies in eastern North America. *Oecologia 120*, 397–404. https://doi.org/10.1007/s004420050872

Hu, G., Stefanescu, C., Oliver, T.H., Roy, D.B., Brereton, T., Van Swaay, C., Reynolds, D.R., Chapman, J.W., 2021. Environmental drivers of annual population fluctuations in a trans-Saharan insect migrant. Proc. *Natl. Acad. Sci. U. S. A. 118*. https://doi.org/10.1073/pnas.2102762118

Hu, L., Chartrand, M.M.G., St-Jean, G., Lopes, M., Bataille, C.P., 2020. Assessing the Reliability of Mobility Interpretation From a Multi-Isotope Hair Profile on a Traveling Individual. *Front. Ecol. Evol. 8*. https://doi.org/10.3389/fevo.2020.568943

Janzen, A., Bataille, C., Copeland, S.R., Quinn, R.L., Ambrose, S.H., Reed, D., Hamilton, M., Grimes, V., Richards, M.P., le Roux, P., Roberts, P., 2020. Spatial variation in bioavailable strontium isotope ratios ($^{87}Sr/^{86}Sr$) in Kenya and northern Tanzania: Implications for ecology, paleoanthropology, and archaeology. *Palaeogeogr. Palaeoclimatol. Palaeoecol. 560*, 109957. https://doi.org/10.1016/j.palaeo.2020.109957

Jarvis, A., Reuter, H.I., Nelson, A., Guevara, E., 2008. Hole-filled SRTM for the globe Version 4, available from the CGIAR-CSI SRTM 90m Database, http://srtm.csi.cgiar.org.

Jiguet, F., Burgess, M., Thorup, K., Conway, G., Arroyo Matos, J.L., Barber, L., Black, J., Burton, N., Castelló, J., Clewley, G., Copete, J.L., Czajkowski, M.A., Dale, S., Davis, T., Dombrovski, V., Drew, M., Elts, J., Gilson, V., Grzegorczyk, E., Henderson, I., Holdsworth, M., Husbands, R., Lorrilliere, R., Marja, R., Minkevicius, S., Moussy, C., Olsson, P., Onrubia, A., Pérez, M., Piacentini, J., Piha, M., Pons, J.-M., Procházka, P., Raković, M., Robins, H., Seimola, T., Selstam, G., Skierczyński, M., Sondell, J., Thibault, J.-C., Tøttrup, A.P., Walker, J., Hewson, C., 2019a. Desert crossing strategies of migrant songbirds vary between and within species. *Sci. Rep. 9*, 20248. https://doi.org/10.1038/s41598-019-56677-4

Jiguet, F., Robert, A., Lorrillière, R., Hobson, K.A., Kardynal, K.J., Arlettaz, R., Bairlein, F., Belik, V., Bernardy, P., Copete, J.L., Czajkowski, M.A., Dale, S., Dombrovski, V., Ducros, D., Efrat, R., Elts, J., Ferrand, Y., Marja, R., Minkevicius, S., Olsson, P., Pérez, M., Piha, M., Raković, M., Schmaljohann, H., Seimola, T., Selstam, G., Siblet, J.-P., Skierczyǹski, M.,

Sokolov, A., Sondell, J., Moussy, C., 2019b. Unravelling migration connectivity reveals unsustainable hunting of the declining ortolan bunting. *Sci. Adv. 5*. https://doi.org/10.1126/sciadv.aau2642

Klaassen, R.H.G., Hake, M., Strandberg, R., Koks, B.J., Trierweiler, C., Exo, K.-M., Bairlein, F., Alerstam, T., 2014. When and where does mortality occur in migratory birds? Direct evidence from long-term satellite tracking of raptors. *J. Anim. Ecol. 83*, 176–184. https://doi.org/10.1111/1365-2656.12135

Knight, E.C., Harrison, A., Scarpignato, A.L., Van Wilgenburg, S.L., Bayne, E.M., Ng, J.W., Angell, E., Bowman, R., Brigham, R.M., Drolet, B., Easton, W.E., Forrester, T.R., Foster, J.T., Haché, S., Hannah, K.C., Hick, K.G., Ibarzabal, J., Imlay, T.L., Mackenzie, S.A., Marsh, A., McGuire, L.P., Newberry, G.N., Newstead, D., Sidler, A., Sinclair, P.H., Stephens, J.L., Swanson, D.L., Tremblay, J.A., Marra, P.P., 2021. Comprehensive estimation of spatial and temporal migratory connectivity across the annual cycle to direct conservation efforts. *Ecography (Cop.)*. 44, 665–679. https://doi.org/10.1111/ecog.05111

Koleček, J., Procházka, P., El-Arabany, N., Tarka, M., Ilieva, M., Hahn, S., Honza, M., de la Puente, J., Bermejo, A., Gürsoy, A., Bensch, S., Zehtindjiev, P., Hasselquist, D., Hansson, B., 2016. Cross-continental migratory connectivity and spatiotemporal migratory patterns in the great reed warbler. *J. Avian Biol. 47*, 756–767. https://doi.org/10.1111/jav.00929

Kramer, R.T., Kinaston, R.L., Holder, P.W., Armstrong, K.F., King, C.L., Sipple, W.D.K., Martin, A.P., Pradel, G., Turnbull, R.E., Rogers, K.M., Reid, M., Barr, D., Wijenayake, K.G., Buckley, H.R., Stirling, C.H., Bataille, C.P., 2022. A bioavailable strontium ($^{87}Sr/^{86}Sr$) isoscape for Aotearoa New Zealand: Implications for food forensics and biosecurity. *PLoS One 17*, e0264458. https://doi.org/10.1371/journal.pone.0264458

Kuhn, M., 2008. Building predictive models in R using the caret package. *J. Stat. Softw. 28*, 1–26. https://doi.org/10.18637/jss.v028.i05

Larsen, T., 1975. Provisional notes of migrant butterflies in Lebanon. Atlanta 6.

Larsen, T.B., 1984. The Zoogeographical Composition and Distribution of the Arabian Butterflies (Lepidoptera; Rhopalocera). *J. Biogeogr. 11*, 119. https://doi.org/10.2307/2844685

Lindroos, E.E., Bataille, C.P., Holder, P.W., Talavera, G., Reich, M.S., 2023. Temporal stability of δ^2H in insect tissues: Implications for isotope-based geographic assignments. *Front. Ecol. Evol. 11*, 1–12. https://doi.org/10.3389/fevo.2023.1060836

Lok, T., Overdijk, O., Piersma, T., 2015. The cost of migration: spoonbills suffer higher mortality during trans-Saharan spring migrations only. *Biol. Lett. 11*, 20140944. https://doi.org/10.1098/rsbl.2014.0944

López-Mañas, R., Pascual-Díaz, J.P., García-Berro, A., Bahleman, F., Reich, M.S., Pokorny, L., Bataille, C.P., Vila, R., Domingo-Marimon, C., Talavera, G., 2022. Erratic spatiotemporal vegetation growth anomalies drive population outbreaks in a trans-Saharan insect migrant. *Proc. Natl. Acad. Sci. U. S. A. 119*, 3–5. https://doi.org/10.1073/pnas.2121249119

Lu, B., Hardin, J., 2022. A Unified Framework for Random Forest Prediction Error Estimation [WWW Document]. URL chrome-extension://efaidnbmnnnibpcajpcglclefindmkaj/https://cran.r-project.org/web/packages/forestError/forestError.pdf (accessed 8.24.23).

Lv, H., Zhai, M., Zeng, J., Zhang, Y., Zhu, F., Shen, H., Qiu, K., Gao, B., Reynolds, D.R., Chapman, J.W., Hu, G., 2023. Changing patterns of the East Asian monsoon drive shifts in migration and abundance of a globally important rice pest. *Glob. Chang. Biol. 29*, 2655–2668. https://doi.org/10.1111/gcb.16636

Ma, C., Vander Zanden, H.B., Wunder, M.B., Bowen, G.J., 2020. assignR: An r package for isotope-based geographic assignment. *Methods Ecol. Evol. 11*, 996–1001. https://doi.org/10.1111/2041-210X.13426

Magozzi, S., Bataille, C.P., Hobson, K.A., Wunder, M.B., Howa, J.D., Contina, A., Vander Zanden, H.B., Bowen, G.J., 2021. Calibration chain transformation improves the comparability of organic hydrogen and oxygen stable isotope data. *Methods Ecol. Evol. 12*, 732–747. https://doi.org/10.1111/2041-210X.13556

Marcacci, G., Briedis, M., Diop, N., Diallo, A.Y., Kebede, F., Jacot, A., 2023. A roadmap integrating research, policy, and actions to conserve Afro-Palearctic migratory landbirds at a flyway scale. *Conserv. Lett. 16*. https://doi.org/10.1111/conl.12933

Marx, M., Korner-Nievergelt, F., Quillfeldt, P., 2016. Analysis of Ring Recoveries of European Turtle Doves Streptopelia turtur — Flyways, Migration Timing and Origin Areas of Hunted Birds. Acta *Ornithol. 51*, 55–70. https://doi.org/10.3161/00016454AO2016.51.1.005

Meier-Augenstein, W., Chartrand, M.M.G., Kemp, H.F., St-Jean, G., 2011. An inter-laboratory comparative study into sample preparation for both reproducible and repeatable forensic 2 H isotope analysis of human hair by continuous flow isotope ratio mass spectrometry. Rapid *Commun. Mass Spectrom. 25*, 3331–3338. https://doi.org/10.1002/rcm.5235

Menchetti, M., Guéguen, M., Talavera, G., 2019. Spatio-temporal ecological niche modelling of multigenerational insect migrations. *Proc. R. Soc. B Biol. Sci. 286*. https://doi.org/10.1098/rspb.2019.1583

Meynard, C.N., Gay, P.E., Lecoq, M., Foucart, A., Piou, C., Chapuis, M.P., 2017. Climate-driven geographic distribution of the desert locust during recession periods: Subspecies' niche differentiation and relative risks under scenarios of climate change. Glob. *Chang. Biol. 23*, 4739–4749. https://doi.org/10.1111/gcb.13739

Mooney, W.D., Laske, G., Masters, T.G., 1998. CRUST 5.1: A global crustal model at 5° × 5°. J. *Geophys. Res. 103*, 727–747. https://doi.org/10.1029/97jb02122

Moore, L.J., Murphy, T.J., Barnes, I.L., Paulsen, P.J., 1982. Absolute Isotopic Abundance Ratios and Atomic Weight of a Reference Sample of Strontium. J. *Res. Natl. Bur. Stand. (1934). 87*, 1. https://doi.org/10.6028/jres.087.001

Morrison, C.A., Alves, J.A., Gunnarsson, T.G., Þórisson, B., Gill, J.A., 2019. Why do earlier-arriving migratory birds have better breeding success? *Ecol. Evol. 9*, 8856–8864. https://doi.org/10.1002/ece3.5441

Nelson, D.M., Braham, M., Miller, T.A., Duerr, A.E., Cooper, J., Lanzone, M., Lemaître, J., Katzner, T., 2015. Stable hydrogen isotopes identify leapfrog migration, degree of connectivity, and summer distribution of Golden Eagles in eastern North America. Condor 117, 414–429. https://doi.org/10.1650/CONDOR-14-209.1

Newton, I., 2007. Weather-related mass-mortality events in migrants. Ibis (Lond. 1859). 149, 453–467. https://doi.org/10.1111/j.1474-919X.2007.00704.x

Paritte, J.M., Kelly, J.F., 2009. Effect of cleaning regime on stable-isotope ratios of feathers in Japanese quail (Coturnix japonica). Auk 126, 165–174. https://doi.org/10.1525/auk.2009.07187

Pedgley, D.E., Reynolds, D.R., Tatchell, G.M., 1995. Long-range insect migration in relation to climate and weather: Africa and Europe, in: Insect Migration. Cambridge University Press, pp. 3–30. https://doi.org/10.1017/CBO9780511470875.002

Pelton, E.M., Schultz, C.B., Jepsen, S.J., Black, S.H., Crone, E.E., 2019. Western Monarch Population Plummets: Status, Probable Causes, and Recommended Conservation Actions. *Front. Ecol. Evol. 7*. https://doi.org/10.3389/fevo.2019.00258

Pittaway, T., 1981. Further notes on the butterflies and hawkmoths (Lepidoptera) of Eastern Saudi Arabia.

Pye, K., 2004. Isotope and trace element analysis of human teeth and bones for forensic purposes. Geol. Soc. London, Spec. Publ. 232, 215–236. https://doi.org/10.1144/GSL.SP.2004.232.01.20

R Core Team, 2023. R: A Language and Environment for Statistical Computing [WWW Document]. URL https://www.r-project.org/ (accessed 5.6.23).

Reich, M. S., Shipilina, D., Talla, V., Bahleman, F., Kébé, K., Berger, J., Backström, N., Talavera, G., Bataille, C. P. (*in prep.*). Intercontinental panmixia despite distinct migratory distances in the trans-Saharan butterfly migrant *Vanessa cardui*.

Reich, M.S., Flockhart, D.T.T., Norris, D.R., Hu, L., Bataille, C.P., 2021. Continuous-surface geographic assignment of migratory animals using strontium isotopes: A case study with monarch butterflies. *Methods Ecol. Evol. 2021*, 1–13. https://doi.org/10.1111/2041-210X.13707

Reppert, S.M., de Roode, J.C., 2018. Demystifying Monarch Butterfly Migration. *Curr. Biol. 28*, R1009–R1022. https://doi.org/10.1016/j.cub.2018.02.067

Salih, A.A.M., Baraibar, M., Mwangi, K.K., Artan, G., 2020. Climate change and locust outbreak in East Africa. *Nat. Clim. Chang. 10*, 584–585. https://doi.org/10.1038/s41558-020-0835-8

Sanderson, F.J., Donald, P.F., Pain, D.J., Burfield, I.J., van Bommel, F.P.J., 2006. Long-term population declines in Afro-Palearctic migrant birds. *Biol. Conserv. 131*, 93–105. https://doi.org/10.1016/j.biocon.2006.02.008

Satterfield, D.A., Sillett, T.S., Chapman, J.W., Altizer, S., Marra, P.P., 2020. Seasonal insect migrations: massive, influential, and overlooked. *Front. Ecol. Environ. 18*, 335–344. https://doi.org/10.1002/fee.2217

Schmaljohann, H., Liechti, F., Bruderer, B., 2007. Songbird migration across the Sahara: the non-stop hypothesis rejected! *Proc. R. Soc. B Biol. Sci. 274*, 735–739. https://doi.org/10.1098/rspb.2006.0011

Serna, A., Prates, L., Mange, E., Salazar-García, D.C., Bataille, C.P., 2020. Implications for paleomobility studies of the effects of quaternary volcanism on bioavailable strontium: A test case in North Patagonia (Argentina). *J. Archaeol. Sci. 121*, 105198. https://doi.org/10.1016/j.jas.2020.105198

Somveille, M., Manica, A., Rodrigues, A.S.L., 2019. Where the wild birds go: explaining the differences in migratory destinations across terrestrial bird species. *Ecography (Cop.). 42*, 225–236. https://doi.org/10.1111/ecog.03531

Stefanescu, C., Alarcón, M., Izquierdo, R., Páramo, F., Àvila, A., 2011. Moroccan Source Areas of the Painted Lady Butterfly Vanessa cardui (Nymphalidae: Nymphalinae) Migrating into Europe in *Spring. J. Lepid. Soc. 65*, 15–26. https://doi.org/10.18473/lepi.v65i1.a2

Stefanescu, C., ASKEW, R.R., CORBERA, J., SHAW, M.R., 2012. Parasitism and migration in southern Palaearctic populations of the painted lady butterfly, *Vanessa cardui* (Lepidoptera: Nymphalidae). Eur. J. Entomol. 109, 85–94. https://doi.org/10.14411/eje.2012.011

Stefanescu, C., Paramo, F., 2010. Frogs eat butterflies: Temporary prey-specialization on the Painted Lady butterfly, Vanessa cardui, by Sahara frog, Pelophylax saharicus, in the Moroccan Anti Atlas. Nota Lepid. 127–131.

Stefanescu, C., Páramo, F., Åkesson, S., Alarcón, M., Ávila, A., Brereton, T., Carnicer, J., Cassar, L.F., Fox, R., Heliölä, J., Hill, J.K., Hirneisen, N., Kjellén, N., Kühn, E., Kuussaari, M., Leskinen, M., Liechti, F., Musche, M., Regan, E.C., Reynolds, D.R., Roy, D.B., Ryrholm, N., Schmaljohann, H., Settele, J., Thomas, C.D., van Swaay, C., Chapman, J.W., 2013. Multi-generational long-distance migration of insects: Studying the painted lady butterfly in the Western Palaearctic. *Ecography (Cop.). 36*, 474–486. https://doi.org/10.1111/j.1600-0587.2012.07738.x

Stefanescu, C., Soto, D.X., Talavera, G., Vila, R., Hobson, K.A., 2016. Long-distance autumn migration across the Sahara by painted lady butterflies: Exploiting resource pulses in the tropical savannah. *Biol. Lett. 12*, 6–9. https://doi.org/10.1098/rsbl.2016.0561

Stefanescu, C., Ubach, A., Wiklund, C., 2021. Timing of mating, reproductive status and resource availability in relation to migration in the painted lady butterfly. *Anim. Behav. 172*, 145–153. https://doi.org/10.1016/j.anbehav.2020.12.013

Suchan, T., Bataille, C. P., Reich, M. S., Toro-Delgado, E., Vila, R., Pierce, N. E., Talavera, G. (*in review*). A trans-oceanic flight of 1 over 4,200 km by painted lady butterflies

Talavera, G., Bataille, C., Benyamini, D., Gascoigne-Pees, M., Vila, R., 2018. Round-trip across the Sahara: Afrotropical Painted Lady butterflies recolonize the Mediterranean in early spring. *Biol. Lett. 14*. https://doi.org/10.1098/rsbl.2018.0274

Talavera, G., García-Berro, A., N K Talla, V., Bahleman, F., Kébé, K., 2023. The Afrotropical breeding grounds of the Palearctic-African migratory painted lady butterflies (*Vanessa cardui*). *Proc. Natl. Acad. Sci. 120*, 10. https://doi.org/10.1073/pnas

Talavera, G., Vila, R., 2017. Discovery of mass migration and breeding of the painted lady butterfly *Vanessa cardui* in the Sub-Sahara: The Europe-Africa migration revisited. *Biol. J. Linn. Soc. 120*, 274–285. https://doi.org/10.1111/bij.12873

Taylor, C.M., Norris, D.R., 2010. Population dynamics in migratory networks. *Theor. Ecol. 3*, 65–73. https://doi.org/10.1007/s12080-009-0054-4

Tessnow, A.E., Nagoshi, R.N., Meagher, R.L., Fleischer, S.J., 2023. Revisiting fall armyworm population movement in the United States and Canada. *Front. Insect Sci. 3*. https://doi.org/10.3389/finsc.2023.1104793

Trabucco, A., Zomer, R., 2019. Global Aridity Index and Potential Evapotranspiration (ET0) Climate Database v2. figshare. Fileset.

van der Merwe, N.J., Lee-Thorp, J.A., Thackeray, J.F., Hall-Martin, A., Kruger, F.J., Coetzee, H., Bell, R.H. V., Lindeque, M., 1990. Source-area determination of elephant ivory by isotopic analysis. *Nature 346*, 744–746. https://doi.org/10.1038/346744a0

Vandenbosch, R., 2007. What do monarch population time series tell us about eastern and western population mixing? *J. Lepid. Soc. 61*, 28–31.

Vickery, J.A., Ewing, S.R., Smith, K.W., Pain, D.J., Bairlein, F., Škorpilová, J., Gregory, R.D., 2014. The decline of Afro-Palaearctic migrants and an assessment of potential causes. Ibis (Lond. 1859). 156, 1–22. https://doi.org/10.1111/ibi.12118

Wang, X., Bocksberger, G., Lautenschläger, T., Finckh, M., Meller, P., O'Malley, G.E., Oelze, V.M., 2023. A bioavailable strontium isoscape of Angola with implications for the archaeology of the transatlantic slave trade. *J. Archaeol. Sci. 154*. https://doi.org/10.1016/j.jas.2023.105775

Wassenaar, L.I., Hobson, K.A., 1998. Natal origins of migratory monarch butterflies at wintering colonies in Mexico: New isotopic evidence. Proc. Natl. Acad. Sci. U. S. A. 95, 15436–15439. https://doi.org/10.1073/pnas.95.26.15436

Webster, M.S., Marra, P.P., Haig, S.M., Bensch, S., Holmes, R.T., 2002. Links between worlds: unraveling migratory connectivity. *Trends Ecol. Evol. 17*, 76–83. https://doi.org/10.1016/S0169-5347(01)02380-1

Zylstra, E.R., Ries, L., Neupane, N., Saunders, S.P., Ramírez, M.I., Rendón-Salinas, E., Oberhauser, K.S., Farr, M.T., Zipkin, E.F., 2021. Changes in climate drive recent monarch butterfly dynamics. *Nat. Ecol. Evol. 5*, 1441–1452. https://doi.org/10.1038/s41559-021-01504-1

Conclusion

Summary

A strong relationship was found between δ^2H in resident butterfly wings and δ^2H in the growing season precipitation isoscape, facilitating the construction of an insect wing-specific isoscape across the Afro-Palearctic range. The tissue-specific δ^2H isoscape displayed strong gradients between the Palearctic and Afro-tropic realms, holding promise for studies focused on tracking the long-distance migration or one-way dispersal of insect species at a trans-continental scale. This study identified the controls of hydrogen isoscape uncertainty, highlighting the significant influence of high evaporation rates and relative humidity which can increase spatial uncertainty and reduce hydrogen's specificity as a provenance tracer.

The most accurate $^{87}Sr/^{86}Sr$ predictions in bioavailable strontium was generated for the Afro-Palearctic range using the latest climatic geospatial data. This research demonstrated that spatial interpolation ensemble machine learning outperformed the random forest regression framework in predicting bioavailable $^{87}Sr/^{86}Sr$. The framework using spatial interpolation ensemble machine learning, provided a more precise assessment of uncertainty, resulting in a spatially explicit map with reduced variability. While the process of mapping bioavailable strontium isoscapes is still evolving (Holt et al., 2021), my study's contribution in developing a new framework using ensemble machine learning has advanced this field.

Finally, my study employed dual δ^2H and $^{87}Sr/^{86}Sr$ -based geographic assignments to unravel the spatiotemporal trans-Saharan migratory connectivity of *Vanessa cardui*. Through this approach, valuable insights into the species migratory behavior were obtained during both northward and southward movements. The study revealed connectivity patterns that are moderate among butterflies migrating between the Palearctic and Afrotropical regions with a more pronounced latitudinal influence rather than a longitudinal one. Notably, my isoscapes led to the identification of the phenomenon of leapfrog migration in *Vanessa cardui*'s southward migration, mirroring patterns observed in vertebrates. This discovery represents one of the first documented instances of leapfrog migration in insects with implications for the understanding of migratory behaviour and patterns, as well as conservation.

Limitations of our study

While this study has provided valuable tools for insect dispersal and migration patterns in the Afro-Palearctic region, it is essential to acknowledge several limitations. For hydrogen isotopes, significant uncertainty of the model predictions persists in various tropical areas, primarily due to the need for improved precipitation δ^2H data and more known-origin δ^2H data across the African continent (Gutiérrez-Expósito et al., 2015; Seifert et al., 2018). These efforts will enable us to better capture hydrogen's isotopic heterogeneity and significantly enhance the precision of geographic assignments. Additionally, incorporating more refined modeling of δ^2H variations within this region that will account for monthly resolution climate variability could further enhance the accuracy of geographic assignments. My research highlights a substantial intra-site δ^2H variation, emphasizing the key intrinsic limitations of using hydrogen isotopes as an insect geolocation tool particularly in tropical regions. This intra-site isotopic variability poses a considerable challenge in achieving higher levels of geolocation precision.

For strontium isotopes, Africa has a notably limited amount of bioavailable $^{87}Sr/^{86}Sr$ data compared to the Palearctic, which likely introduces significant geographic biases and results in a lack of predictive power across the African continent (Bataille et al., 2020). While machine learning offers the potential to create isoscapes over large areas, these models still require accurate local data for effective training and usability in addressing specific research questions. Also, there may be issues with incorporating geological data into isoscapes, because older rocks have been found to have increasingly diverse $^{87}Sr/^{86}Sr$ ratios (Bataille et al., 2020) making it difficult to predict in the absence of empirical testing. Lastly, even at a regional scale, $^{87}Sr/^{86}Sr$ are almost never unique which implies that strontium isotope analysis by itself is insufficient to fully answer research questions (Holt et al., 2021).

For the case study, areas of natal origin identified through dual assignments can remain quite large. In some instances, the geographic assignments displayed extensive potential areas of origin, primarily due to the high redundancy of certain isotope signatures across the landscape. Such unspecific estimates of natal origin may introduce inaccuracies such as poor estimates of migration distance (Hallworth et al., 2018). Even with the dual isotope framework, geographic assignments are not constrained enough spatially. Isotope geolocation evidence should, in

general, be interpreted in conjunction with other evidence to further refine geolocation precision. These may include ecological niche modeling (Menchetti et al., 2019), pollen metabarcoding analysis (Suchan et al., 2019), wind trajectory modeling (Åkesson et al., 2016), and the incorporation of additional isotopes. Triple or quadruple isotope studies have been found to be more effective for provenancing biological materials (e.g., Bataille et al., 2021; Hobson et al., 2012b; Veen et al., 2014). By pursuing these research directions, we can deepen our understanding of insect movement, support conservation efforts, and have strong evidence-based management strategies for the Afro-Palearctic region.

Future work and perspectives

My novel hydrogen and strontium isoscapes provided valuable tools to investigate the migration and connectivity of *V. cardui* individuals across the Sahara Desert. Looking forward, my study has opened up exciting possibilities for future research. Many questions regarding the ecology and behavioral adaptations of insects crossing the Sahara remain unanswered. Future studies could explore various legs of *V. cardui*'s migration cycle.

My δ^2H isoscapes could be applied to various other insect studies, including tracing forest pest movements across European forest (Muñoz-Adalia and Colinas, 2020), mapping long-distance migration routes of butterflies (e.g., Chapman et al., 2015; Hawkes et al., 2022), and assessing the impacts of climate change on the mobility of long-distance migratory insect populations. While strontium isotopes could be applied in combination with hydrogen isotopes for the applications mentioned above, the applications of our novel strontium isoscape extend beyond entomology. They hold immense potential in fields like archaeology (Copeland et al., 2011). For example, strontium isotopes have been use to reconstruct the movements and history of ancient human populations, such as tracing the origins of African slaves buried in other regions of the word (Wang et al., 2023). Strontium isotopes can also aid paleontologists and paleoecologists in studying prehistoric species' migration (Hamilton et al., 2021). For example, reconstructing paleomigration of extinct and extant megafauna (e.g., wildebeest, elephants) might help understand the drivers of their population decline or of their extinction with key lessons for the future. The field of food science can use strontium isoscapes to determine the origins of food products from Africa (e.g., coffee, cocoa), enhancing traceability for fair-trade

and quality control (Voerkelius et al., 2010). Lastly, my strontium isoscape can play a vital role in forensic science, helping identify the poaching or trade of illegal material from Africa (e.g., drugs, ivory, wood) (Van Der Merwe et al., 1990) or the identification of human remains (Degryse et al., 2012).

Appendix

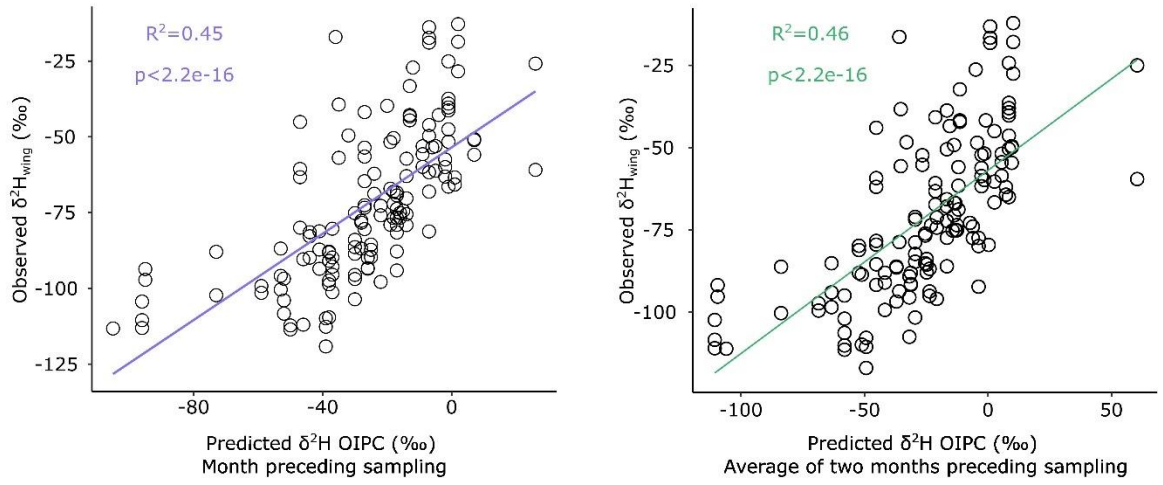

Figure S1.7. Linear model between δ^2H_{wing} and δ^2H values of monthly precipitation isoscapes using The Online Isotopes in Precipitation Calculator (OIPC v3.1) A. Predicted δ^2H from OIPC v3.2 (‰) for one month preceding sampling, B. Predicted δ^2H from OIPC v3.2 (‰) for the average of two months preceding sampling

Table S1.2. | Known-origin dataset (including outliers). Metadata includes sample ID, genus and species, sampling date (month, date and year), country of sampling, elevation of sampling site (m), latitude and longitude (decimal degree) and δ^2H values (‰).

(All data can be downloaded from the supporting information here: Ghouri, Sana, et al. "A Hydrogen Isoscape for Tracing the Migration of Herbivorous Lepidopterans across the Afro-Palearctic Range." Rapid Communications in Mass Spectrometry, vol. 38, no. 3, 2024, p. e9675, https://doi.org/10.1002/rcm.9675)

Table S2.1. | Template with newly compiled bioavailable $^{87}Sr/^{86}Sr$ ratio database across the Afro-Palearctic based on Bataille et al. 2020 with the locality name of collection, sample type, sampling date (month, date and year) their associated $^{87}Sr/^{86}Sr$ ratio, geographic coordinates of latitude and longitude (Decimal Degree), method details and source of data. This template is designed for the upload of new $^{87}Sr/^{86}Sr$ data and their associated metadata.

(All data can be downloaded from here: https://isobank.tacc.utexas.edu/)

Table S2.4. | Capture date and location of each painted lady sample (n = 118) and the hydrogen isotope value (δ^2H) and strontium isotope ratio (^{87}Sr/^{86}Sr) measured in the wing tissue.

ID	Date	Country	δ^2H	δ^2H publication	^{87}Sr/^{86}Sr	Analytical Uncertainty (δ^2H and ^{87}Sr/^{86}Sr)	^{87}Sr/^{86}Sr publication
GTcoll19B405	22.III.2019	Cyprus	-46	this study	0.7084	2 std	this study
GTcoll19B407	22.III.2019	Cyprus	-34	this study	0.70887	2 std	this study
GTcoll19B408	22.III.2019	Cyprus	-41	this study	0.70846	2 std	this study
GTcoll19B412	5.IV.2019	Cyprus	-27	this study	0.70949	2 std	this study
GTcoll19D088	19.III.2019	Italy	-40	this study	0.71094	2 std	this study
GTcoll19D089	19.III.2019	Italy	-43	this study	0.71102	2 std	this study
GTcoll19D125	23.III.2019	Israel	-33	this study	0.70826	2 std	this study
GTcoll19D178	20.III.2019	Israel	-24	this study	0.70897	2 std	this study
GTcoll19D209	21.III.2019	Israel	-27	this study	0.70852	2 std	this study
GTcoll19D268	11.III.2019	Israel	-30	this study	0.70891	2 std	this study
GTcoll19D270	5.IV.2019	Israel	-40	this study	0.70879	2 std	this study
GTcoll19D274	7.IV.2019	Israel	-69	this study	0.70858	2 std	this study
GTcoll19D309	3.III.2019	Israel	-53	this study	0.70924	2 std	this study
GTcoll19D311	8.III.2019	Israel	-16	this study	0.70854	2 std	this study
GTcoll19D347	6.I.2019	Spain	-55	this study	0.70996	2 std	this study
GTcoll19D358	9.I.2019	Spain	-43	this study	0.71072	2 std	this study
GTcoll19D366	14.III.2019	Spain	-39	this study	0.7102	2 std	this study
GTcoll19D421	26.IV.2019	Spain	-55	this study	0.71149	2 std	this study
GTcoll19D505	12.III.2019	Jordan	-17	this study	0.70879	2 std	this study
GTcoll19D509	12.III.2019	Jordan	-40	this study	0.70934	2 std	this study
GTcoll19D635	20.III.2019	Jordan	-32	this study	0.70898	2 std	this study
GTcoll19D639	20.III.2019	Jordan	-19	this study	0.70933	2 std	this study
GTcoll19D727	28.III.2019	Syria	-12	this study	0.7086	2 std	this study

GTcoll19D729	4.IV.2019	Syria	-36	this study	0.70853	2 std	this study
GTcoll19D737	4.IV.2019	Syria	-47	this study	0.70858	2 std	this study
GTcoll19D742	12.IV.2019	Syria	-30	this study	0.70903	2 std	this study
GTcoll19D757	18.IV.2019	Italy	-68	this study	0.7099	2 std	this study
GTcoll19D784	8.IV.2019	Italy	-16	this study	0.70973	2 std	this study
GTcoll19D858	27.IV.2019	Spain	-48	this study	0.70989	2 std	this study
GTcoll19F038	9.III.2019	Spain	-36	this study	0.71327	2 std	this study
GTcoll19F064	9.III.2019	Spain	-50	this study	0.70933	2 std	this study
GTcoll19F065	9.III.2019	Spain	-64	this study	0.71141	2 std	this study
GTcoll19F156	11.IV.2019	Israel	-28	this study	0.70875	2 std	this study
GTcoll19F216	6.XII.2018	Kenya	-26	this study	0.70785	2 std	this study
RVcoll17G997	28.XI.2017	Kenya	-60	this study	0.7079	2 std	this study
RVcoll17H061	29.XI.2017	Kenya	-67	this study	0.70712	2 std	this study
RVcoll17H062	29.XI.2017	Kenya	-51	this study	0.7071	2 std	this study
RVcoll17H084	29.XI.2017	Kenya	-59	this study	0.70843	2 std	this study
RVcoll17H159	30.XI.2017	Kenya	-47	this study	0.70694	2 std	this study
RVcoll17H163	30.XI.2017	Kenya	-51	this study	0.7083	2 std	this study
RVcoll17H173	30.XI.2017	Kenya	-49	this study	0.70782	2 std	this study
RVcoll17H244	1.XII.2017	Kenya	-57	this study	0.70876	2 std	this study
RVcoll17H335	4.XII.2017	Kenya	-65	this study	0.70707	2 std	this study
RVcoll17H342	4.XII.2017	Kenya	-56	this study	0.70699	2 std	this study
RVcoll17H357	4.XII.2017	Kenya	-50	this study	0.70818	2 std	this study
RVcoll17H360	4.XII.2017	Kenya	-69	this study	0.70896	2 std	this study
RVcoll17H384	5.XII.2017	Uganda	-61	this study	0.70834	2 std	this study
RVcoll17H397	6.XII.2017	Uganda	-32	this study	0.71214	2 std	this study
RVcoll17H760	18.XII.2017	Kenya	-40	this study	0.70992	2 std	this study
RVcoll14M265	27.IV.2012	Spain	-49	Talavera et al 2018	0.70915	2 std	this study
RVcoll14M274	28.IV.2012	Spain	-51	Talavera et al 2018	0.7092	2 std	this study
RVcoll14M281	28.IV.2012	Spain	-48	Talavera et al 2018	0.70834	2 std	this study

RVcoll14M282	28.IV.2012	Spain	-49	Talavera et al 2018	0.70896	2 std	this study
RVcoll16C403	24.II.2016	Spain	-57	Talavera et al 2018	0.71086	2 std	this study
RVcoll16C407	23.II.2016	Spain	-58	Talavera et al 2018	0.71088	2 std	this study
RVcoll16C409	25.II.2016	Spain	-38	Talavera et al 2018	0.71036	2 std	this study
RVcoll16C413	16.II.2016	Spain	-25	Talavera et al 2018	0.71066	2 std	this study
RVcoll16C416	25.II.2016	Spain	-47	Talavera et al 2018	0.70982	2 std	this study
RVcoll16C425	16.II.2016	Spain	-35	Talavera et al 2018	0.7121	2 std	this study
RVcoll17A040	24.II.2017	Morocco	-38	Talavera et al 2018	0.70994	2 std	this study
RVcoll17A094	27.II.2017	Morocco	-46	Talavera et al 2018	0.71234	2 std	this study
RVcoll17A114	27.II.2017	Morocco	-53	Talavera et al 2018	0.71015	2 std	this study
RVcoll17A139	28.II.2017	Morocco	-52	Talavera et al 2018	0.70962	2 std	this study
RVcoll17A157	28.II.2017	Morocco	-48	Talavera et al 2018	0.71042	2 std	this study
RVcoll17A159	28.II.2017	Morocco	-43	Talavera et al 2018	0.70932	2 std	this study
RVcoll17A162	28.II.2017	Morocco	-25	Talavera et al 2018	0.71187	2 std	this study
RVcoll17A167	28.II.2017	Morocco	-39	Talavera et al 2018	0.70978	2 std	this study
RVcoll17A173	28.II.2017	Morocco	-49	Talavera et al 2018	0.71063	2 std	this study
RVcoll17A174	28.II.2017	Morocco	-53	Talavera et al 2018	0.71	2 std	this study
RVcoll17A175	28.II.2017	Morocco	-48	Talavera et al 2018	0.70976	2 std	this study
RVcoll17A179	28.II.2017	Morocco	-48	Talavera et al 2018	0.71033	2 std	this study
RVcoll17A184	28.II.2017	Morocco	-35	Talavera et al 2018	0.71083	2 std	this study
RVcoll17A187	28.II.2017	Morocco	-34	Talavera et al 2018	0.71013	2 std	this study
RVcoll17A209	24.II.2017	Morocco	-45	Talavera et al 2018	0.71047	2 std	this study
Rvcoll14T075	3.X.2014	Chad	-71	Stefanescu et al 2016	0.71419	2 std	this study
Rvcoll14T186	5.X.2014	Chad	-85	Stefanescu et al 2016	0.71659	2 std	this study
Rvcoll14T192	5.X.2014	Chad	-71	Stefanescu et al 2016	0.716	2 std	this study
Rvcoll14T202	6.X.2014	Chad	-58	Stefanescu et al 2016	0.715	2 std	this study
Rvcoll14T240	6.X.2014	Chad	-77	Stefanescu et al 2016	0.717	2 std	this study
Rvcoll14T273	7.X.2014	Chad	-48	Stefanescu et al 2016	0.724	2 std	this study
Rvcoll14T280	7.X.2014	Chad	-51	Stefanescu et al 2016	0.717	2 std	this study

Rvcoll14T305	8.X.2014	Chad	-64	Stefanescu et al 2016	0.716	2 std	this study
Rvcoll14T339	10.X.2014	Chad	-49	Stefanescu et al 2016	0.721	2 std	this study
Rvcoll14T366	11.X.2014	Chad	-81	Stefanescu et al 2016	0.716	2 std	this study
Rvcoll14T378	11.X.2014	Chad	-80	Stefanescu et al 2016	0.714	2 std	this study
Rvcoll14T597	21.X.2014	Benin	-71	Stefanescu et al 2016	0.7121	2 std	this study
Rvcoll14T630	21.X.2014	Benin	-56	Stefanescu et al 2016	0.71374	2 std	this study
Rvcoll14T645	22.X.2014	Benin	-81	Stefanescu et al 2016	0.71092	2 std	this study
Rvcoll14T653	22.X.2014	Benin	-78	Stefanescu et al 2016	0.71322	2 std	this study
Rvcoll14T715	22.X.2014	Benin	-85	Stefanescu et al 2016	0.714	2 std	this study
Rvcoll14T867	26.X.2014	Benin	-44	Stefanescu et al 2016	0.7142	2 std	this study
Rvcoll14T876	26.X.2014	Benin	-55	Stefanescu et al 2016	0.71434	2 std	this study
Rvcoll14T967	2.XI.2014	Senegal	-70	Stefanescu et al 2016	0.713	2 std	this study
Rvcoll14U004	4.XI.2014	Senegal	-66	Stefanescu et al 2016	0.714	2 std	this study
Rvcoll14U014	4.XI.2014	Senegal	-68	Stefanescu et al 2016	0.714	2 std	this study
Rvcoll14U016	4.XI.2014	Senegal	-65	Stefanescu et al 2016	0.715	2 std	this study
Rvcoll14U018	4.XI.2014	Senegal	-64	Stefanescu et al 2016	0.714	2 std	this study
Rvcoll14U050	5.XI.2014	Senegal	-59	Stefanescu et al 2016	0.716	2 std	this study
Rvcoll14U061	5.XI.2014	Senegal	-45	Stefanescu et al 2016	0.715	2 std	this study
Rvcoll14U074	6.XI.2014	Senegal	-41	Stefanescu et al 2016	0.716	2 std	this study
GTcoll18B699	8.IX.2018	Senegal	-101	Reich et al in prep	0.71063	2 std	Reich et al in prep
GTcoll18B705	7.IX.2018	Senegal	-86	Reich et al in prep	0.71021	2 std	Reich et al in prep
GTcoll18B720	13.IX.2018	Senegal	-100	Reich et al in prep	0.71438	2 std	Reich et al in prep
GTcoll18B721	13.IX.2018	Senegal	-109	Reich et al in prep	0.71522	2 std	Reich et al in prep
GTcoll18B722	13.IX.2018	Senegal	-69	Reich et al in prep	0.71543	2 std	Reich et al in prep
GTcoll18B773	23.IX.2018	Benin	-84	Reich et al in prep	0.71298	2 std	Reich et al in prep
GTcoll18B774	23.IX.2018	Benin	-81	Reich et al in prep	0.71516	2 std	Reich et al in prep

GTcoll18B775	23.IX.2018	Benin	-76	Reich et al in prep	0.71327	2 std	Reich et al in prep
GTcoll18B782	22.IX.2018	Benin	-79	Reich et al in prep	0.71367	2 std	Reich et al in prep
GTcoll19H115	29.IX.2019	Senegal	-79	Reich et al in prep	0.71013	2 std	Reich et al in prep
GTcoll19H116	29.IX.2019	Senegal	-81	Reich et al in prep	0.70971	2 std	Reich et al in prep
GTcoll19H119	26.X.2019	Senegal	-91	Reich et al in prep	0.7098	2 std	Reich et al in prep
GTcoll19H120	26.X.2019	Senegal	-72	Reich et al in prep	0.71019	2 std	Reich et al in prep
GTcoll19H121	9.XI.2019	Senegal	-65	Reich et al in prep	0.70997	2 std	Reich et al in prep
GTcoll19H128	15.IX.2019	Benin	-83	Reich et al in prep	0.72613	2 std	Reich et al in prep
GTcoll19H129	15.VIII.2019	Benin	-77	Reich et al in prep	0.72074	2 std	Reich et al in prep
GTcoll19H137	9.X.2019	Benin	-83	Reich et al in prep	0.71756	2 std	Reich et al in prep
GTcoll19H140	7.XI.2019	Benin	-84	Reich et al in prep	0.71525	2 std	Reich et al in prep

References

Åkesson, S., Bianco, G., Hedenstrom, A., 2016. Negotiating an ecological barrier: Crossing the Sahara in relation to winds by common swifts. Philos. Trans. R. Soc. B Biol. Sci. 371. https://doi.org/10.1098/rstb.2015.0393

Bataille, C.P., Bowen, G.J., 2012. Mapping 87Sr/ 86Sr variations in bedrock and water for large scale provenance studies. Chem. Geol. 304–305, 39–52. https://doi.org/10.1016/j.chemgeo.2012.01.028

Bataille, C.P., Crowley, B.E., Wooller, M.J., Bowen, G.J., 2020. Advances in global bioavailable strontium isoscapes. Palaeogeogr. Palaeoclimatol. Palaeoecol. 555, 109849. https://doi.org/10.1016/j.palaeo.2020.109849

Bataille, C.P., Jaouen, K., Milano, S., Trost, M., Steinbrenner, S., Crubézy, É., Colleter, R., 2021. Triple sulfur-oxygen-strontium isotopes probabilistic geographic assignment of archaeological remains using a novel sulfur isoscape of western Europe. PLoS One 16, 1–21. https://doi.org/10.1371/journal.pone.0250383

Borisov, S.N., Iakovlev, I.K., Borisov, A.S., Ganin, M.Y., Tiunov, A. V., 2020. Seasonal migrations of pantala flavescens (Odonata: Libellulidae) in middle asia and understanding of the migration model in the afro-asian region using stable isotopes of hydrogen. Insects 11, 1–12. https://doi.org/10.3390/insects11120890

Bowen, G.J., Wassenaar, L.I., Hobson, K.A., 2005. Global application of stable hydrogen and oxygen isotopes to wildlife forensics. Oecologia 143, 337–348. https://doi.org/10.1007/s00442-004-1813-y

Bowen, G.J., West, J.B., 2018. Chapter 3 - Isoscapes for Terrestrial Migration Research, Second Edi. ed, Tracking Animal Migration with Stable Isotopes. Elsevier Inc. https://doi.org/10.1016/B978-0-12-814723-8.00003-9

Brattström, O., Bensch, S., Wassenaar, L.I., Hobson, K.A., Åkesson, S., 2010. Understanding the migration ecology of European red admirals Vanessa atalanta using stable hydrogen isotopes. Ecography (Cop.). 33, 720–729. https://doi.org/10.1111/j.1600-0587.2009.05748.x

Chapman, J.W., Reynolds, D.R., Wilson, K., 2015. Long-range seasonal migration in insects: Mechanisms, evolutionary drivers and ecological consequences. Ecol. Lett. 18, 287–302. https://doi.org/10.1111/ele.12407

Chowdhury, S., Fuller, R.A., Dingle, H., Chapman, J.W., Zalucki, M.P., 2021. Migration in butterflies: a global overview. Biol. Rev. 96, 1462–1483. https://doi.org/10.1111/brv.12714

Clem, C.S., Hobson, K.A., Harmon-Threatt, A.N., 2022. Do Nearctic hover flies (Diptera: Syrphidae) engage in long-distance migration? An assessment of evidence and mechanisms. Ecol. Monogr. 92, 1–20. https://doi.org/10.1002/ecm.1542

Copeland, S.R., Cawthra, H.C., Fisher, E.C., Lee-Thorp, J.A., Cowling, R.M., le Roux, P.J., Hodgkins, J., Marean, C.W., 2016. Strontium isotope investigation of ungulate movement patterns on the Pleistocene Paleo-Agulhas Plain of the Greater Cape Floristic Region, South

Africa. Quat. Sci. Rev. 141, 65–84. https://doi.org/10.1016/j.quascirev.2016.04.002

Copeland, S.R., Sponheimer, M., De Ruiter, D.J., Lee-Thorp, J.A., Codron, D., Le Roux, P.J., Grimes, V., Richards, M.P., 2011. Strontium isotope evidence for landscape use by early hominins. Nature 474, 76–78. https://doi.org/10.1038/nature10149

Degryse, P., De Muynck, D., Delporte, S., Boyen, S., Jadoul, L., De Winne, J., Ivaneanu, T., Vanhaecke, F., 2012. Strontium isotopic analysis as an experimental auxiliary technique in forensic identification of human remains. Anal. Methods 4, 2674–2679. https://doi.org/10.1039/c2ay25035g

Flockhart, D.T., Wassenaar, L.I., Martin, T.G., Hobson, K.A., Wunder, M.B., Norris, D.R., 2013. Tracking multi-generational colonization of the breeding grounds by monarch butterflies in eastern North America. Proc. R. Soc. B Biol. Sci. 280. https://doi.org/10.1098/rspb.2013.1087

Flockhart, D.T.T., Kyser, T.K., Chipley, D., Miller, N.G., Norris, D.R., 2015. Experimental evidence shows no fractionation of strontium isotopes (87Sr/86Sr) among soil, plants, and herbivores: implications for tracking wildlife and forensic science. Isotopes Environ. Health Stud. 51, 372–381. https://doi.org/10.1080/10256016.2015.1021345

Flockhart, T.T., Brower, L.P., Ramirez, M.I., Hobson, K.A., Wassenaar, L.I., Altizer, S., Norris, D.R., 2017. Regional climate on the breeding grounds predicts variation in the natal origin of monarch butterflies overwintering in Mexico over 38 years. Glob. Chang. Biol. 23, 2565–2576. https://doi.org/10.1111/gcb.13589

Gao, B., Hedlund, J., Reynolds, D.R., Zhai, B., Hu, G., Chapman, J.W., 2020. The 'migratory connectivity' concept, and its applicability to insect migrants. Mov. Ecol. 8, 1–13. https://doi.org/10.1186/s40462-020-00235-5

García-Berro, A., Talla, V., Vila, R., Wai, H.K., Shipilina, D., Chan, K.G., Pierce, N.E., Backström, N., Talavera, G., 2023. Migratory behaviour is positively associated with genetic diversity in butterflies. Mol. Ecol. 32, 560–574. https://doi.org/10.1111/mec.16770

Gutiérrez-Expósito, C., Ramírez, F., Afán, I., Forero, M.G., Hobson, K.A., 2015. Toward a deuterium feather isoscape for sub-saharan Africa: Progress, challenges and the path ahead. PLoS One 10, 1–12. https://doi.org/10.1371/journal.pone.0135938

Hallworth, M.T., Marra, P.P., McFarland, K.P., Zahendra, S., Studds, C.E., 2018. Tracking dragons: Stable isotopes reveal the annual cycle of a long-distance migratory insect. Biol. Lett. 14. https://doi.org/10.1098/rsbl.2018.0741

Hamilton, M.I., Fernandez, D.P., Nelson, S. V., 2021. Using strontium isotopes to determine philopatry and dispersal in primates: a case study from Kibale National Park. R. Soc. Open Sci. 8, rsos.200760. https://doi.org/10.1098/rsos.200760

Hawkes, W.L.S., Walliker, E., Gao, B., Forster, O., Lacey, K., Doyle, T., Massy, R., Roberts, N.W., Reynolds, D.R., Özden, Ö., Chapman, J.W., Wotton, K.R., 2022. Huge spring migrations of insects from the Middle East to Europe: quantifying the migratory assemblage and ecosystem services. Ecography (Cop.). 2022, 1–15. https://doi.org/10.1111/ecog.06288

Hobson, K.A., 2008. Applying Isotopic Methods to Tracking Animal Movements. Terr. Ecol. 2,

45–78. https://doi.org/10.1016/S1936-7961(07)00003-6

Hobson, K.A., Kardynal, K.J., Koehler, G., 2019. Expanding the isotopic toolbox to track monarch butterfly (Danaus plexippus) origins and migration: On the utility of stable oxygen isotope (δ18O) measurements. Front. Ecol. Evol. 7, 1–8. https://doi.org/10.3389/fevo.2019.00224

Hobson, K.A., Soto, D.X., Paulson, D.R., Wassenaar, L.I., Matthews, J.H., 2012a. A dragonfly (δ2h) isoscape for North America: A new tool for determining natal origins of migratory aquatic emergent insects. Methods Ecol. Evol. 3, 766–772. https://doi.org/10.1111/j.2041-210X.2012.00202.x

Hobson, K.A., Van Wilgenburg, S.L., Wassenaar, L.I., Powell, R.L., Still, C.J., Craine, J.M., 2012b. A multi-isotope (δ 13 C, δ 15 N, δ 2 H) feather isoscape to assign Afrotropical migrant birds to origins. Ecosphere 3, art44. https://doi.org/10.1890/es12-00018.1

Hobson, K.A., Wassenaar, L.I., Taylor, O.R., 1999. Stable isotopes (δD and δ13C) are geographic indicators of natal origins of monarch butterflies in eastern North America. Oecologia 120, 397–404. https://doi.org/10.1007/s004420050872

Holder, P.W., Armstrong, K., Van Hale, R., Millet, M.A., Frew, R., Clough, T.J., Baker, J.A., 2014. Isotopes and trace elements as natal origin markers of Helicoverpa armigera - An experimental model for biosecurity pests. PLoS One 9, 1–13. https://doi.org/10.1371/journal.pone.0092384

Holt, E., Evans, J.A., Madgwick, R., 2021. Strontium (87Sr/86Sr) mapping: A critical review of methods and approaches. Earth-Science Rev. 216, 103593. https://doi.org/10.1016/j.earscirev.2021.103593

Hu, G., Lim, K.S., Horvitz, N., Clark, S.J., Reynolds, D.R., Sapir, N., Chapman, J.W., 2016. Mass seasonal bioflows of high-flying insect migrants. Science (80-.). 354, 1584–1587. https://doi.org/10.1126/science.aah4379

Janzen, A., Bataille, C., Copeland, S.R., Quinn, R.L., Ambrose, S.H., Reed, D., Hamilton, M., Grimes, V., Richards, M.P., le Roux, P., Roberts, P., 2020. Spatial variation in bioavailable strontium isotope ratios (87Sr/86Sr) in Kenya and northern Tanzania: Implications for ecology, paleoanthropology, and archaeology. Palaeogeogr. Palaeoclimatol. Palaeoecol. 560, 109957. https://doi.org/10.1016/j.palaeo.2020.109957

Lindroos, E.E., Bataille, C.P., Holder, P.W., Talavera, G., Reich, M.S., 2023. Temporal stability of δ2H in insect tissues: Implications for isotope-based geographic assignments. Front. Ecol. Evol. 11, 1–12. https://doi.org/10.3389/fevo.2023.1060836

Magozzi, S., Vander Zanden, H.B., Wunder, M.B., Bowen, G.J., 2019. Mechanistic model predicts tissue–environment relationships and trophic shifts in animal hydrogen and oxygen isotope ratios. Oecologia 191, 777–789. https://doi.org/10.1007/s00442-019-04532-8

Menchetti, M., Guéguen, M., Talavera, G., 2019. Spatio-temporal ecological niche modelling of multigenerational insect migrations. Proc. R. Soc. B Biol. Sci. 286. https://doi.org/10.1098/rspb.2019.1583

Menz, M.H.M., Reynolds, D.R., Gao, B., Hu, G., Chapman, J.W., Wotton, K.R., 2019.

Mechanisms and Consequences of Partial Migration in Insects. Front. Ecol. Evol. 7, 1–9. https://doi.org/10.3389/fevo.2019.00403

Muñoz-Adalia, E.J., Colinas, C., 2020. The invasive moth Paysandisia archon in Europe: Biology and control options. J. Appl. Entomol. 144, 341–350. https://doi.org/10.1111/jen.12746

Newton, J., 2021. An insect isoscape of UK and Ireland. Rapid Commun. Mass Spectrom. 35, 1–8. https://doi.org/10.1002/rcm.9126

Qin, Z., Shi, J., 2020. Feasibility of species origin traceability by hydrogen stable isotopes: Sample case of lymantria dispar l. (lepidoptera: Erebidae). Forests 11, 1–10. https://doi.org/10.3390/f11111209

Reich, M.S., Flockhart, D.T.T., Norris, D.R., Hu, L., Bataille, C.P., 2021. Continuous-surface geographic assignment of migratory animals using strontium isotopes: A case study with monarch butterflies. Methods Ecol. Evol. 2021, 1–13. https://doi.org/10.1111/2041-210X.13707

Reichlin, T.S., Hobson, K.A., Van Wilgenburg, S.L., Schaub, M., Wassenaar, L.I., Martín-Vivaldi, M., Arlettaz, R., Jenni, L., 2013. Conservation through connectivity: Can isotopic gradients in Africa reveal winter quarters of a migratory bird? Oecologia 171, 591–600. https://doi.org/10.1007/s00442-012-2418-5

Satterfield, D.A., Sillett, T.S., Chapman, J.W., Altizer, S., Marra, P.P., 2020. Seasonal insect migrations: massive, influential, and overlooked. Front. Ecol. Environ. 18, 335–344. https://doi.org/10.1002/fee.2217

Seifert, N., Ambrosini, R., Bontempo, L., Camin, F., Liechti, F., Rubolini, D., Scandolara, C., Saino, N., Hahn, S., 2018. Matching geographical assignment by stable isotopes with African non-breeding sites of barn swallows Hirundo rustica tracked by geolocation. PLoS One 13, 1–16. https://doi.org/10.1371/journal.pone.0202025

Suchan, T., Talavera, G., Sáez, L., Ronikier, M., Vila, R., 2019. Pollen metabarcoding as a tool for tracking long-distance insect migrations. Mol. Ecol. Resour. 19, 149–162. https://doi.org/10.1111/1755-0998.12948

Talavera, G., Bataille, C., Benyamini, D., Gascoigne-Pees, M., Vila, R., 2018. Round-trip across the Sahara: Afrotropical Painted Lady butterflies recolonize the Mediterranean in early spring. Biol. Lett. 14. https://doi.org/10.1098/rsbl.2018.0274

Talavera, G., García-Berro, A., N K Talla, V., Bahleman, F., Kébé, K., 2023. The Afrotropical breeding grounds of the Palearctic-African migratory painted lady butterflies (Vanessa cardui). Proc. Natl. Acad. Sci. 120, 10. https://doi.org/10.1073/pnas

Talavera, G., Vila, R., 2017. Discovery of mass migration and breeding of the painted lady butterfly Vanessa cardui in the Sub-Sahara: The Europe-Africa migration revisited. Biol. J. Linn. Soc. 120, 274–285. https://doi.org/10.1111/bij.12873

Van Der Merwe, N.J., Lee-Thorp, J.A., Thackeray, J.F., Hall-Martin, A., Kruger, F.J., Coetzee, H., Bell, R.H.V., Lindeque, M., 1990. Source-area determination of elephant ivory by isotopic analysis. Nature 346, 744–746. https://doi.org/10.1038/346744a0

van der Merwe, N.J., Lee-Thorp, J.A., Thackeray, J.F., Hall-Martin, A., Kruger, F.J., Coetzee, H., Bell, R.H. V., Lindeque, M., 1990. Source-area determination of elephant ivory by isotopic analysis. Nature 346, 744–746. https://doi.org/10.1038/346744a0

Vander Zanden, H.B., Wunder, M.B., Hobson, K.A., Van Wilgenburg, S.L., Wassenaar, L.I., Welker, J.M., Bowen, G.J., 2014. Contrasting assignment of migratory organisms to geographic origins using long-term versus year-specific precipitation isotope maps. Methods Ecol. Evol. 5, 891–900. https://doi.org/10.1111/2041-210X.12229

Veen, T., Hjernquist, M.B., Van Wilgenburg, S.L., Hobson, K.A., Folmer, E., Font, L., Klaassen, M., 2014. Identifying the African wintering grounds of hybrid flycatchers using a multi-isotope (δ2H, δ13C, δ 15N) assignment approach. PLoS One 9. https://doi.org/10.1371/journal.pone.0098075

Vickery, J.A., Mallord, J.W., Adams, W.M., Beresford, A.E., Both, C., Cresswell, W., Diop, N., Ewing, S.R., Gregory, R.D., Morrison, C.A., Sanderson, F.J., Thorup, K., Van Wijk, R.E., Hewson, C.M., 2023. The conservation of Afro-Palaearctic migrants: What we are learning and what we need to know? Ibis (Lond. 1859). https://doi.org/10.1111/ibi.13171

Voerkelius, S., Lorenz, G.D., Rummel, S., Quétel, C.R., Heiss, G., Baxter, M., Brach-Papa, C., Deters-Itzelsberger, P., Hoelzl, S., Hoogewerff, J., Ponzevera, E., Van Bocxstaele, M., Ueckermann, H., 2010. Strontium isotopic signatures of natural mineral waters, the reference to a simple geological map and its potential for authentication of food. Food Chem. 118, 933–940. https://doi.org/10.1016/j.foodchem.2009.04.125

Wang, X., Bocksberger, G., Lautenschläger, T., Finckh, M., Meller, P., O'Malley, G.E., Oelze, V.M., 2023. A bioavailable strontium isoscape of Angola with implications for the archaeology of the transatlantic slave trade. J. Archaeol. Sci. 154. https://doi.org/10.1016/j.jas.2023.105775

Wassenaar, L.I., Hobson, K.A., 1998. Natal origins of migratory monarch butterflies at wintering colonies in Mexico: New isotopic evidence. Proc. Natl. Acad. Sci. U. S. A. 95, 15436–15439. https://doi.org/10.1073/pnas.95.26.15436

Wotton, K.R., Gao, B., Menz, M.H.M., Morris, R.K.A., Ball, S.G., Lim, K.S., Reynolds, D.R., Hu, G., Chapman, J.W., 2019. Mass Seasonal Migrations of Hoverflies Provide Extensive Pollination and Crop Protection Services. Curr. Biol. 29. https://doi.org/10.1016/j.cub.2019.05.036

Wunder, M.B., Kester, C.L., Knopf, F.L., Rye, R.O., 2005. A test of geographic assignment using isotope tracers in feathers of known origin. Oecologia 144, 607–617. https://doi.org/10.1007/s00442-005-0071-y